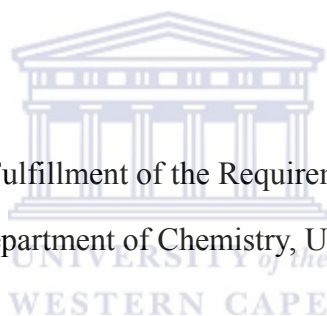


# **Proton conducting polymer composite membrane development for Direct Methanol Fuel Cell applications**

Hongze Luo

A Thesis Submitted in Fulfillment of the Requirements for the Degree of Doctor  
of Philosophy in the Department of Chemistry, University of the Western Cape.



Supervisor: Dr. Guntars Vaivars

May 2008

**KEYWORDS**

Direct Methanol Fuel Cell (DMFC)

Proton conducting membranes (Proton exchange membranes)

Composite

Sulfonation

Methanol permeability

Proton conductivity

Chlorosulfonation

Cross-linking

Water uptake

Sulfonated and sulfinated PEEK



**DECLARATION**

I declare that *Proton conducting polymer composite membrane development for Direct Methanol Fuel Cell applications* is my own work, and that it has not been submitted for any degree or examination in any other university, and that all sources I have used or quoted have been indicated and acknowledged by complete references.



Hongze Luo

May, 2008

Signed:

## ACKNOWLEDGEMENTS

I would like to express my sincere gratitude to all those who helped me with my study at UWC. I wish to thank the following people:

- ✧ Prof. V. Linkov for affording me the opportunity to be part of his research group;
- ✧ Supervisor Dr. Guntars. Vaivars, for guidance throughout and constant advice, and most especially for his assistance with the many technical aspects of membrane technology;
- ✧ Dr. S. Ji, for his friendship and his assistance in SPEEK/ZP membrane;
- ✧ Dr. S. Titinchi and Dr. M. Zou in characterization of SCPEEK;
- ✧ Dr. H. Zheng, for her assistance with the electric chemical analysis and constant support;
- ✧ I would also like to express my sincerest gratitude to Dr. A. Nechaev, Dr. B. Bladergroen, Dr. L. Khotseng, Dr. P. Ndungu, Dr. S. Pasupathi for all their helpful guidance and assistance during my time at SAIAMC;
- ✧ Mrs. L. Petrik, Prof. F. Ameer, Prof. D. Key staff, Prof. I.R. Green, and Mr. T. Lesch, members of the chemistry department of the University of Western Cape for their assistance;
- ✧ I. Sprinceana, B. Rodgers for their assistance in the laboratory;
- ✧ The members of SAIAMC;
- ✧ Mr. A. Josephs in the Physics Department for their assistance with the SEM measurements;
- ✧ My parents and brother, for their patience, unending support, love and understanding during the time of my studies;
- ✧ Finally, I would like to thank my Changhong Wu, for always being there for me. Thank you for your constant and endless love, support, understanding, patience and encouragement.

**LIST OF ABBREVIATIONS**

AFC	Alkaline Fuel Cell
3-APTES	Acid-functionalized 3-aminopropyl triethoxysilane
BDSA	2,2'-benzidinedisulfonic acid
BPO4	Boron orthophosphate
CV	Cyclic Voltammetry
DC	Degree of Chlorosulfonation
DMAc	Dimethylacetamide
DMF	Dimethylformamide
DMFC	Direct Methanol Fuel Cell
DMSO	Dimethyl sulfoxide
DS	Degree of Sulfonation
DT	Degree of Total Substitution
EDX	Energy Dispersive X-Ray
FTIR	Fourier Transform Infra-Red
GC	Gas Chromatograph
GPC	Gel Permeation Chromatography
H <sub>2</sub> -PEMFC	H <sub>2</sub> Proton Exchange Membrane Fuel Cell
I	Current density [A/cm <sup>2</sup> ]
IEC	Ion Exchange Capacity
L	Membrane thickness [cm]
MCFC	Molten Carbonate Fuel Cell
MEA	Membrane Electrode Assembly
NMP	1-Methyl-2-pyrrolidinone
P	Methanol permeability [cm <sup>2</sup> /s]
PAFC	Phosphoric Acid Fuel Cell
PBI	Polybenzimidazole
PEEK	Poly Ether Ether Ketone

## List of Abbreviations

---

PEK	Poly Ether Ketone
PEM	Proton Exchange Membrane
PEMFC	Proton Exchange Membrane Fuel Cell
PSU	Polysulfone
PTFE	Polytetrafluoroethylene
R	Resistance [ $\Omega$ ]
S	Surface area [ $\text{cm}^2$ ]
SEM	Scanning Electron Microscopy
SOFC	Solid Oxide Fuel Cell
SCPEEK	Sulfonated and Chlorosulfonated Poly Ether Ether Ketone
SPEEK	Sulfonated Poly Ether Ether Ketone
SPEEK/ZP	Sulfonated Poly Ether Ether Ketone/Phosphorized Zirconium oxide nano-particles
SsPEEK	Sulfonated and sulfinated Poly Ether Ether Ketone
SPI	Sulfonated Polyimide
TEM	Transmission Electron Microscopy
TGA	Thermal Gravimetric Analysis
V	Voltage [V]
XRD	X-Ray Diffraction
ZP	Phosphorized Zirconium oxide nano-particles

## ABSTRACT

The proton conducting membrane, usually termed “proton exchange membrane” is one key component of the direct methanol fuel cell (DMFC). For a direct methanol fuel cell (DMFC), the proton exchange membrane must conduct protons and be a good methanol barrier. Currently the membranes most referred to are DuPont’s Nafion<sup>®</sup>. The high cost of the DMFC components, and high methanol crossover, are the main issues preventing its commercialisation and DMFC performance. The main objective of this study was thus to prepare highly proton conductive membranes that are cheap to manufacture and have low methanol permeability. Two different kinds of membranes (composite and cross-linked) based on poly(etheretherketone) (PEEK) have been developed and studied in this thesis.

Chapter 3 and Chapter 4 respectively present those two membranes, different but relatively based on poly(etheretherketone) (PEEK).

In Chapter 3, SPEEK/phosphorized zirconium oxide nano-particles (ZP) composite membranes were prepared by incorporating various ratios of ZP into SPEEK. SPEEK/ZP membranes showed many improved properties compared with that of pure SPEEK. Key amongst these are increased proton conductivity, reduced water uptake and the 28 % methanol permeability reduction of a membrane with 5 wt.% of ZP compared with that of SPEEK membrane, it is 12 times lower than that of Nafion<sup>®</sup> 117. SPEEK/ZP composite membrane with low incorporated ZP content is considered for DMFC application.

Chapter 4 presents a novel type of cross-kinked membrane which prepared by an original and simple method. The membranes are highly conductive, low methanol permeable and stable, cheap and easy to prepare.

The properties of the cross-linked membranes were effected on the cross-linking degree of the membranes. Water uptake, methanol permeability reduces with increasing cross-linking degree. The water uptake of a highly cross-linked membrane was only 28 wt.% at room temperature, with only moderate increases with temperature. Although the proton conductivity of the cross-linked membrane was slightly compromised, the highly cross-linked membranes still exhibited high proton conductivity (comparable with Nafion<sup>®</sup>), much lower methanol permeability and high stability. In the DMFC test, a highly cross-linked PEEK membrane demonstrated a better performance compared to the commercial membrane Nafon<sup>®</sup>. Due to the low cost, higher proton conductivity, suitable water uptake and low methanol permeability, these cross-linked PEEK membranes are considered for use in DMFC (also for H<sub>2</sub>-PEMFC) as alternatives to Nafion<sup>®</sup>.



**TABLE OF CONTENTS**

KEYWORDS .....	ii
DECLARATION.....	iii
AKNOWLEDGEMENTS.....	iv
LIST OF ABBREVIATIONS.....	v
ABSTRACT.....	vii
TABLE OF CONTENTS .....	ix
LIST OF FIGURES.....	xv
LIST OF TABLES.....	xx
CHAPTER 1:                      Introduction.....	1
1.1. Background .....	1
1.2. Objectives.....	2
1.3. Steps towards attaining solutions .....	3
CHAPTER 2:                      Literature Review .....	4
2.1. Fuel cells .....	4
2.1.1. Introduction.....	4
2.1.2. Advantages of Fuel Cells compared to conventional technologies.....	5
2.1.3. Types of fuel cells .....	6



## Table of Contents

---

2.2. Proton Exchange Membrane Fuel Cells (PEMFC).....	7
2.2.1. H <sub>2</sub> -Proton Exchange Membrane Fuel Cell.....	7
2.2.2. Direct Methanol Fuel Cell (DMFC).....	8
2.2.2.1. Advantages and comparison of DMFC with H <sub>2</sub> -PEMFC .....	8
2.2.2.2. Principle of operating of the Direct Methanol Fuel Cell.....	9
2.2.2.3. Components of a Direct Methanol Fuel Cell .....	10
2.3. Proton Exchange Membranes .....	11
2.3.1. Introduction.....	11
2.3.2. Fluorinated membranes and composite fluorinated membranes.....	13
2.3.2.1. Homogeneous fluorinated membranes.....	13
2.3.2.2. Partially fluorinated membranes .....	15
2.3.2.3. Composites fluorinated membranes.....	16
2.3.3. Non-Fluorinated Membranes and its composite .....	19
2.3.3.1. Sulfonated polymers .....	19
2.3.3.2. Cross-linked membranes based on sulfonated polymer.....	23
2.3.3.3. Composite Non-fluorinated membranes .....	24
2.3.4. Other membranes Phosphonated Polyphosphazene.....	27
2.4. The significance of the review .....	28

## Table of Contents

---

CHAPTER 3: Preparation and Characterization of SPEEK/ZP Composite Proton Conducting Membranes .....	30
3.1. Introduction.....	30
3.2. Experimental .....	32
3.2.1. Materials.....	32
3.2.2. Preparation of SPEEK.....	32
3.2.3. Preparation of phosphorized zirconia nano-particles (ZP).....	32
3.2.4. Membrane preparation .....	33
3.2.4.1. Preparation of SPEEK membranes .....	33
3.2.4.2. Preparation of SPEEK/ZP composite membrane.....	33
3.2.5. Characterization of the polymers and membranes.....	34
3.2.5.1. Fourier Transform Infrared (FTIR) study .....	34
3.2.5.2. X-Ray Diffraction (XRD) .....	34
3.2.5.3. Transmission Electron Microscopy (TEM).....	35
3.2.5.4. Thermal Gravimetric Analysis (TGA) .....	35
3.2.5.5. Ion Exchange Capacity (IEC) .....	35
3.2.5.6. Water uptake.....	37
3.2.5.7. Methanol permeability measurements .....	37

## Table of Contents

---

3.2.5.8. Scanning Electron Microscope (SEM).....	40
3.2.5.9. Proton conductivity measurements .....	41
3.3. Results and discussions .....	43
3.3.1. Thermal properties and degree of sulfonation .....	43
3.3.2. Ion Exchange Capacity (IEC) .....	46
3.3.3. Fourier Transform Infrared (FTIR) spectroscopy .....	47
3.3.4. X- Ray Diffraction (XRD) .....	49
3.3.5. Transmission Electron Microscopy (TEM).....	51
3.3.6. Water uptake of the membranes .....	53
3.3.7. Solubility of SPEEK .....	55
3.3.8. Proton conductivity of the membrane .....	56
3.3.9. Methanol permeability (Methanol crossover).....	59
3.3.10. Morphology studies by SEM .....	61
3.4. ConcluSions .....	63
CHAPTER 4: Preparation and characterization of cross-linked PEEK membranes .....	64
4.1. Introduction .....	64
4.2. Experimental .....	66

## Table of Contents

---

4.2.1. Chemicals and Materials .....	66
4.2.2. Modification of PEEK .....	67
4.2.3. Preparation of cross-linked PEEK membranes .....	67
4.2.4. Characterization of the polymer and membranes.....	68
4.2.4.1. Fourier Transform Infrared (FTIR) .....	68
4.2.4.2. Viscosity measurement.....	68
4.2.4.3. Ion Exchange Capacity (IEC) .....	69
4.2.4.4. Determination of chloride by the Mohr method .....	69
4.2.4.5. Redox titration for determination of the sulfinate.....	69
4.2.4.6. Proton conductivity measurement.....	70
4.2.4.7. Water uptake.....	70
4.2.4.8. Methanol permeability (methanol crossover) measurements ..	70
4.2.4.9. Electrochemical stability by cyclic voltammetry measurement	71
4.2.4.10. TGA.....	71
4.2.4.11. DMFC test .....	71
4.3. Results and discussion .....	74
4.3.1. Modification of PEEK by chlorosulfonic acid.....	74
4.3.2. FTIR of investigated polymers and membranes .....	75

## Table of Contents

---

4.3.3. Viscosity of SCPEEK.....	77
4.3.4. IEC of SCPEEK.....	79
4.3.5. Chlorine analysis.....	81
4.3.6. Degree of substitution.....	83
4.3.7. Redox titration for determination of the sulfinate.....	84
4.3.8. IEC of the cross-linked membranes.....	84
4.3.9. Water uptake of the cross-linked membranes.....	86
4.3.10. Proton conductivity of the cross-linked membranes.....	89
4.3.11. Methanol permeability (methanol crossover).....	92
4.3.12. SEM of the cross-linked membrane.....	95
4.3.13 Thermal stability of the cross-linked membrane.....	96
4.3.14. Electrochemical stability.....	97
4.3.15 Performance of membranes in DMFC.....	100
4.4. Conclusions.....	102
CHAPTER 5: Overall summary and recommendations.....	103
5.1. Overall summary.....	103
5.2. Recommendations.....	104

**LIST OF FIGURES**

CHAPTER 2:

Figure 2. 1: Basic description of a Direct Methanol Fuel Cell operation. .... 10

Figure 2.2: A view of a DMFC stack and an exploded view of a single cell <sup>[51]</sup>.  
 ..... 11

Figure 2. 3: Chemical Structure of Nafion<sup>®</sup> Membrane <sup>[60]</sup> ..... 13

Figure 2. 4: Chemical structure of Dow ionomer membrane <sup>[62, 67]</sup> ..... 14

Figure 2. 5: Structure of Pall membrane R-1010 <sup>[107]</sup> ..... 18

Figure 2.6: Chemical structure of sulfonated polyetherketone ..... 21

Figure 2. 7: Poly[2,20-(*m*-phenylene)-5,50-bibenzimidazole] (PBI)..... 26

CHAPTER 3:

Figure 3. 1: Schematic diagram of methanol permeability measurement..... 38

Figure 3.2. Schematic representation of the cell for measuring proton conductivity ..... 42

Figure 3. 3: Thermo-gravimetric curves of PEEK, SPEEK and SPEEK/ZP. 44

Figure 3. 4: Degree of sulfonation of SPEEK with the sulfonation time..... 45

Figure 3. 5: Structure and atom numbering of SPEEK,  $x + y = n$ ,  
 $y/(x + y) = DS$  <sup>[189]</sup> ..... 45

Figure 3. 6: Ion exchange capacity of SPEEK and prepared membranes..... 46

## List of Figures

---

Figure 3. 7: Structures of DMF and DMAc and a possible configuration of hydrogen-bonding between SO <sub>3</sub> H groups of SPEEK and DMF molecules <sup>[190]</sup> .....	47
Figure 3. 8: FTIR spectra of PEEK and sulfonated PEEK with different DS values. ....	48
Figure 3. 9: FTIR spectra of ZrO <sub>2</sub> and ZP.....	49
Figure 3. 10: XRD patterns of nano-sized ZrO <sub>2</sub> and ZP. ....	50
Figure 3. 11: TEM image of ZP nano-particles.....	51
Figure 3. 12: TEM image of ZrO <sub>2</sub> nano-particles. ....	52
Figure 3. 13: High resolution TEM of ZP nano-particle powder. ....	53
Figure 3. 14: Water uptake as a function of DS at room temperature and at 80 °C. ....	54
Figure 3. 15: The water uptake for membranes with different ZP content at different temperatures. ....	55
Figure 3. 16: Proton conductivity of the membranes with different DS.....	56
Figure 3. 17: The proton conductivity of SPEEK/ZP membranes as a function of temperature. ....	58
Figure 3. 18: Effect of ZP content on proton conductivity at 80 °C and room temperature.....	59
Figure 3. 19: Effect of the incorporated ZP content on methanol permeability. ....	60

## List of Figures

---

Figure 3. 20: SEM micrographs of SPEEK and SPEEK/ZP composite membrane:.....	62
CHAPTER 4:	
Figure 4. 1: The procedures of membrane-electrode assembly.....	72
Figure 4. 2: Lynntech endplates. ....	73
Figure 4. 3: FTIR spectra of PEEK, SPEEK, SCPEEK, SsPEEK and one of the cross-linked membranes.....	75
Figure 4. 4: Enlarged FTIR spectra of PEEK, SPEEK, SCPEEK, SsPEEK and one of the cross-linked membranes.....	77
Figure 4. 5: Viscosities of SCPEEK.....	79
Figure 4. 6: Ion exchange capacity of SCPEEK. ....	80
Figure 4. 7: Structure of PEEK positions marked with arrows are possible sites of substitution.....	80
Figure 4. 8: Substitution of SO <sub>2</sub> Cl and degree of chlorosulfonation. ....	82
Figure 4. 9: Energy Dispersive X-ray spectroscopy of SCPEEK. ....	82
Figure 4. 10: Degree of substitutions of SCPEEK.....	83
Figure 4. 11: IEC of the cross-linked membranes.....	85
Figure 4. 12: Image of the prepared membranes.....	86
Figure 4. 13: Water uptake of the cross-linked membranes.....	87

## List of Figures

---

Figure 4. 14: The dependence of water uptake on cross-linking degree.....	88
Figure 4. 15: Schematic diagram of the cross-linking membrane. ....	88
Figure 4. 16: proton conductivity of the membranes as a function of temperature.....	89
Figure 4. 17: Effect proton conductivity on cross-linking degree. ....	90
Figure 4. 18: Arrhenius plot of proton conductivity as a function of temperature for the cross-linked membranes and Nafion <sup>®</sup> 117 membrane. ....	91
Figure 4. 19: Cyclic voltammetry curves for the methanol at various concentrations. ....	93
Figure 4. 20: The relation between peak current and methanol concentration. ....	94
Figure 4. 21: The influence of cross-linking degree on methanol permeability of the cross-linked PEEK membranes. ....	95
Figure 4. 22: The SEM cross section images of the cross-linked membranes. ....	96
Figure 4. 23: The TGA curves of cross-linked membranes M-1 and M-5....	97
Figure 4. 24: Cyclic voltammetry of prepared membrane in 1 M KOH solution. ....	98
Figure 4. 25: Cyclic voltammetry of prepared membrane in 0.5 M H <sub>2</sub> SO <sub>4</sub> ..	99
Figure 4. 26: The cell performance of a cross-linked membrane single cell vs.	

Nafion<sup>®</sup> 117 single cell. .... 101

CHAPTER 5:

Figure 5. 1: Schematic diagram of a cross-linked membrane..... 105



**LIST OF TABLES**

CHAPTER 2:

Table 2. 1: Types of Fuel Cells <sup>[27-29]</sup> ..... 6

Table 2. 2: Comparison of the membrane parameters <sup>[108]</sup> ..... 19

CHAPTER 3:

Table 3. 1: The specifications and working parameters of XRD. .... 35

Table 3. 2: Gas chromatography (HP 5890) parameters. .... 40

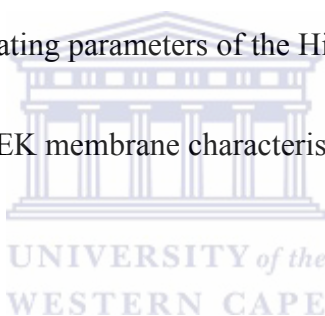
Table 3. 3: The operating parameters of the Hitachi x650 SEM..... 41

Table 3. 4: The SPEEK membrane characteristic parameters..... 47

CHAPTER 4:

Table 4. 1: List of the used chemicals and materials..... 66

Table 4. 2: Chemical stability of cross-linked membranes. .... 100



**1.1. BACKGROUND**

Energy may be the most important factor that will influence the shape of society in the 21<sup>st</sup> century <sup>[1]</sup>. Fuel cells are electrochemical energy converters, transforming chemical energy directly into electricity <sup>[2]</sup>. They are forming an attractive new technology of electricity generation due to their many benefits. In the next few years, strides in fuel cell technology will forever change our concept of alternative energy systems and will become the driver of the next growth wave of the world's economy. As well as offering a high theoretical efficiency, especially at low temperatures, fuel cells emit low or zero levels of pollutants. They can run on a wide range of fuels –from the gaseous, such as hydrogen and natural gas to the liquid fuels such as methanol and gasoline <sup>[3]</sup>.

Among various types of fuel cells, the direct methanol fuel cell (DMFC) uses methanol as the fuel. Methanol is a low cost liquid fuel having high electrochemical activity. It has a high energy density with respect to its volume, which allows for greater efficiency over traditional combustion engines. Presently, DMFCs are becoming very attractive for transportation and portable applications as they offer important advantages such as elimination of fuel reforming, ease of refuelling, and simplified system design <sup>[3]</sup>.

Proton conducting membranes, also known as proton exchange membranes which play the major role in DMFC. They affect the performance and the cost of DMFC. Since, the proton exchange membranes based on fluorinated polymer, such as Nafion<sup>®</sup> membranes, exhibit high proton conductivity and stability <sup>[4]</sup>, they are widely used as the electrolyte.

However, the high price of fluorine-based Nafion<sup>®</sup> is the major factor influencing the cost of the DMFC system. The commercialization of DMFC is thus limited by the high cost of the available fluorinated membranes<sup>[4]</sup>. A shortcoming of the fluorinated membranes especially related to their application in DMFC is their high methanol permeability, which drastically reduces DMFC performance<sup>[5]</sup>. Therefore developing cheap membranes with low methanol permeability have become an active area of research.

## 1.2. OBJECTIVES

The main objective of this project is to develop the cheap proton exchange membranes with low methanol permeability and high proton conductivity. The main focus of this study includes:

- A search for cheaper membrane non-fluorinated materials.
- The synthesis of proton conducting membranes for DMFC, which are:
  - ✧ Highly proton conductive (of the order of  $1 \times 10^{-2}$  S/cm),
  - ✧ Mechanically strong,
  - ✧ Chemically and thermally stable, (especially stable in DMFC),
  - ✧ Low methanol permeability.
- Preparation of membranes, and developing effective membrane preparation methods.
- Modification of the membrane structure to improve the properties of the membrane.
- Characterizing the prepared membrane using various techniques.
- Assembling the single cell of DMFC using prepared membrane, and evaluating its performance.

### 1.3. STEPS TOWARDS ATTAINING SOLUTIONS

#### 1. Establishing the starting material

The starting material poly(etheretherketone) (PEEK) was established after the literature review. PEEK is high chemical inertness, relatively low cost.

#### 2. Composite membranes

The sulfonation of PEEK by concentrated sulphuric acid and the membranes prepared by using those sulfonated PEEK with various levels degree of sulfonation was studied. In order to improve the properties of the membranes, a series of PEEK/ZP composite membranes were subsequently prepared by incorporating a nano-sized inorganic proton conductor, phosphorized zirconium oxide in SPEEK polymer matrix. Chapter 3 gives a detailed synthesis of SPEEK/ZP membranes, characterization of SPEEK/ZP composite membranes, results and discussion.

#### 3. Cross-linked membranes

For developing highly proton conductive and stable membrane, PEEK was modified to SCPEEK via sulfonation and chlorosulfonation. After reducing SCPEEK to SsPEEK, the membranes were prepared by cross-linking in order to prepare the stable membranes with high proton conductivity. Chapter 4 gives a detailed preparation of cross-linked PEEK membranes, characterization, results, discussions and performance of a DMFC using prepared cross-linked membrane.

**2.1. FUEL CELLS****2.1.1. Introduction**

Fuel cells are electrochemical devices that convert chemical energy in fuels into electrical energy directly<sup>[6]</sup> without a combustion process, promising power generation with high efficiency (Fuel cells are not limited by Carnot efficiency)<sup>[7]</sup> and low environmental impact.

Fuel cells have gained popular recognition and are under serious consideration as an economically and technically viable power source. They are considered a prime candidate for the future.

The origin of fuel cell technology in 1839, is credited to William Robert Grove (1811-1896) who was a British jurist and amateur physicist<sup>[8, 9]</sup> Ludwig Mond (1839-1909) with assistant Carl Langer conducted experiments with a hydrogen fuel cell in 1888 that produced 6 amps per square foot at 0.73 volts<sup>[10]</sup>. Francis Thomas Bacon invented the first alkaline fuel cell (AFC) in 1932<sup>[11]</sup>. 27 years later, he made a 5 kW fuel cell for practical application.

From 1839, it took 120 years until National Aeronautics and Space Administration (NASA) demonstrated some potential applications in providing power during space flight. During that time, the first PEMFC was invented and developed<sup>[12, 13]</sup>. As a result of these successes, industry recognized the commercial potential of fuel cells in the 1960s, but encountered technical barriers and high investment costs. Since 1984, the Office of Transportation Technologies

at the U.S. Department of Energy has been supporting research and development of fuel cell technology<sup>[14, 15]</sup>. Hundreds of companies around the world are working towards making fuel cell technology pay off. In 1993, Ballard Corporation made the first fuel cell car in Canada. Just as in the commercialization of the electric light bulb nearly one hundred years ago, today's companies are being driven by technical, economic, and social forces such as high performance characteristics, reliability, durability, low cost, and environmental benefits<sup>[16, 17]</sup>.

### **2.1.2. Advantages of Fuel Cells compared to conventional technologies**

Fuel cells are not Carnot cycle (thermal energy based) engines<sup>[18, 19]</sup>. Since the fuel is converted directly to electricity, a fuel cell has the potential to operate at much higher efficiencies than in conventional energy conversion processes, thereby extracting more electricity from the same amount of fuel, while providing the heat of condensation of the water vapour in the products. Fuel cells have low emission profiles. If a hydrogen fuel is used, the only waste product is water<sup>[20]</sup>. Fuel cells are mechanically ideal because these devices have no moving parts thereby making them quiet and reliable sources of power<sup>[3]</sup>.

In principle, a fuel cell operates like a battery<sup>[21]</sup>. Unlike a battery, a fuel cell does not run down or require recharging<sup>[22, 23]</sup>. A fuel cell will be able to continually generate energy as long as fuel and the oxidant are provided to the cell. This is distinctly different from typical batteries, which are merely energy storage devices. Since it is a storage appliance, the battery is dead (or discharged) when the stored reactants are exhausted. The fuel for fuel cells is stored external to the actual device, and therefore, cannot become internally depleted<sup>[24]</sup>.

### 2.1.3. Types of fuel cells

Fuel cell types are generally classified by different electrolyte material <sup>[25]</sup>. The electrolyte is the substance between the positive and negative electrode, acting as the conductor (but it does not conduct electrons) for the ion exchange that produces electrical current <sup>[26]</sup>. There are five kinds of fuel cell undergoing study (Table 2.1), development and demonstration, in various stages of commercial availability. These five types of fuel cell are significantly different from each other in many respects that the key distinguishing feature is the electrolyte material. All fuel cells have the same basic operating principle.

Table 2. 1: Types of Fuel Cells <sup>[27-29]</sup>.

Type	Alkaline Fuel Cell (AFC)	Molten Carbonate fuel cells (MCFC)	Phosphoric Acid Fuel Cells (PAFC)	Solid Oxide fuel cells (SOFC)	Proton Exchange Membrane Fuel Cells (PEMFC)
Type of electrolyte	Typically aqueous KOH solution	Typically, molten $\text{Li}_2\text{CO}_3/\text{K}_2\text{CO}_3$ eutectics	$\text{H}_3\text{PO}_4$ solutions	Stabilized ceramic matrix with free oxide ions	Proton exchange membrane
Typical construction	Plastic, metal	High temp metals, porous ceramic	Carbon, porous ceramics	Ceramic, high temp metals	Plastic, metal, or carbon
Operational temperature	(60-260 °C)	(650-700 °C)	(150-210 °C)	(650-1000 °C)	(60-120 °C)
Primary contaminate sensitivities	$\text{CO}$ , $\text{CO}_2$ , and Sulfur	Sulfur	$\text{CO} < 1\%$ , Sulfur	Sulfur	$\text{CO}$ , Sulfur, and $\text{NH}_3$
Applications	Military space	Electric utility	Electric utility, transportation	Electric utility	Electric utility, portable power, transportation
Advantages	Cathode reaction faster in alkaline electrolyte — therefore high performance	High temperature advantages	Up to 85 % efficiency in co-generation of electricity and heat. Impure $\text{H}_2$ as fuel	High temperature advantages. Solid electrolyte advantages	Solid electrolyte reduces corrosion & management problems. Low temperature. Quick start-up
Disadvantages	Expensive removal of $\text{CO}_2$ from fuel and air streams required	High temperature enhances corrosion and breakdown of cell components	Pt catalyst. Low current and power. Large size.	High temperature enhances breakdown of cell components	Low temperature requires expensive catalysts. High sensitivity to fuel impurities

## 2.2. PROTON EXCHANGE MEMBRANE FUEL CELLS (PEMFC)

PEMFCs offer high energy conversion efficiency, at low operating temperatures, which can rapid start-up<sup>[30]</sup>. These traits and the ability to rapidly change power output are some of the characteristics that make the PEMFCs the most promising fuel cell technique for large-scale application in, for example, portable electronics, automobiles or stationary power supplies<sup>[31]</sup>.

H<sub>2</sub>-PEMFC and DMFC are classified as PEMFC because they all use a solid proton exchange membrane as the electrolyte. The main difference between the DMFC and the H<sub>2</sub>-PEMFC is the type of fuel used for the production of electrical power: methanol in the case of DMFC and H<sub>2</sub> in the case of H<sub>2</sub>-PEMFC<sup>[32]</sup>.

### 2.2.1. H<sub>2</sub>-Proton Exchange Membrane Fuel Cell

The first H<sub>2</sub>-PEMFC device was developed in the 1960's by the General Electric Company for use as auxiliary power sources in the Gemini space missions<sup>[33-35]</sup>. It emits no environmental pollutants. The H<sub>2</sub>-PEMFC uses Platinum (Pt) catalyst and hydrogen fuel for the anode electrode and Pt and air or O<sub>2</sub> for the cathode electrode. Pt is extremely sensitive to CO poisoning<sup>[36-38]</sup>. So, their fuels must be purified. Pure hydrogen fuel cells give the best performance in H<sub>2</sub>-PEMFCs<sup>[39-41]</sup>. But, because of hydrogen storage and transportation problems, alternate fuels have been sought.

According to Dr. Ferdinand Panik (DaimlerChrysler Fuel Cell Project Head) following the Cross-Country Trek of Methanol-Fueled NECAR 5, June 4, 2002;

*“Hydrogen is an ideal fuel for fuel cell applications, but the problem with hydrogen is storing it on-board the vehicle. I don't believe we will find a solution in the next few years, so in my opinion, hydrogen will be limited to fleets with*

*limited range. For individual transportation, I believe we need a liquid fuel and methanol is an excellent hydrogen carrier.”* [37]

## **2.2.2. Direct Methanol Fuel Cell (DMFC)**

### 2.2.2.1. Advantages and comparison of DMFC with H<sub>2</sub>-PEMFC

The alternative PEMFC is DMFC. DMFC technology has become widely accepted as a viable fuel cell technology, and DMFCs have been successfully demonstrated in powering cars, mobile phones and laptop computers [26, 42-45]. DMFCs will be widely used in future years. In a DMFC system, liquid methanol is fed directly into the fuel cell without the intermediate step of reforming the fuel into hydrogen. Methanol is a cheap liquid at room temperature, easy to store, has high energy density and can be generated from a variety of sources such as natural gas, coal and even biomass. It also is biodegradable. Furthermore, it is not corrosive for the frame of the DMFC. DMFC offers to many applications a technology with endless possibilities [46].

Comparing with the catalyst of H<sub>2</sub>-PEMFC, in addition to platinum, other catalysts like ruthenium (Ru) have to be added to break methanol bond in the anodic reaction. The electrolyte and the operating temperature in DMFCs are basically the same as those used in H<sub>2</sub>-PEMFCs, which would typically operate in a temperature range of 50 - 100 °C. Higher efficiencies are achieved at higher temperatures. The main difference is the anode reaction where methanol is oxidized instead of hydrogen as in the H<sub>2</sub>-PEMFC. DMFC uses catalysts and a methanol solution (typically 1 - 2 M) at the anode electrode, Pt catalyst and air or O<sub>2</sub> at the cathode electrode. The electrochemical oxidation reaction of methanol is more complicated than the oxidation reaction of hydrogen.

### 2.2.2.2. Principle of operating of the Direct Methanol Fuel Cell

A DMFC is comprised of an anode (which is negative electrode that repels electrons) on one side of an electrolyte (membrane) in the centre with a cathode on the other side. A methanol and water mixture is fed to the anode catalyst where the catalyst particles present in the anode help to separate the methanol molecule into hydrogen atoms and carbon dioxide (CO<sub>2</sub>) (shown in Figure 2.1). The separated hydrogen atoms are then typically stripped of their electrons to form protons, and passed through the membrane to the cathode side of the cell [47, 48]. At the cathode catalyst, the protons react with the oxygen in air to form water minus an electron. By connecting a conductive wire from the anode to the cathode side, the electrons stripped from the hydrogen atoms on the anode side can travel to the cathode side and combine with the electron deficient species [49].

The reaction of the DMFC:



For the formation of the final product -CO<sub>2</sub>- water is required. The six electrons are passing the load resistance of the outer circuit and are consumed at the cathode together with six protons [50].

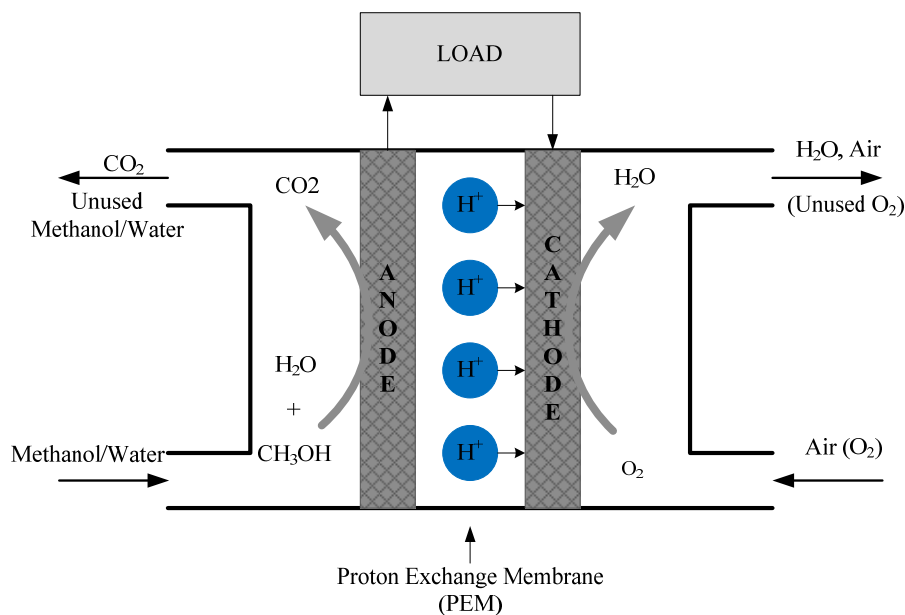


Figure 2. 1: Basic description of a Direct Methanol Fuel Cell operation.

### 2.2.2.3. Components of a Direct Methanol Fuel Cell

An exploded view of a DMFC stack is presented in Figure 2.2. A single cell is the basic unit of a DMFC stack which consists of many individual cells to produce electricity. The Membrane-Electrode Assembly (MEA) together with the plates make up a single DMFC cell which consists of a proton exchange membrane and two electrodes<sup>[40]</sup>. A stack electrically connects many single cells in series or parallel to produce the overall voltage and current levels desired. The plates serve as the electrical connections between individual cells and serve as the channels through which fuel and oxidant can flow. The number of fuel cells connected in series in the stack determines the stack voltage. The total surface area of the cells determines the total current produced. Additional components are required for electrical connections and/or insulation and the flow of methanol, water, CO<sub>2</sub>, oxidant.

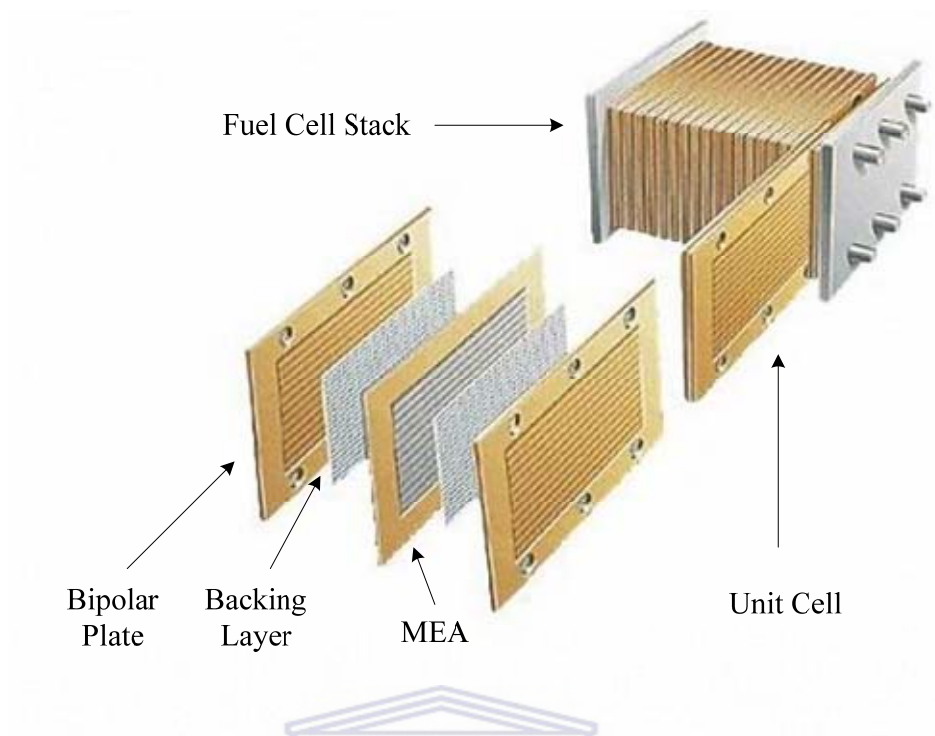


Figure 2.2: A view of a DMFC stack and an exploded view of a single cell <sup>[51]</sup>.

The MEA is the heart of a single DMFC. MEA consists of two electrodes and Proton Exchange Membrane (electrolyte). A major disadvantage of DMFC is the high cost of the system resulting from the high price of catalysts and that of membranes <sup>[52, 53]</sup>. That means the high cost of DMFC system resulting from the high price of the MEA.

## 2.3. PROTON EXCHANGE MEMBRANES

### 2.3.1. Introduction

The function of the proton exchange membrane is to provide a proton conductive path while at the same time separating the reactants. However, the membrane material is an electrical insulator. It is also a film barrier that separates fuel and oxidant in the anode and cathode compartments of the fuel cell. It acts as

the separating layer in a fuel cell. The proton exchange membrane is the key component of a fuel cell system because only highly stable membranes can resist the cruel chemical and physical environment in a fuel cell.

The largest current problem with the DMFC is methanol permeability which is the undesirable transport of fuel from the anode side through the membrane to the cathode side where it is oxidized by chemical reaction with the oxidant present without any contribution to power generation, resulting in poor cell performance. Methanol permeability also deactivates the cathode electro-catalyst resulting in further efficiency losses, limits the applicable working temperature and decreases the cell potential.

Proton exchange membranes with low methanol permeation may allow the use of fuels with high methanol concentration and thereby increase the energy density, which is particularly attractive for portable electronic applications.

Furthermore, the cost of existing membranes is one of the key issues influencing the cost of the fuel cell system.

The membrane is an excellent proton conductor when it is saturated with water, but it does not conduct electrons. To achieve high efficiency in PEMFCs, the following membrane properties are required: (a) chemical and electrochemical stability under operating conditions; (b) mechanical strength and stability; (c) compatibility with and good adhesion to the components of the PEMFC; (d) extremely low crossover to the reactants ( $H_2$ , methanol,  $O_2$ ) to maximize coulombic efficiency; (e) high electrolyte transport to maintain uniform electrolyte content and to prevent local drying; (f) high proton conductivity to support high currents with minimal resistive losses and zero electronic conductivity; (g) production costs compatible with the intended application<sup>[54]</sup>.

Membranes can be either inorganic or organic. Many membranes have been developed, and many membranes are still ongoing research. Some representative membranes are discussed below.

### 2.3.2. Fluorinated membranes and composite fluorinated membranes

#### 2.3.2.1. Homogeneous fluorinated membranes

Fluorinated membranes are based on a polytetrafluoroethylene (PTFE) backbone with attached sulfonic acid groups. The best known materials of this class are the DuPont Nafion<sup>®</sup> membranes<sup>[55]</sup>. Nafion<sup>®</sup> is by far the leading type of commercial membrane, and widely used in H<sub>2</sub>-PEMFC and DMFC<sup>[56]</sup>. It was first conceived during the space programme in the 1960's<sup>[12, 57]</sup>. The hydrophobic PTFE backbone of Nafion<sup>®</sup> provides thermal and chemical stability, while, the fluorinated side chains terminating with hydrophilic sulfonic acid (SO<sub>3</sub>H) provides the channels for proton transport<sup>[58, 59]</sup>. The macromolecule of Nafion<sup>®</sup>, shown in Figure 2.3 below, is both hydrophobic and hydrophilic.

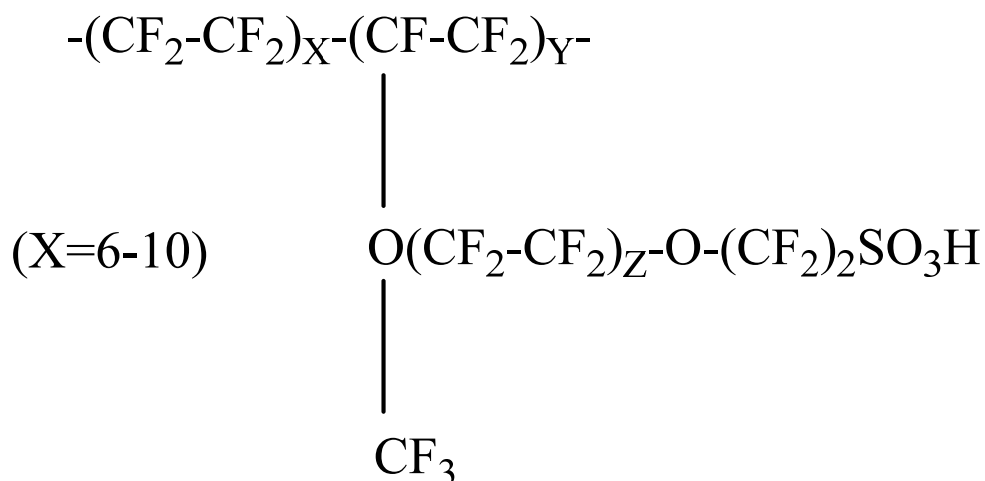


Figure 2. 3: Chemical Structure of Nafion<sup>®</sup> Membrane<sup>[60]</sup>.

The Nafion<sup>®</sup> membrane is relatively durable (unsurpassed longevity > 60,000 h in the PEMFC) and has high ionic conductivity and chemical stability<sup>[61]</sup>. However, it is too expensive for large-scale applications. High methanol cross over reduces the efficiency of the fuel cell. Moreover, the operating temperature is limited (< 80 °C) and high humidification is required due to the dehydration at high temperatures.

One of fluorinated membrane, Dow product Dow<sup>®</sup> membranes (Figure 2.4) is prepared by the co-polymerisation of tetrafluoroethylene with a vinylene monomer. The difference between Dow<sup>®</sup> and Nafion<sup>®</sup> is that the side chain of the Dow<sup>®</sup> membrane is shorter than the side chain of Nafion<sup>®</sup><sup>[62-65]</sup>. The specific conductance of the 800 and 850 EW (equivalent weight, grams of dry polymer per mole of ion exchange sites) membranes is 0.2 and 0.12 Ω<sup>-1</sup> cm<sup>-1</sup>, respectively<sup>[66]</sup>.

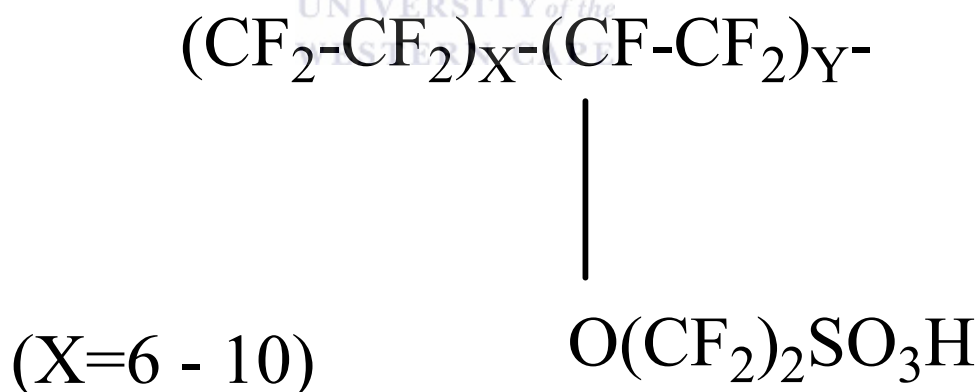


Figure 2. 4: Chemical structure of Dow ionomer membrane<sup>[62, 67]</sup>.

Dow<sup>®</sup> membranes have higher methanol permeability ( $4 \times 10^{-10}$  A cm<sup>-2</sup>) than Nafion<sup>®</sup> 117 ( $2.7 \times 10^{-10}$  A cm<sup>-2</sup>)<sup>[68]</sup>. Performance testing of a Dow membrane in a six cell Ballard Power Systems PEMFC MK4 stack in 1988 showed better performance than with Nafion<sup>®</sup><sup>[66]</sup>.

The German company 3P-energy developed a fluorinated sulfonic acid (PFSA) membrane. The 3P-membranes have 20 times lower methanol permeability than Nafion<sup>®</sup> membrane. However, other properties such as mechanical durability and lifetime data for the 3P-membranes were not available in the open literature.

The membranes of other known firms such as Asahi Glass Engineering (Flemion<sup>®</sup> membranes), Asahi Kasei (Aciplex<sup>®</sup> membranes) are also members of the fluorinated membrane family, have also been investigated for use in H<sub>2</sub>-PEMFC and DMFCs [69-72]. Both the Aciplex and the Flemion membranes have a bi-layer structure that is comprised of sulfonic acid functional groups on the anode side and carboxylic acid functional groups on the cathode side. Flemion and Aciplex membranes can be made thinner while still providing the same acid activity and thus a higher proton exchange capacity, and therefore a better proton conductivity [73].

The main drawbacks of these polymers are their high price (about \$ 800/m<sup>2</sup>) and the production process which includes strongly toxic and environment-unfriendly intermediates [74]. A shortcoming of the fluorinated ionomers especially related to their application in DMFC is their high methanol permeability which drastically reduces the performance of DMFCs [5, 75].

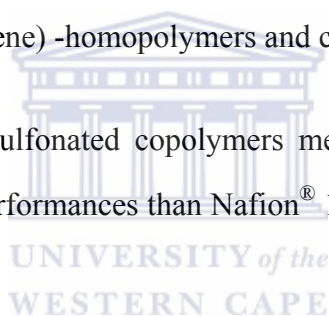
#### 2.3.2.2. Partially fluorinated membranes

Partially fluorinated membranes are still the subject of ongoing research, for example, the Paul Scherrer Institute, Villigen, Switzerland [76, 77]. These proton exchange membranes showed good performance when being applied in H<sub>2</sub>-PEMFC and DMFCs. Grafted ionomer membranes based on poly (vinylidene fluoride) have been developed by Sundholm [78].

A shortcoming of these membranes is the use of styrene and divinylbenzene monomers from where it known that their oxidation stability is limited this is due to the presence of tertiary C–H bonds in the styrene/divinylbenzene graft chains which are sensitive to O<sub>2</sub> and hydrogen peroxide attack.

The Ballard Corporation has developed a number of partially fluorinated proton exchange membranes which consist of sulfonated<sup>[79]</sup> or phosphonated<sup>[80]</sup> polymerisates of unmodified  $\alpha$ ,  $\beta$ ,  $\beta$ -trifluorostyrene and  $\alpha$ ,  $\beta$ ,  $\beta$ -trifluorostyrene modified with radicals R. Disadvantages of these membrane types include the complicated production process for the monomer  $\alpha$ ,  $\beta$ ,  $\beta$ -trifluorostyrene<sup>[81]</sup> and the difficult sulfonation<sup>[79]</sup> and phosphonation<sup>[80]</sup> procedures for poly( $\alpha$ ,  $\beta$ ,  $\beta$ -trifluorostyrene)-homopolymers and copolymers.

Partially fluorinated sulfonated copolymers membranes showed better initial and long-term DMFC performances than Nafion<sup>®</sup> 112 due to their lower methanol permeabilities<sup>[82]</sup>.



### 2.3.2.3. Composites fluorinated membranes

Penner and Martin prepared the first composite membranes by the impregnation of Gore-Tex<sup>®</sup> with Nafion<sup>®</sup><sup>[83]</sup>. Kolde *et al.* applied the Gore-Select<sup>™</sup> membrane in fuel cells. Gore-Select<sup>™</sup> membranes were found to have good mechanical strength in both the swollen and unswollen state.

The composite fluorinated membranes can be prepared with the addition of: (1). hydrophilic inorganic materials, such as SiO<sub>2</sub>, clay and zeolite<sup>[84-92]</sup>, which maintain high water content and prevent the Nafion<sup>®</sup> dehydration at high temperatures; (2). solid acids, such as sulfonated ZrO<sub>2</sub><sup>[84, 85]</sup> and zirconium phosphate<sup>[86-88]</sup> which increase the concentration of acid sites to promote proton

migration within the membrane; (3). heteropolyacids, such as phosphotungstic acid ( $\text{H}_3\text{PW}_{12}\text{O}_{40}$ )<sup>[89-91]</sup>, and phosphoric acid<sup>[67]</sup>. The performance of fluorinated membranes is significantly improved via the addition of these materials.

The composite fluorinated membranes also can be prepared with the addition of polymer, such as poly(vinylidene fluoride) (PVDF)<sup>[92-97]</sup>, polybenzimidazole (PBI)<sup>[98, 99]</sup>, polytetrafluoroethylene (PTFE)<sup>[86, 100-102]</sup>.

Nafion<sup>®</sup>-polyfurfuryl alcohol nanocomposite membranes can be synthesized by in situ polymerisation of furfuryl alcohol within commercial Nafion<sup>®</sup> membranes. The amount of polyfurfuryl alcohol in the membranes had a significant effect on the properties of the Nafion–furfuryl alcohol nanocomposite membranes. Single cell at room temperature and 60 °C and ambient air showed a much higher cell performance for the MEA with the nanocomposite membranes<sup>[103]</sup>.

Nafion<sup>®</sup> composite membrane modified by phosphoric acid-functionalized 3-aminopropyl triethoxysilane (3-APTES) was prepared and studied<sup>[104]</sup>. Methanol permeability for the composite membranes was found to be at least 50 % lower than for Nafion<sup>®</sup>. The proton conductivity of the membrane showed maximum proton conductivity of 0.07 S/cm at 3 wt.% of APTES, which was comparable with the proton conductivity of Nafion<sup>®</sup>. The performance of the fuel cell has not been reported yet.

The Gore Corporation has developed micro-reinforced composite membranes with the trade name Gore-Select<sup>®</sup>, which consist of a microporous stretched PTFE membrane whose pores are filled with fluorinated ionomer<sup>[76, 105]</sup>. Compared to Nafion<sup>®</sup>, these membranes could be reduced in thickness to 5  $\mu\text{m}$ , leading to a proton conductivity of the Gore-Select<sup>®</sup> membranes which is a factor 10 higher than the proton conductivity of Nafion<sup>®</sup>.

Pall Gelman Sciences Inc. developed Pall IonClad<sup>®</sup> membranes, which are based on tetra-fluoroethylene/perfluoropropylene. IonClad<sup>®</sup> R-1010 (shown in Figure 2.5) and IonClad<sup>®</sup> R-4010 have 2.5 – 3 times lower methanol cross over than Nafion<sup>®</sup> 117 [106].

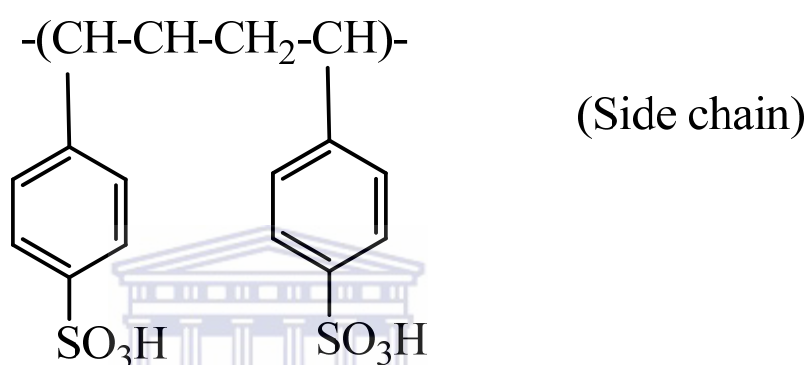


Figure 2. 5: Structure of Pall membrane R-1010 [107].

A comparison of all three membranes studied is shown in Table 2.2. The stability of the Pall membranes for a PEMFC was estimated to be 500 h [107].

Table 2. 2: Comparison of the membrane parameters <sup>[108]</sup>.

Temperature (°C)	Pall R-4010	Pall R-1010	Nafion <sup>®</sup> 117
Proton conductivity (mS cm <sup>-1</sup> )			
20	73	80	79
Methanol permeability ( $\times 10^7$ ), cm <sup>2</sup> s <sup>-1</sup>			
60	9.4	13.7	34.4

The price of the above mentioned composite membranes is still high due to the high cost of the based fluorinated polymer or membranes.

### 2.3.3. Non-Fluorinated Membranes and its composite

#### 2.3.3.1. Sulfonated polymers

Poly(arylene ether)s such as poly(ethersulfone)s, poly(etherketone)s or poly(etheretherketone)s are well known engineering plastics that display excellent thermal and mechanical properties as well as resistance to oxidation and acid catalyzed hydrolysis. The favourable properties displayed by this class of polymers now form the focus of attention as promising candidates for fuel cell membranes.

#### *Sulfonated poly(arylethersulfone) membranes*

Polysulfone (PSU) has very good chemical stability, and it is cheap. The synthesis and characterization of sulfonated polysulfone (SPSU) has been achieved by Johnson *et al.* <sup>[109]</sup> and Nolte *et al.* <sup>[110]</sup>. The shortcomings identified were that membranes cast from SPSU (Udel<sup>™</sup> P-1700) solutions were completely water soluble <sup>[110-112]</sup> and become very brittle when drying out which can happen

in the fuel cell application under intermittent conditions <sup>[113]</sup>.

Kerres and co-workers developed promising alternative composite membranes which have been cross-linked by S-alkylation of PSU sulfonate groups with di-halogenoalkanes. These membranes show very good performance in H<sub>2</sub>-PEMFC and DMFC <sup>[114-116]</sup>. These membranes also show markedly reduced methanol permeability <sup>[117]</sup>.

#### *Sulfonated poly(aryletherketone) membranes*

Poly(arylether ketone)s consist of sequences of ether and carbonyl linkages between phenyl rings, that can either “ether-rich” like PEEK and PEEKK, or “ketone-rich” like PEK and PEKEKK. The most common materials are poly(etherketone) (PEK), and poly(etheretherketone) (PEEK) which is commercially available under the name Victrex™ PEEK from Imperial Chemical Industries Ltd. A number of groups are developing proton exchange polymer materials based on this classification of materials.

Sulfonated poly(etherketone) membranes have been investigated for use in PEMFCs and DMFCs <sup>[118, 119]</sup> in the last decade. The motivation for these developments was that these polymer families have chemical and mechanical stabilities closest to the fluorinated polymer classes <sup>[120]</sup>. Sulfonated poly(etherketone) membranes consist of a poly(etherketone) backbone that has a sulfonic acid functional group attached to it (shown in Figure 2.6).

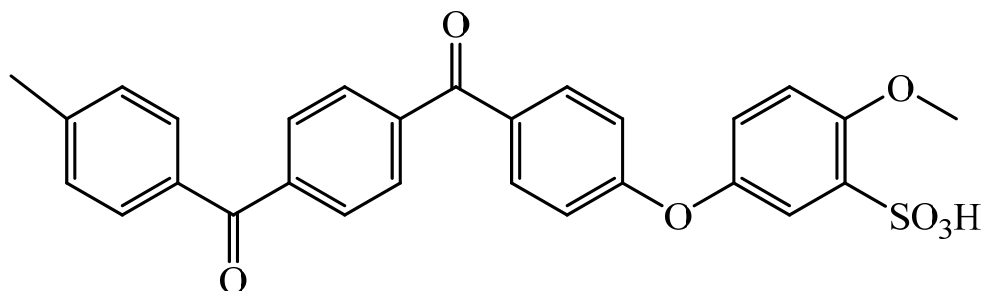


Figure 2.6: Chemical structure of sulfonated polyetherketone.

The backbone is hydrophobic and the sulfonate head is hydrophilic. However, the backbone is less hydrophobic than the PTFE backbone and the sulfonic acid group is less acidic and therefore less hydrophilic<sup>[121, 122]</sup>. The poly(etherketone) backbone is less flexible than the PTFE backbone of the sulfonated fluoropolymer family of membranes<sup>[122]</sup>. As a result of these differences between the two membranes, the sulfonated poly(etherketone) membranes are not separated into a two-phase system as distinctly as the sulfonated fluoropolymer family of membranes. The polyaromatic membranes are easier to manufacture than the sulfonated fluoropolymer membranes, and they are significantly cheaper<sup>[122]</sup>.

Sulfonation of poly(etherketone)s can be carried out directly in concentrated sulfonic acid or oleum, the extent of sulfonation being controlled by the reaction time and temperature<sup>[123, 124]</sup>.

Sulfonated polyaryls have been demonstrated to suffer from hydroxyl radical initiated degradation<sup>[125]</sup>. In contrast to this, SPEEK was found to be durable under fuel cell conditions extending over several thousand hours by Kreuer<sup>[121]</sup>. The brittleness of SPEEK makes their handling difficult and may lead to mechanical membrane failure during operation. These types of membranes become very brittle when drying out.

*Sulfonated polyamides membranes*

Aromatic polyamides such as Nomex<sup>®</sup> and Kevlar<sup>®</sup> are known as polymers of high mechanical strength and high chemical resistance. The preparation of sulfonated and carboxylated copolyaramides with high ion exchange capacities has been described by Sherman<sup>[126]</sup> and Konagaya and Tokai<sup>[127]</sup>. These materials were used for the preparation of reverse osmosis membranes with enhanced rejection properties and chlorine resistance. So far, sulfonated polyaramides have not been mentioned as potential membrane materials in fuel cell applications.

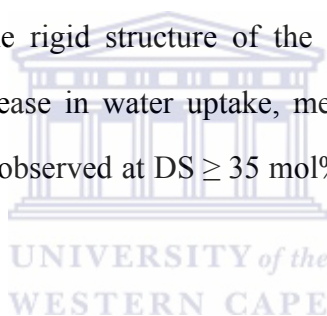
*Sulfonated polyimide membranes*

Sulfonated polyimides have successfully developed in several laboratories. Sulfonated polyimides present very interesting swelling properties in addition to good ionic conductivities, so they can be considered as promising materials for fuel cell<sup>[128-136]</sup>. It is well known that polyimides possess many advantages such as excellent thermal stability, high mechanical strength and modulus, superior electric properties, and good chemical resistance, which are just required for the PEMs used in fuel cell systems. The synthesis of sulfonated polyimide was generally performed by polymerization of a typical six-membered ring dianhydride monomer, 1,4,5,8-naphthalenetetracarboxylic dianhydride, a sulfonated diamine, and common nonsulfonated diamine monomers. The ion exchange capacity (IEC) of a sulfonated polyimide can be precisely controlled by regulating the molar ratio between the sulfonated diamine and the non-sulfonated one. However, many researches have identified that 2,2'-benzidinedisulfonic acid (BDSA) BDSA-based SPIs have rather poor water stability which needs to be improved.

Gunduz and McGrath<sup>[137]</sup> recently described the synthesis of sulfonated

polyimides using 2, 5-diaminobenzene sulfonic acid sodium salt as the source of the sulfonated subunits. Polymers with high molecular weights and narrow molecular weight distributions were obtained by the ester–acid procedure in aprotic solvents. Films prepared from polyimides with a DS of 50 and 75 % were tough and creased. A higher DS yielded brittle films, especially when completely dried. As expected, the hydrophilicity increased with increasing DS.

Woo *et al.* [138] have studied the properties of sulfonated polyimides derived from the reaction of 3,3,4,4-benzophenonetetracarboxylic acid dianhydride with 4,4-diaminobiphenyl-2,2-disulfonic acid and 4,4-oxydianiline. The water uptake was found to be five times lower than that of Nafion<sup>®</sup> 117 at comparable IEC, and which was related to the rigid structure of the polyimides leading to a lesser swelling. A sudden increase in water uptake, methanol permeability as well as proton conductivity was observed at DS  $\geq$  35 mol%. However, data from fuel cell tests were not available.



### 2.3.3.2. Cross-linked membranes based on sulfonated polymer

Guo *et al.* prepared and characterized UV-cross-linked proton exchange membranes from sulfonated poly[bis(3-methylphenoxy)phosphazene] [139]. The cross-linking was carried out after sulfonation by dissolving benzophenone (BP) photo initiator in the membrane casting solution and then exposing the dried membranes to UV light. Those cross-linked membranes looked promising for possible proton exchange membrane fuel cell applications. A cross-linked membrane swelled less than Nafion<sup>®</sup> 117 in water. The proton conductivity of the membrane at temperatures between 25 and 65 °C was only 30 % lower than that of Nafion<sup>®</sup> 117 and the water and methanol permeability were very low (e.g.,  $1.62 \times 10^{-8}$  cm<sup>2</sup>/s for methanol at 30 °C), as compared to the in Nafion<sup>®</sup>

$(6.5 \times 10^{-6} \text{ cm}^2/\text{s}$  at  $30 \text{ }^\circ\text{C}$ ).

Carter *et al.* developed proton exchange membranes which were prepared from blends of sulfonated poly[bis(3-methylphenoxy) phosphazene] (SPOP) and polyacrylonitrile (PAN)<sup>[140]</sup>. After membrane formation, the polyphosphazene was cross-linked using UV radiation. Fuel cell performance was essentially the same as that with Nafion<sup>®</sup> 117 at low current densities, while the methanol permeability flux was three to four times lower than that with Nafion<sup>®</sup> 117. At high current densities, the cell voltage dropped rapidly due to the low ionic conductivity of the blended membranes (0.008 S/cm).

The most representative cross-linked membranes were developed in developed in Stuttgart University (Germany). Kerres and co-workers investigated cross-linked sulfonated polymer membrane based on sulfonated polymer via covalently and ionically cross-linking<sup>[118, 141, 142]</sup>. Chemically cross-linked membranes were developed to reduce membrane swelling and increase mechanical strength. Materials prepared by cross-linking are comparable to commercial Nafion<sup>®</sup> in terms of their mechanical strength and proton conductivity<sup>[118, 141-144]</sup>. Although the cross-linked membrane exhibits very good properties, the processes are complex.

The membranes prepared from sulfonated poly(etheretherketone) and cross-linked with simple polyols (ethylene glycol and glycerol), exhibited enhanced strength, stability in hot water and high proton conductivity<sup>[145]</sup>. However, data from fuel cell tests were not available.

### 2.3.3.3. Composite Non-fluorinated membranes

The organic/inorganic composite proton exchange membranes are developed to

overcome the disadvantages of the actual state-of-the-art membranes which require increasing the operating temperature above 100 °C and/or reducing methanol permeability (methanol crossover). In addition, as in many proton conductors with conductivity suitable for electrochemical applications, the proton transfer process takes place on the surface of the inorganic particles; and an increase in surface area (small particle size) increases the proton conductivity [146].

Composite membrane can be fabricated by blending sulfonated poly(etheretherketone) (SPEEK) with boron orthophosphate (BPO<sub>4</sub>) [147, 148]. In comparison with Nafion<sup>®</sup> 117, the composite membranes have demonstrated better methanol separator property. The highest proton conductivity value of the composite membrane was  $3.35 \times 10^{-3}$  S/cm, and this value is adequate for DMFC application even though slightly lower than the proton conductivity of Nafion<sup>®</sup> 117 membrane [148].

Sulfonated poly(etheretherketone)/polyaniline composite proton exchange membrane was prepared by Nagarale *et al.* [149]. The authors claimed SPEEK with 1.5 % of polyaniline is more suitable for fuel cell applications considering optimum physicochemical and electrochemical properties, thermal stability as well as very low methanol permeability.

Mecheri *et al.* prepared composite membranes based on sulfonated polyether ether ketone (SPEEK) and hydrated tin oxide (SnO<sub>2</sub>·*n*H<sub>2</sub>O). The polymer electrolyte membrane doped with 50 wt.% SnO<sub>2</sub>·*n*(H<sub>2</sub>O) possess good proton transport characteristics, reduced methanol uptake and improved stability with respect to a reference unfilled membrane [150].

Acid-base composite membranes can maintain high proton conductivity at elevated temperatures without suffering from dehydration effects.

Polybenzimidazoles are synthesised from aromatic bis-*o*-diamines and dicarboxylates (acids, esters, amides), either in the molten state or in solution. The repeating unit, benzimidazole, has rather remarkable thermal properties when compared to its carbon congener indene, as illustrated by melting and boiling point data<sup>[151]</sup>. The commercially available polybenzimidazole is poly-[2,20-(*m*-phenylene)-5,50-bi-benzimidazole] shown in Figure 2.7 which is synthesized from diphenyl-*iso*-phthalate and tetra-aminobiphenyl, and will be referred to hereafter simply as “PBI”. It has excellent thermal and mechanical stability.

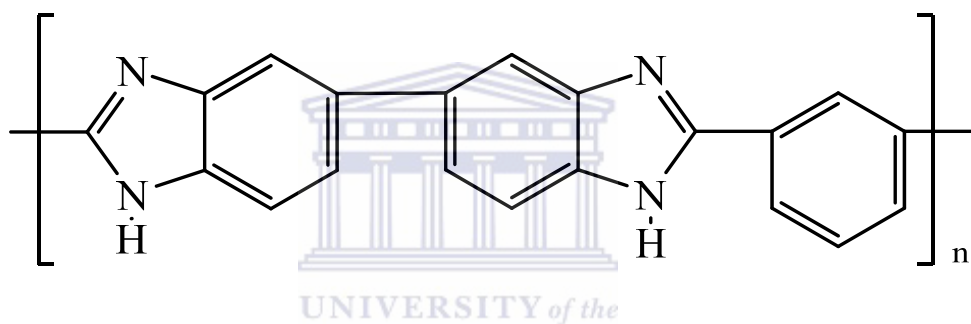


Figure 2. 7: Poly[2,20-(*m*-phenylene)-5,50-bi-benzimidazole] (PBI).

PBI is a suitable basic polymer which can readily be complexed with strong acids<sup>[152-160]</sup>. The immersion of PBI film in aqueous phosphoric acid leads to an increase in both its proton conductivity and thermal stability<sup>[161]</sup>.

Early reports of the proton conductivity of PBI are conflicting. Thus, whereas values in the range  $2 \times 10^{-4} - 8 \times 10^{-4} \text{ Scm}^{-1}$  at relative humidities between 0 and 100 % were published<sup>[157, 162]</sup>, other authors<sup>[151, 162]</sup> observed proton conductivity some two to three orders of magnitude lower. These latter values are those generally accepted for non-modified PBI, and are clearly too low for any use of PBI membranes in fuel cell applications. Two principal routes have been developed to improve the proton conduction properties, and these repose upon the

particular reactivity of PBI – which is twofold – and arises from the  $-N=$  and  $-NH-$  groups of the imidazole ring. PBI is a basic polymer ( $pK_a = 5.5$ ), the membrane can be prepared with inorganic and organic acids [156, 163, 164]. The membranes have good oxidative and thermal stability, and mechanical flexibility at elevated temperatures  $T < 200\text{ }^\circ\text{C}$  [165].

In addition however, the  $-NH-$  group is reactive; hydrogen can be abstracted, and functional groups then grafted onto the anionic PBI polymer backbone [166]. It should also be mentioned that unlike other polyaromatic polymers, the direct sulfonation of PBI using sulfuric or sulfonic acid is not appropriate for the preparation of proton conducting polymers for fuel cell membranes, since it tends to lead to a polymer with a low degree of sulfonation and increased brittleness [167].

The major disadvantage is leaching of the low molecular weight acid in hot methanol solutions. These problems were solved by the addition of high molecular weight phosphotungstic acid as a replacement of the low molecular weight acid. At  $T > 130\text{ }^\circ\text{C}$  the proton conductivity of the doped PBI membrane is similar to Nafion<sup>®</sup> ( $30\text{ mS cm}^{-1}$  at  $130\text{ }^\circ\text{C}$  and  $80\text{ mS cm}^{-1}$  at  $200\text{ }^\circ\text{C}$ ).

As mentioned above, PBI can be doped with strong acids, and it also can be complexed with conductive polymer to prepare a composite membrane [168-173].

#### 2.3.4. Other membranes Phosphonated Polyphosphazene

Allcock *et al.* synthesized poly(aryloxyphosphazene) with side chains containing phenyl phosphonic acid units for use as a proton conducting membrane in direct methanol fuel cells [174]. The phosphonated polyphosphazene membranes were synthesized from

poly[(4-bromophenoxy)(3-methylphenoxy)phosphazene]<sup>[175]</sup>. Ion exchange capacity, proton conductivity, water swelling and methanol cross over were determined. The prepared membranes with ion exchange capacities between 1.17 and 1.43 mmol/g had a proton conductivity between  $10^{-2}$  and  $10^{-1}$  S/cm at room temperature. The water uptake at room temperature was found to be between 11 % and 32 %. The methanol permeability was about 40 times lower than that of Nafion<sup>®</sup> 117.

In a later study, Zhou *et al.* reported on the methanol permeability of polyphosphazene membranes containing either sulfonic or phosphonic acid groups at different temperatures<sup>[176]</sup>. The ion exchange capacity of the membranes was 1.07 and 1.35 mmol/g for sulfonated material and phosphonated polyphosphazene, and all of the membranes were cross-linked by Co  $\gamma$ -radiation. The methanol permeability of the membranes composed of sulfonated polyphosphazene was about 8 times lower than that of the Nafion<sup>®</sup> 117 at room temperature.

Up to now, no phosphonated polyphosphazene membrane has been made into a membrane electrode assembly and tested in a DMFC.

#### 2.4. THE SIGNIFICANCE OF THE REVIEW

The DMFC has become the most promising type of fuel cell due to its many advantages. First, it is an emerging technology that needs to be better understood. Which is being performed worldwide aimed at solving the engineering problems that currently prevent fuel cells from becoming commercially available. The need is to reduce the cost of producing fuel cells. The existing problems of high price and high methanol permeability of the proton exchange membrane results in the high initial cost of DMFC manufacturing and its performance. Furthermore, the

available proton exchange membranes are very limited and expensive. Developing new proton exchange membranes which possess better properties at lower cost is crucial. It is believed that the opportunity to develop new membranes is attractive and will be extremely advantageous for us.



## CHAPTER 3: Preparation and Characterization of SPEEK/ZP Composite Proton Conducting Membranes

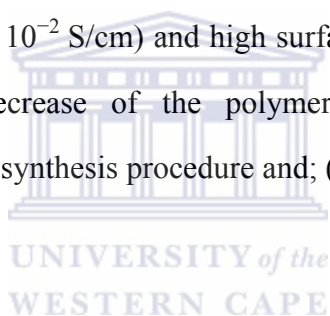
### 3.1. INTRODUCTION

Fuel cell technology is expected to become one of the key technologies of the 21<sup>st</sup> century both for stationary and for portable applications. The proton exchange membrane (PEM) is one the key components of the direct methanol fuel cell (DMFC), which has double functions of conducting protons and separating the fuel from oxidant. Currently fluorinated polymers, such as Nafion<sup>®</sup>, are used in DMFC [177]. However, the high cost of those polymers limits the large-scale commercialization of the proton conducting membrane fuel cells [4]. A shortcoming of the fluorinated membranes especially related to their application in DMFC is their high methanol permeability, which drastically reduces DMFC performance [5]. Therefore developing alternatives have become an active area of research.

In the last decades, numerous types of arylene main chain polymers have been developed. Many of these polymers have also been sulfonated in order to obtain the proton conducting membranes. Among these polymers, SPEEK [119, 120, 124, 178, 179] possesses many of the required properties (such as good thermal stability, chemical inertness, good mechanical properties, low cost and adequate proton conductivity) as a proton conducting membrane for fuel cell applications, which makes it a promising alternative material for fuel cell applications. However, the mechanical properties of PEEK tend to deteriorate progressively with sulfonation degree (DS) [180]. The membrane swelling leads to the loss of their mechanical stability and permeability increase.

In this chapter, initially, a series of SPEEK polymers and membranes were prepared and studied. Subsequently, a series of SPEEK/ZP composite membranes were prepared and investigated; their characterizations were carried out by scanning electron microscopy, methanol permeability, water uptake and proton conductivity measurements. The investigated composite membranes were found to be suitable candidates for fuel cells. They exhibited high proton conductivity within the temperature range of fuel cell application and the methanol permeability lower than that of Nafion<sup>®</sup>.

The phosphorized zirconia nano-particles (ZP) were incorporated into SPEEK because of the following properties: (1). high proton conductivity when humidified (approaching  $10^{-2}$  S/cm) and high surface area as reported by Vaivars *et al.* <sup>[181]</sup>; (2). the decrease of the polymer methanol permeability was reported <sup>[182]</sup>; (3). simple synthesis procedure and; (4) low price.



## 3.2. EXPERIMENTAL

### 3.2.1. Materials

Dimethylacetamide (DMAc) 99 %, poly(etheretherketone) (PEEK) were supplied from *Aldrich*; zirconium oxide nano-particles were purchased from *Degussa*; acetic acid (99.8 %), sulfuric acid (98 %), phosphoric acid (85 %) and methanol (99 %) were supplied by KIMIX.

### 3.2.2. Preparation of SPEEK

The basic polymer, SPEEK was prepared via a sulfonation reaction using concentrated sulfuric acid at room temperature. PEEK pellets were dried in a vacuum oven at 100 °C for overnight. 10 g of PEEK pellets were added slowly to 200 ml concentrated sulfuric acid (98 %) with vigorous magnetic stirring. After the prescribed time, the sulfonated polymer was precipitated in a large excess of ice-water. The polymer precipitate was filtered and washed several times with deionized water until the pH = 7. The filtered polymer (SPEEK) was dried under vacuum at 60 °C for one week. Degree of sulfonation of the prepared SPEEK was determined by TGA according to the method of Zaidi *et al.* <sup>[120]</sup>. The method is based on the assumption that the first degradation step between 318 - 400 °C is entirely caused by SO<sub>3</sub> release. The 5 wt.% SPEEK solutions in dimethylacetamide (DMAc) were used for membrane preparation.

### 3.2.3. Preparation of phosphorized zirconia nano-particles (ZP)

ZP was prepared by an phosphorization of ZrO<sub>2</sub> nano-particles according to the method described in <sup>[183]</sup>. A ZrO<sub>2</sub> nano-particles suspension was prepared by mixing 3 g of ZrO<sub>2</sub> nano-particles powder with 97 g of 2 M acetic acid solution. The mixture was stirred with a magnetic stirrer until a milky solution was

obtained and mixed with 8 % phosphoric acid solution (in mass relation 1 ZrO<sub>2</sub> : 2 phosphoric acid). The mixture was slowly heated up to 80 °C, then dried in a vacuum oven at 80 °C.

### 3.2.4. Membrane preparation

#### 3.2.4.1. Preparation of SPEEK membranes

Subsequently, the polymer solution was cast onto a flat glass plate to give a thin film. The cast membrane was allowed to evaporate the DMAc solvent and dried in a vacuum oven at 60 °C for 48 h, followed by 120 °C for 24 h. After the evaporation of the solvent, and cooling to room temperature, the resultant membrane was peeled off from the glass in deionized water. A series of SPEEK membranes with different DS were prepared.

#### 3.2.4.2. Preparation of SPEEK/ZP composite membrane

The SPEEK membrane with DS = 0.79 which possesses high proton conductivity and suitable water uptake was established to prepare the composite membrane.

The SPEEK solution was mixed with different amounts of ZP on magnetic stirrer and heated up to 60 °C for 2 h, then placed in an ultrasonic bath for 1 h for better dispersion. After further magnetic stirring for 1 h, the mixture was cast on a flat glass plate. The glass plate was kept in a vacuum oven at 60 °C for 48 h and at 120 °C for 24 h for solvent removal. After cooling down to room temperature, the resultant membranes were peeled off from the glass plate after immersion in deionized water for 30 minutes.

A series of composite membranes with different ratios of SPEEK/ZP were prepared. The membranes were immersed in a 1 M sulfuric acid solution at 80 °C for 24 h. The composite membranes were kept in deionized water before use. The thickness of the dried composite membranes was in the 0.09 - 0.2 mm size range (measured using micrometer).

### 3.2.5. Characterization of the polymers and membranes

#### 3.2.5.1. Fourier Transform Infrared (FTIR) study

Fourier Transform Infrared spectroscopy (FTIR) is a powerful tool used for chemical bond identification. FTIR is useful for identifying chemicals that are either organic or inorganic. Structural data of PEEK, SPEEK, ZP and SPEEK/ZP were obtained via FTIR analysis.

FTIR spectra were recorded on Perkin Elmer Paragon 1000 Fourier transform spectrometer. The powdered samples (PEEK, ZrO<sub>2</sub> and ZP) were milled with KBr. The powder was compressed into thin pellets which were used for analysis. The pellets were composed of 98 wt.% KBr and 2 wt.% of the analyzed sample. The spectra of SPEEK and SPEEK/ZP were recorded by using the dried thin films. For the thin films, the spectra were recorded using air as a background. Potassium bromide (KBr) is transparent in the infrared (IR) range, and was thus used as a background for powdered samples. FTIR spectra were recorded in a scanning range of 600 - 4000 cm<sup>-1</sup>.

#### 3.2.5.2. X-Ray Diffraction (XRD)

The chemical composition and crystalline structure of the prepared ZP and ZrO<sub>2</sub> were determined by XRD. The XRD was performed using Philips equipment. The specifications and the working parameters are given in Table 3.1.

Table 3. 1: The specifications and working parameters of XRD.

Goniometer	PW1050
Detector	PW3011
X-Ray tube	PW2233 Cu NF
Automatic divergence slit	12 mm
Anti scatter slit	4 degrees
Receiving slit	0.1 mm
The software used	Philips X'Pert software
Working angle	between 0 and 90°

#### 3.2.5.3. Transmission Electron Microscopy (TEM)

TEM pictures of the nano-particles from aged and fresh ZP nano-particle suspensions were obtained and compared.

Transmission Electron Microscopy (TEM) pictures were obtained using a Jeol electron microscope. The sample was ground into a fine powder, then suspended in methanol and placed on a carbon-coated copper grid. The grid was sealed with a polymer (5 wt.% Butyar in chloroform). For taking high resolution pictures a Hitachi H7500 TEM instrument was used, operating at 120 kV.

#### 3.2.5.4. Thermal Gravimetric Analysis (TGA)

Samples (10mg) were analyzed in a N<sub>2</sub> atmosphere by using Thermal analyzer STA 1500 (CCI-3, *Rheometric Scientific*) in a temperature range from 20 °C to 800 °C at a heating rate of 10 °C/min.

#### 3.2.5.5. Ion Exchange Capacity (IEC)

The Ion Exchange Capacity (IEC) of SPEEK and the membranes were

determined by acid-base titration using following procedure: a dry weight of ~0.5 g of the polymer or membrane in the  $\text{SO}_3\text{H}^+$  form was immersed in 20 ml of saturated NaCl solution and equilibrated for 24 h. All  $\text{H}^+$  ions of the polymer were released by the large excess of  $\text{Na}^+$  ions. The solution was then titrated with a 0.01 M NaOH solution and phenolphthalein was used as an acid-base indicator. The IEC was calculated by using following equations:

$$\text{IEC} = \frac{\text{Moles}_{\text{H}^+}}{\text{Mass}_{\text{sample}}} \cdot 1000 \text{ (mmol/g)} \quad (3.1)$$

The sulfonation degree can thus be calculated as:

$$\text{DS} = \frac{\text{molar number of SPEEK unit}}{(\text{molar number of SPEEK unit} + \text{molar number of PEEK unit})} \quad (3.2)$$

The molar number ( $N_1$ ) of the SPEEK unit in 1 g SPEEK is:

$$N_1 = 0.001 \cdot \text{IEC} \quad (3.3)$$

The molar number ( $N_2$ ) of the PEEK unit in 1g SPEEK is:

$$N_2 = \frac{(1 - 0.001 \cdot \text{IEC} \cdot M_1)}{M_2} \quad (3.4),$$

where  $M_1$ ,  $M_2$  are the molecular weights of SPEEK unit, and PEEK unit, respectively:

$$M_1 = 368 \text{ (Dalton)}$$

$$M_2 = 288 \text{ (Dalton)}$$

With these and inserting equations 3.3 and 3.4 into equation 3.2 gives:

$$\text{DS} = \frac{288 \cdot \text{IEC}}{(1000 - 80 \cdot \text{IEC})} \quad (3.5)$$

When DS = 100 %, the limit IEC of SPEEK is:

$$\text{IEC}_{\text{max}} \approx 2.72 \text{ (mmol/g)} \quad (3.6)$$

#### 3.2.5.6. Water uptake

The water uptake of the membranes was determined by measuring the weight difference between the fully hydrated membrane and the dried membrane. The membrane (1 × 5 cm) was kept in deionized water at a room temperature for one day before the measurement. The membrane was saturated with water until no further weight gain was observed. The water uptake also measured at 80 °C. The membranes were immersed in water at 80 °C for one hour before the weight determination. The liquid water from the surface of the wet membrane was quickly removed using tissue paper, and immediately weighed. Subsequently, the membranes were dried in an oven at 100 °C for 6 h and reweighed. The percentage weight gain with respect to the weight of a dried membrane was taken as a water uptake. The following formula was used:

$$\text{Water uptake} = \frac{G_w - G_d}{G_d} \times 100\% \quad (3.7),$$

where  $G_w$  is the weight of the wet membrane, and  $G_d$  is the weight of the dry membrane.

#### 3.2.5.7. Methanol permeability measurements

The membrane permeability (also termed methanol permeability) was examined by using a diaphragm diffusion cell (shown in Figure 3.1). A plastic cell containing solutions A and B in two identical compartments separated by the membrane was utilized for methanol permeability tests. Compartment A was

filled with 1 M methanol solution while compartment B was filled with deionized water. The membrane was placed between the two compartments by a screw clamp and both compartments were placed in an ultrasonic bath while measuring. The concentration of the methanol in solution B was measured as a function of a permeation time using a Hewlett Packard 5890 series II model gas chromatography. The methanol permeability  $P$  was calculated from the slope of the straight line plot of methanol concentration versus permeation time.

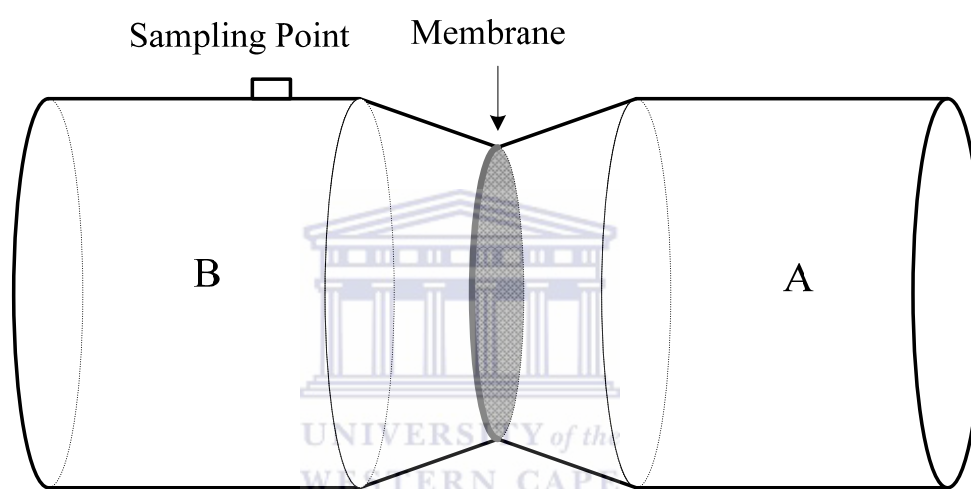


Figure 3. 1: Schematic diagram of methanol permeability measurement.

Methanol permeability was calculated according to the following equation [106, 184].

$$C_B(t) = \frac{A}{V_B} \frac{P}{L} C_A(t - t_0), \quad (3.8)$$

where  $A$ : membrane area available for diffusion;  $C_A$ : initial methanol concentration;  $C_B$ : final methanol concentration;  $L$ : membrane thickness;  $P$ : membrane crossover;  $(t - t_0)$ : permeation time;  $V_B$ : volume of the receiving compartment.

Methanol permeability was calculated using the following equation:

$$P = \frac{L}{A} \times \frac{V_B}{C_A} \times \frac{\Delta C}{\Delta t} \quad (3.9)$$

The gas chromatograph used for methanol permeability determination was a Hewlett Packard 5890 series II model. The column was used a Porapak Q with the following specifications:

Length                      6 feet

Inside diameter          2.2 mm

Outside diameter        1/8 inches

The GC parameters and settings are shown in Table 3.2.

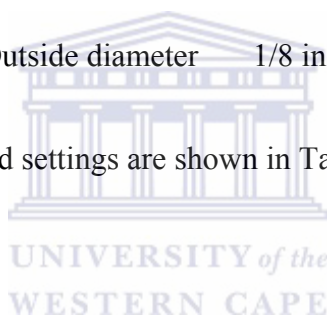


Table 3. 2: Gas chromatography (HP 5890) parameters.

GC parameters	Settings
Helium flow rate	30 ml/min
Hydrogen flow rate	25 ml/min
Air flow rate	450 ml/min
Column	80/100 Hayesep R, 1.8m x 2mm
Column temperature	175 °C
Injector temperature	150 °C
Detector temperature	250 °C
Sampling loop volume	1 $\mu$ l

#### 3.2.5.8. Scanning Electron Microscope (SEM)

The membrane surface and the cross section morphology were studied using a Hitachi x650 Scanning Electron Microscope (SEM). SEM is more powerful as compared to ordinary microscope. The combination of higher magnification, larger depth of focus, greater resolution, and ease of sample observation makes the SEM one of the basic research tools.

Specimens for the SEM were prepared by freezing the dry membrane sample in liquid nitrogen and subsequently breaking the membrane into small pieces. Thereafter, the fragment of the fractured membrane was mounted on aluminium stub and coated with a thin layer of gold by vacuum sputtering for 3 minutes in order to facilitate the proton conductivity.

The SEM operating conditions are described in Table 3.3.

Table 3. 3: The operating parameters of the Hitachi x650 SEM.

<b>SEM Parameter</b>	<b>Setting</b>
Accelerating voltage	25 kV
Aperture	0.4 mm
Tilt Angle	0°
Resolution	6 nm
Working distance	5 mm

#### 3.2.5.9. Proton conductivity measurements

The impedance of the membrane was measured in a temperature range from ambient to 100 °C by using Hioki 3560 AC milliohmmeter (HiTester). A schematic representation of the cell for proton conductivity measurements is shown on Figure 3.2.

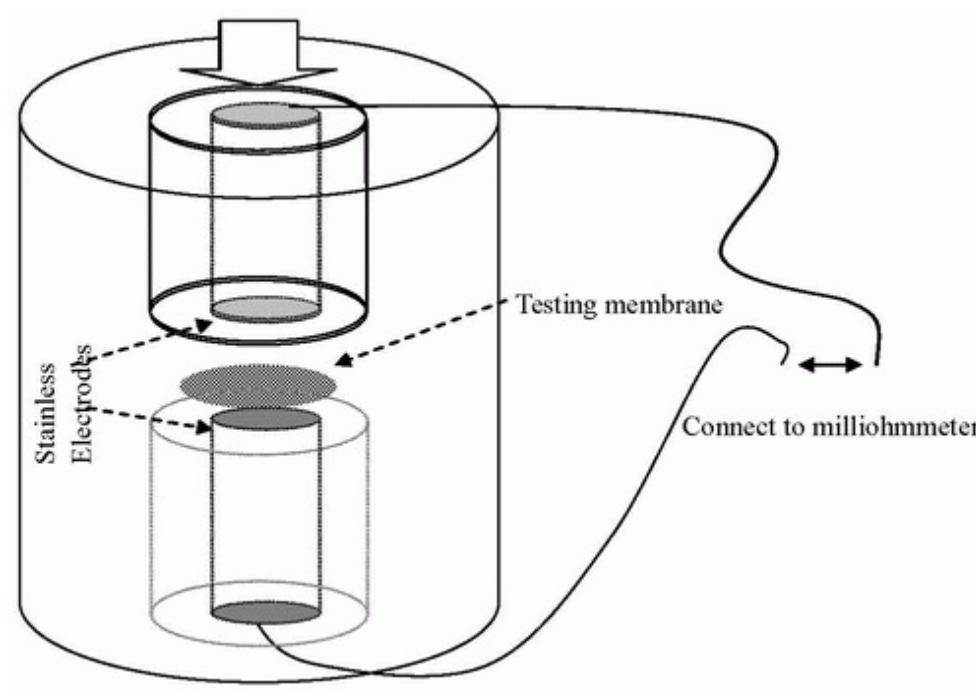


Figure 3.2. Schematic representation of the cell for measuring proton conductivity.

The membrane was pressed under a 2 kg pressure in-between two stainless steel electrodes with a contact area of  $0.28 \text{ cm}^2$ . Before the proton conductivity test, the membrane was kept in a 1 M sulfuric acid solution for 6 h at a room temperature. The membrane was then rinsed with deionized water several times to remove any excess  $\text{H}_2\text{SO}_4$  and then immersed in deionized water for 6 h at  $60^\circ\text{C}$ . All membranes were stored in deionized water at a room temperature.

The membrane proton conductivity  $\sigma$  was calculated, using the relationship:

$$\sigma = L/RS, \quad (3.10)$$

where L, R and S is the thickness, resistance and face area of the membrane, respectively.

### 3.3. RESULTS AND DISCUSSIONS

#### 3.3.1. Thermal properties and degree of sulfonation

All the sulfonated PEEK and neat PEEK powder were analyzed by TGA in order to characterize their thermal stability and determine the degree of sulfonation.

TGA analysis has been used to determine the DS of SPEEK according to the method of Zaidi *et al.* [120] which attributes the second weight loss step entirely to SO<sub>3</sub> release. The results in Table 3.4 show that the DS values obtained from TGA. The PEEK was sulfonated for different reaction times ranging from 14 to 163 h to produce SPEEK polymers with various DS. It is known that the DS of SPEEK can be controlled by changing reaction time, acid concentration and temperature [185]. In this study, the DS was controlled by changing reaction time due to simplicity to control it.

The thermal stability of the membrane is crucial for fuel cell applications. The characteristic TG curves for PEEK, SPEEK and SPEEK/ZP composite membranes are presented in Figure 3.3. PEEK is thermally stable up to 550 °C. The onset of weight loss for PEEK began at about 550 °C. This weight loss is due to the main chain decomposition, which results in the formation of phenols and benzene. Three weight loss steps are observed for SPEEK and SPEEK/ZP membranes, which are related to: 1) physically absorbed water (20 - 200 °C), 2) the splitting off of the sulfonic group (200 - 450 °C) [186], and 3) the decomposition of the main chain of PEEK (> 450 °C). The main chain decomposition temperature of SPEEK is lower than that of PEEK because of the catalytic decomposition of the polymer chain caused by SO<sub>3</sub>H. The thermal stability of the composite membrane is quite similar to that of pure SPEEK

membrane. The results suggest that these composite membranes have adequate thermal properties for application in low temperature fuel cells. At the same time, the composite membrane contains larger amount of physically absorbed water as compared to SPEEK.

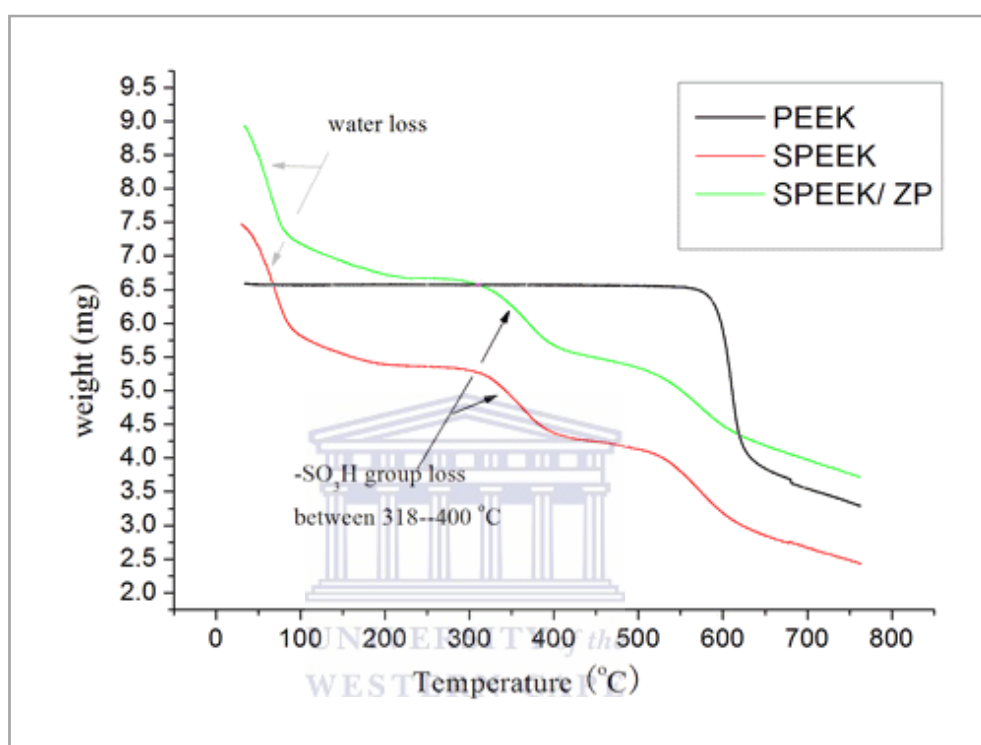


Figure 3. 3: Thermo-gravimetric curves of PEEK, SPEEK and SPEEK/ZP.

Figure 3.4 shows DS as a function of sulfonation time. The sulfonation of SPEEK proceeded rapidly first 60 h, but progressed more slow after that and did not exceed 1.

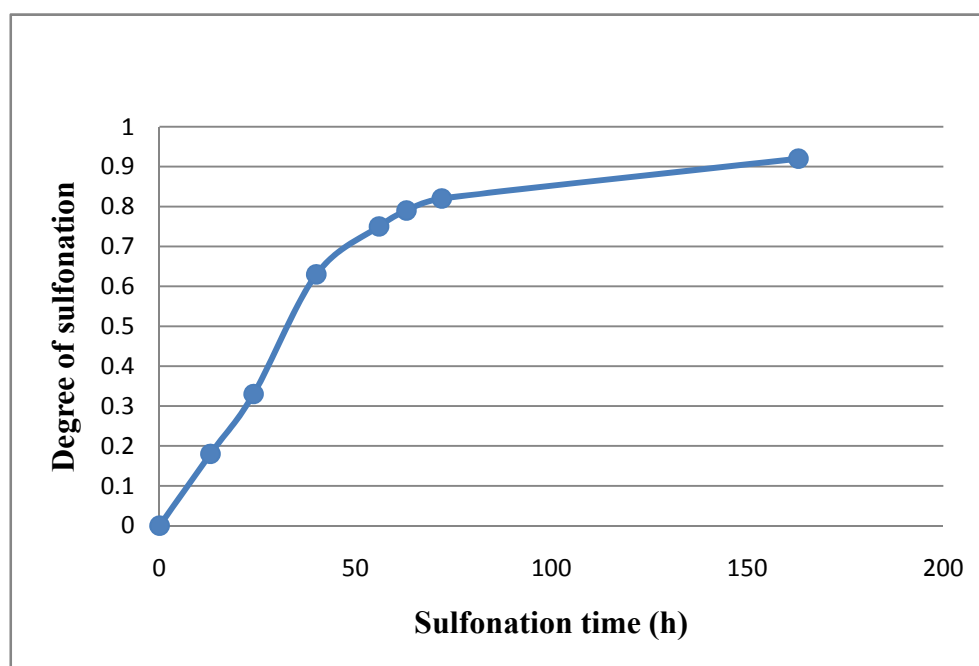


Figure 3. 4: Degree of sulfonation of SPEEK with the sulfonation time.

These results are consistent with the reports of Jin *et al.* [185] that sulfonation by using concentrated sulfuric acid at room temperature is limited to DS = 1.0. It was suggested that sulfonation occurs exclusively on the hydroquinone segment [187, 188] and the electron removal from the SO<sub>3</sub>H group once it is introduced in that ring will show deactivating effect, which is the reason for DS limiting. The other two phenyl rings connected through ether linkages are therefore deactivated for electrophilic sulfonation by the electron-withdrawing effect of the carbonyl group.

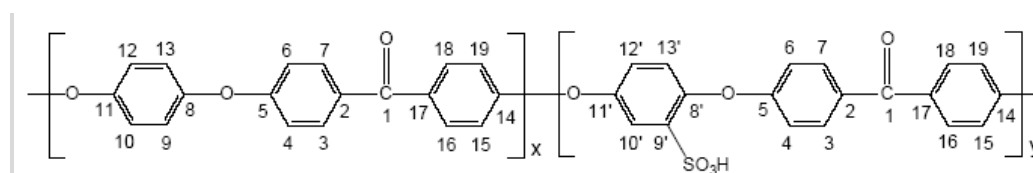


Figure 3. 5: Structure and atom numbering of SPEEK,  $x + y = n$ ,  $y/(x + y) = DS$  [189].

### 3.3.2. Ion Exchange Capacity (IEC)

The Ion Exchange Capacity (IEC) indicates the number of sulfonic groups in SPEEK polymer and prepared membrane.

Figure 3.6 shows IEC of the SPEEK and prepared membranes as function of sulfonation time. IEC of the membranes is slightly reduced compared with that of basic SPEEK polymer. It is consistent with the results published by Kaliaguine *et al.* [190].

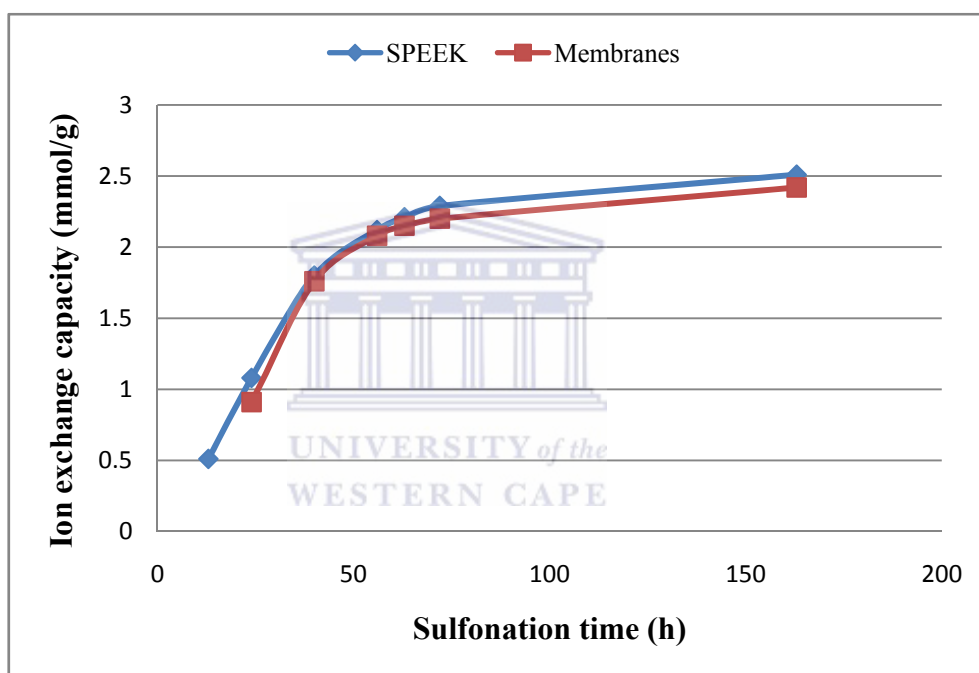


Figure 3. 6: Ion exchange capacity of SPEEK and prepared membranes.

Kaliaguine *et al.* investigated the effect of the synthesis procedure on the properties of the SPEEK membranes. They found that the casting solvent is important in providing the proton conductivity and the mechanical strength of the membrane. The usage of dimethylformamide (DMF) as a solvent resulted in the highest decrease in proton conductivity, due to the formation of strong hydrogen bound between the DMF and the sulfonic acid groups as shown in the Figure 3.7.

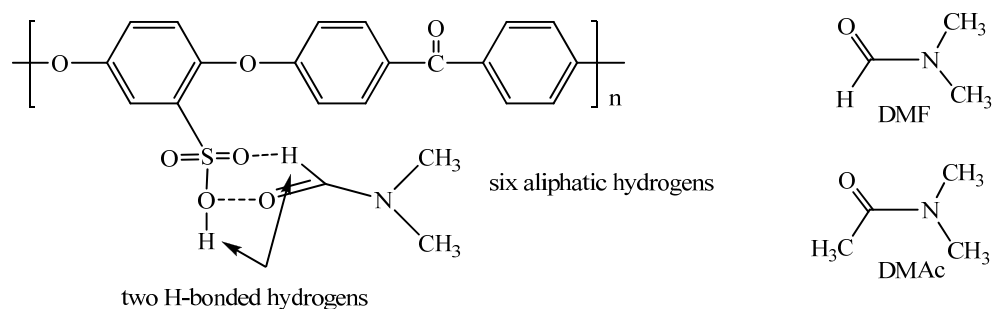


Figure 3. 7: Structures of DMF and DMAc and a possible configuration of hydrogen-bonding between SO<sub>3</sub>H groups of SPEEK and DMF molecules <sup>[190]</sup>.

DS of SPEEK can be also calculated from IEC results. The membrane characteristics are shown in Table 3.4, and both methods (TGA, IEC) gave similar results.

Table 3. 4: The SPEEK membrane characteristic parameters.

Polymer designation	DS from (TGA)	DS from (IEC)	Methanol permeability (cm <sup>2</sup> /s)	Proton conductivity at 20 °C (S/cm)	Water uptake (wt.%) at 20 °C	Water uptake (wt.%) at 80 °C	Sulfonation time (h)
SPEEK18	0.18	0.16	-----	Insoluble in DMAc	-----	-----	13
SPEEK30	0.30	0.28	4.00 × 10 <sup>-9</sup>	5.6 × 10 <sup>-3</sup>	16	20	24
SPEEK63	0.63	0.61	9.00 × 10 <sup>-8</sup>	0.9 × 10 <sup>-2</sup>	18	25	40
SPEEK75	0.75	0.72	1.50 × 10 <sup>-7</sup>	1.3 × 10 <sup>-2</sup>	20	40	56
SPEEK79	0.79	0.77	1.58 × 10 <sup>-7</sup>	1.9 × 10 <sup>-2</sup>	24	60	63
SPEEK82	0.82	0.80	1.80 × 10 <sup>-7</sup>	2.5 × 10 <sup>-2</sup>	32	95	72
SPEEK92	0.92	0.90	-----	Soluble or gel	Soluble or gel	-----	163

### 3.3.3. Fourier Transform Infrared (FTIR) spectroscopy

Fourier Transform Infrared spectroscopy (FTIR) is a powerful tool used to characterize the functional groups of the polymer. FTIR has been successfully utilized before to characterize many sulfonated polymers.

The FTIR spectra of PEEK and SPEEK samples with different DS are shown in Figure 3.8. The broadband in SPEEK samples appearing at  $3450\text{ cm}^{-1}$  was assigned to O-H vibration from sulfonic acid groups interacting with absorbed molecular water. The splitting of aromatic C-C band at  $1488\text{ cm}^{-1}$  for PEEK was observed upon sulfonation due to the new substitution. A new absorption band at  $1078\text{ cm}^{-1}$ , which appeared upon sulfonation was assigned to sulfur-oxygen symmetric vibration O=S=O. The new absorptions at  $1250$ ,  $1078$ , and  $1020\text{ cm}^{-1}$  which appeared in sulfonated samples were assigned to the sulfonic acid group in SPEEK [191].

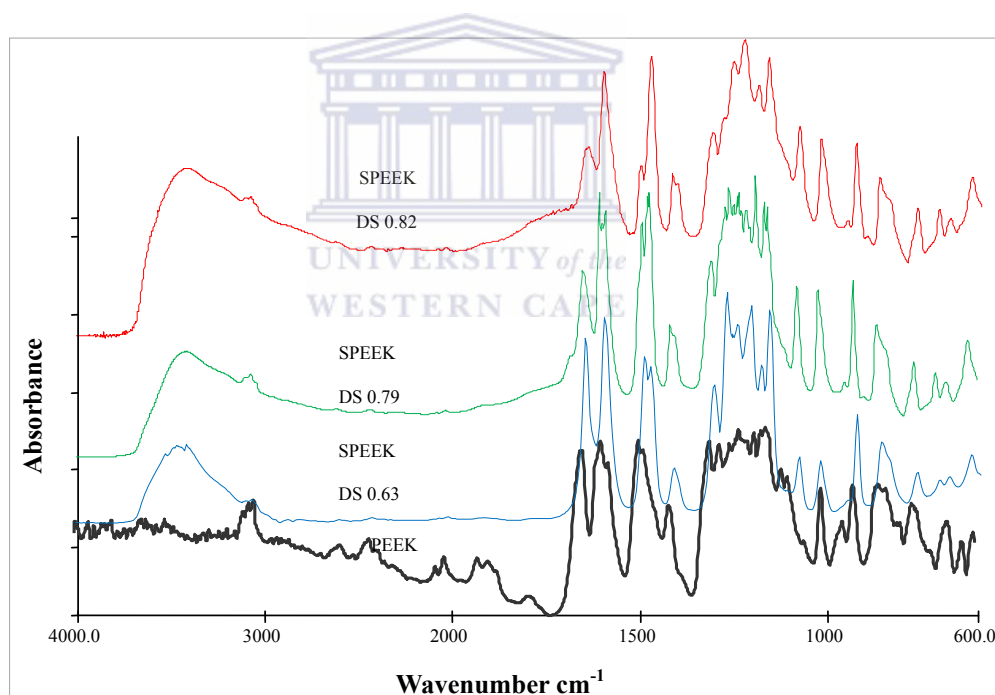


Figure 3. 8: FTIR spectra of PEEK and sulfonated PEEK with different DS values.

The absorption band of SPEEK at  $1078\text{ cm}^{-1}$  assigned to the monosubstituted benzene ring between the ether groups, which decreased with increasing DS. At the same time the intensities of the absorption bands at  $1020\text{ cm}^{-1}$  and  $710\text{ cm}^{-1}$  are attributed to a para-substituted benzene ring and the S-O stretching vibration,

which increased with increasing DS <sup>[191]</sup>, respectively. The FTIR spectral data thus indicate that sulfonation of PEEK in sulfuric acid only takes place at the para position of the terminal phenoxy group.

FTIR is useful for identifying chemicals that are either organic or inorganic. FTIR can be applied to the analysis of solids, liquids, and gases. The FTIR technique proved to be a useful tool to show the presence of zirconium phosphate in composite membranes. The infrared spectra of ZP as compared to the initial zirconium oxide are shown on Figure 3.9. After phosphorization, the new peak at ca.  $1053\text{ cm}^{-1}$  is observed, which is characteristic for the P-O stretching mode of the phosphate group <sup>[192]</sup>. The weak band at  $1650\text{ cm}^{-1}$  results from the P=O vibration.

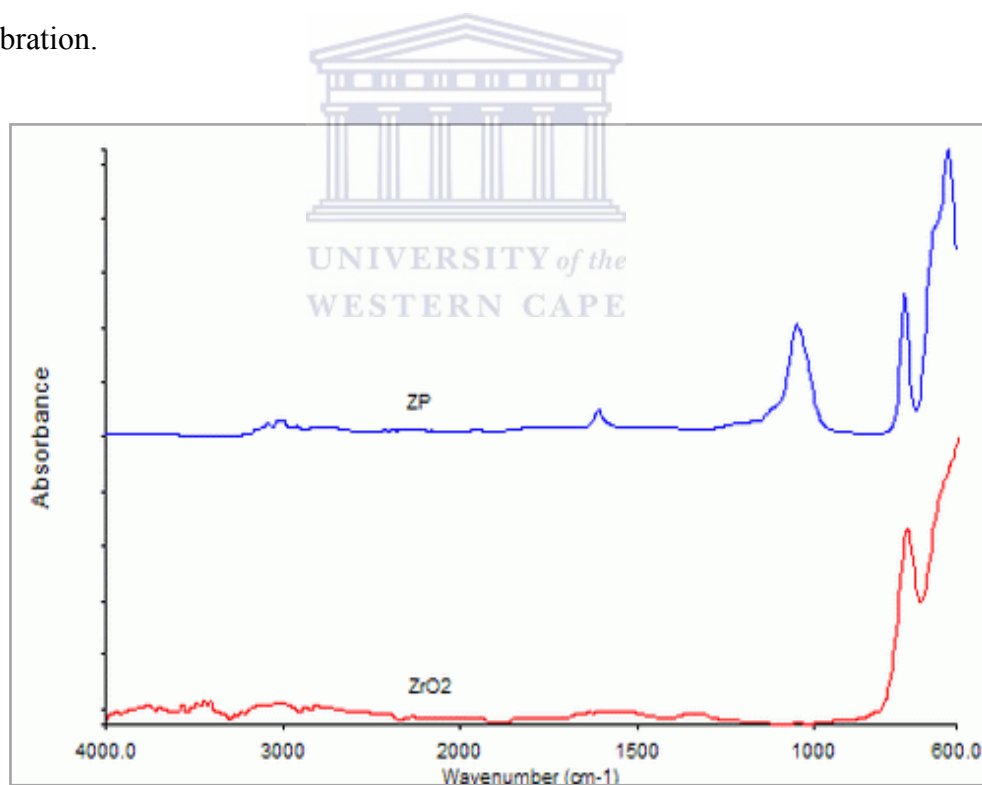


Figure 3. 9: FTIR spectra of ZrO<sub>2</sub> and ZP.

### 3.3.4. X- Ray Diffraction (XRD)

The X-Ray Diffraction pattern of ZrO<sub>2</sub> and ZP are shown in Figure 3.10. The

XRD analysis of  $\text{ZrO}_2$  revealed the presence of both monoclinic and tetragonal structures. The Bragg angles ( $2\theta$ ) of the monoclinic structure appears at  $24.4^\circ$ ,  $28.2^\circ$ ,  $31.5^\circ$ ,  $34.5^\circ$  and  $62.3^\circ$ , whereas the angles for the tetragonal structure are  $30.2^\circ$ ,  $50.2^\circ$ ,  $50.7^\circ$ ,  $59.3^\circ$  and  $60.2^\circ$  [193]. The XRD analysis of ZP is almost the same as that of  $\text{ZrO}_2$ . This shows that crystalline zirconium phosphate does not exist in the ZP sample. It means that the bulk structure of the nano-sized  $\text{ZrO}_2$  did not change after phosphorization by phosphoric acid solution. However, FTIR analysis of phosphated  $\text{ZrO}_2$  shows the presence of zirconium phosphate in phosphated  $\text{ZrO}_2$ . Combining the results of XRD and FTIR, it was suggested that the bulk structure of  $\text{ZrO}_2$  was not changed and that phosphorization only takes place on the surface of the nano-sized  $\text{ZrO}_2$ . The absence of the characteristic powder diffraction peaks of ZP is due to its amorphous nature and also due to the formation of a thin layer of ZP on the surface of the nano-sized  $\text{ZrO}_2$ .

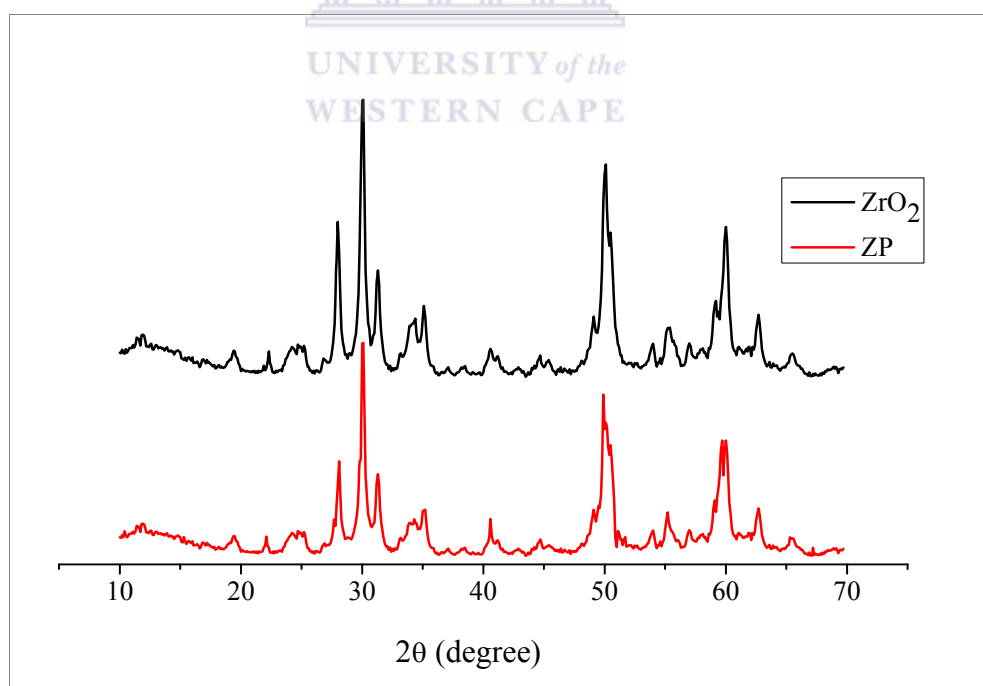


Figure 3. 10: XRD patterns of nano-sized  $\text{ZrO}_2$  and ZP.

### 3.3.5. Transmission Electron Microscopy (TEM)

TEM of nano-sized  $\text{ZrO}_2$  and ZP are presented in Figure 3.11 and Figure 3.12, respectively. The TEM image shows the uniform dispersion and lack of agglomeration of the  $\text{ZrO}_2$  nano-particles. The typical particle size for the  $\text{ZrO}_2$  nano-particles are in range from 10 to 20 nm.



Figure 3. 11: TEM image of ZP nano-particles.

Figure 3.12 shows that the size of nano-particles after phosphorization is in the range 40 – 60 nm (see also high-resolution TEM picture in Figure 3.13).

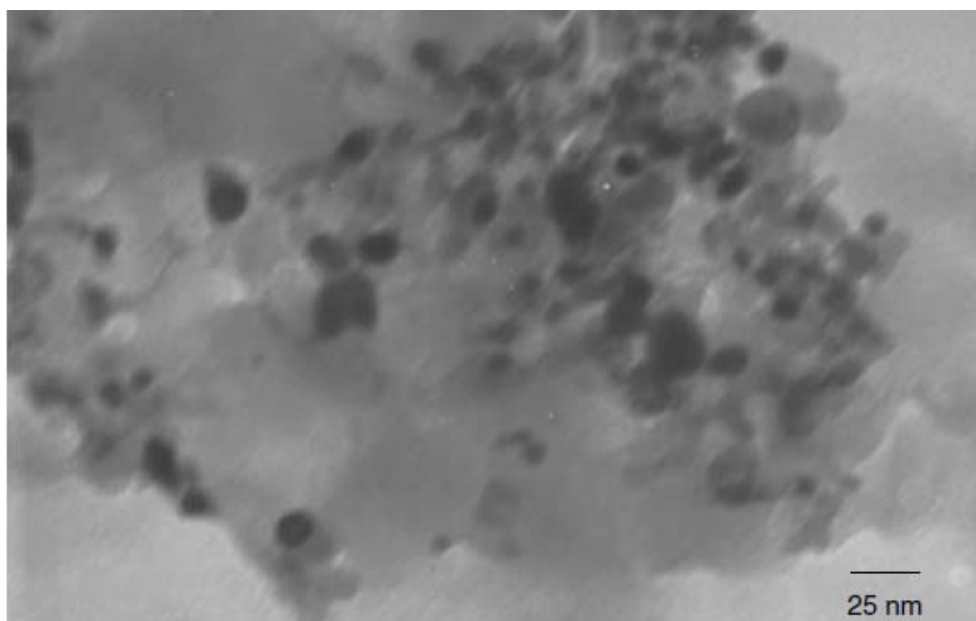


Figure 3. 12: TEM image of ZrO<sub>2</sub> nano-particles.

Figure 3.13 shows the high resolution TEM picture of the phosphorised ZrO<sub>2</sub> nano-particles. The high resolution image confirms that the typical particle size is about 40 nm. The phosphorization thus leads to an increase in the particle size, but the particles maintain the structure of the fine powder. These results are in agreement to those obtained for the XRD analysis, where the ZP peak is not presented. However, the FTIR spectrum confirms the presence of the ZP due to the presence of the ZP peak.

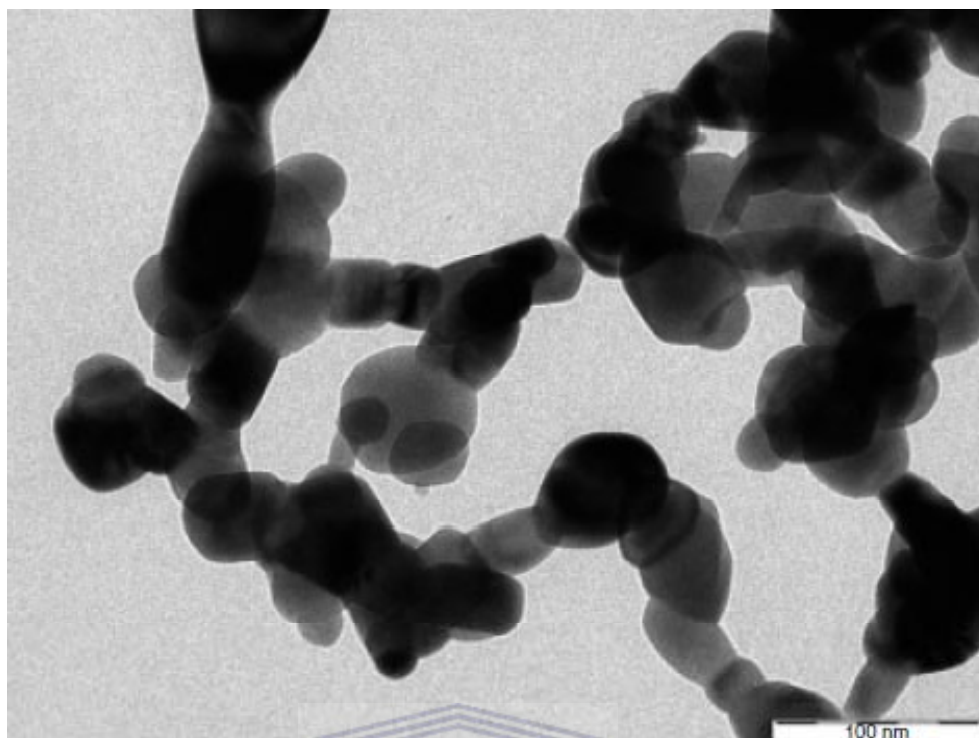


Figure 3. 13: High resolution TEM of ZP nano-particle powder.

### 3.3.6. Water uptake of the membranes

The water uptake of the SPEEK membrane as a function of DS at room temperature and at 80 °C is presented in Figure 3.14. It can be seen that water uptake is enhanced with increasing DS and temperature.

The main purpose of sulfonating PEEK is to enhance acidity and hydrophilicity, as it is known that the presence of water facilitates proton transfer and increases the proton conductivity of solid electrolytes.

It has been reported that the proton conductivity of SPEEK depends on DS, pre-treatment of the membrane, hydration state, temperature and ambient relative humidity<sup>[119]</sup>. The proton conductivity of the membranes depends on the number of available acid groups and their dissociation capability in water, which is

accompanied by the generation of protons. For this reason, the water uptake is an important parameter in studying proton exchange membranes.

Excessively high levels of water uptake can result in membrane dimensional change leading to mechanical disintegration and, in extreme cases, solubility in water at elevated temperatures, so it is important to know the relationship between DS and water uptake for the membranes.

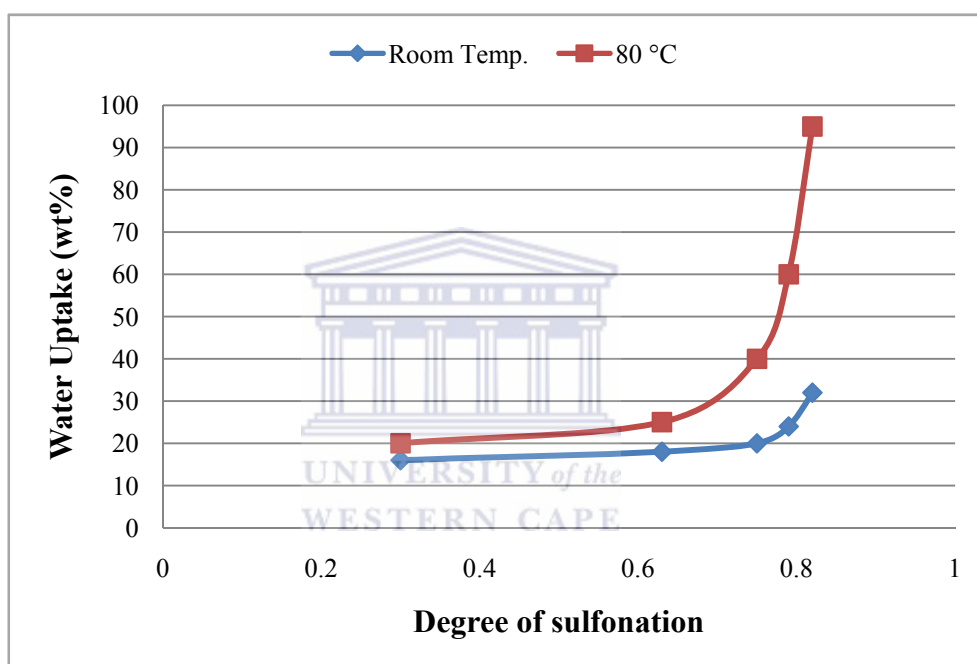


Figure 3. 14: Water uptake as a function of DS at room temperature and at 80 °C.

The water uptake of the composite membranes was determined at a room temperature (20 °C) and at 80 °C (Figure 3.15). The incorporated ZP particles are decreasing the water uptake in both cases. It is believed that the water uptake of the membranes is increased due to the membrane swelling and resulting pore expansion, which is caused by interaction with a solvent. The swelling depends on the temperature and the effect is more clearly observed at higher temperatures.

The incorporated ZP nano-particles are closing pores and by forming hydrogen bonding network strengthen the structure and therefore prevent the swelling.

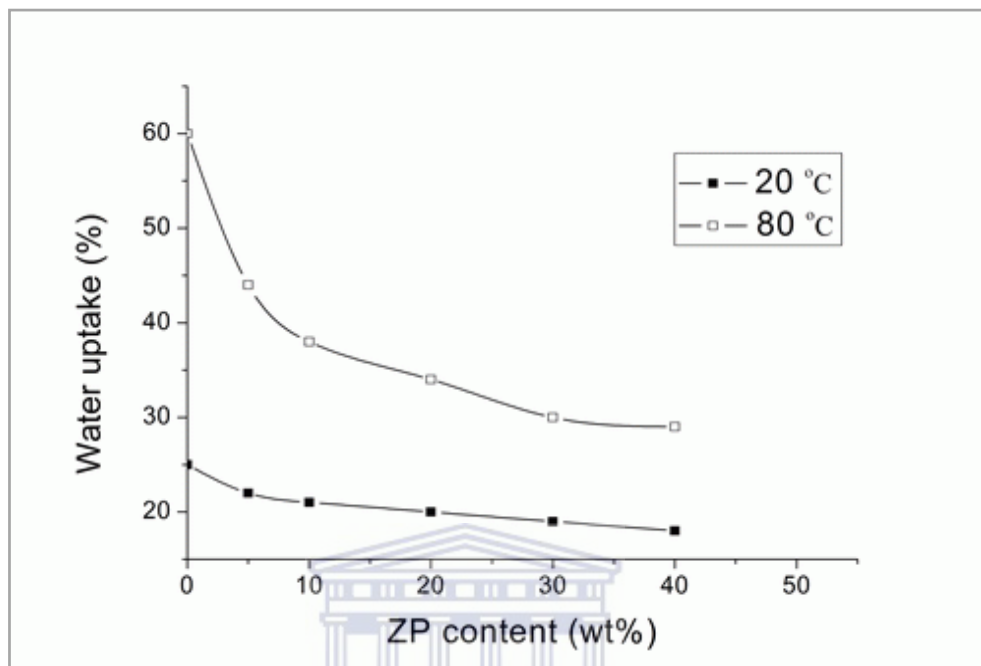


Figure 3. 15: The water uptake for membranes with different ZP content at different temperatures.

### 3.3.7. Solubility of SPEEK

Sulfonation modifies the chemical properties of PEEK, which reduces the crystallinity and affects the solubility of the polymer. It was observed that the SPEEK with DS = 0.18 is soluble only in concentrated H<sub>2</sub>SO<sub>4</sub>. After reaching the DS = 0.3 the SPEEK polymer became soluble in hot DMAc. For samples with DS = 0.63, 0.75 or 0.82, the SPEEK polymer was soluble in the DMAc solvent at room temperature, but insoluble in water. The polymer with DS  $\geq$  0.82 is soluble in hot water. The very high DS leads to a particularly hydrophilic macromolecule that was readily soluble in cold water.

Besides water, SPEEK is also soluble in DMAc, DMF, DMSO, NMP. At the

same time, it is insoluble in chlorohydrocarbons and in hydrocarbon solvents.

### 3.3.8. Proton conductivity of the membrane

The proton conductivity of the polymer membranes was measured in a fully hydrated condition at room temperature. The effect of DS on the proton conductivity of SPEEK membranes at room temperature is shown in Figure 3.16. It shows that proton conductivity increases with the degree of sulfonation of the SPEEK.

The proton conductivity was found to increase with DS and reached a value of  $2.5 \times 10^{-2}$  S/cm at DS = 0.82. This is explained by the SPEEK membrane becoming more hydrophilic and absorbing more water (see Figure 3.16), which facilitates proton transport. Therefore, sulfonation raises the proton conductivity of the PEEK not only by increasing the number of protonated sites ( $\text{SO}_3\text{H}$ ), but also through formation of water mediated pathways for protons.

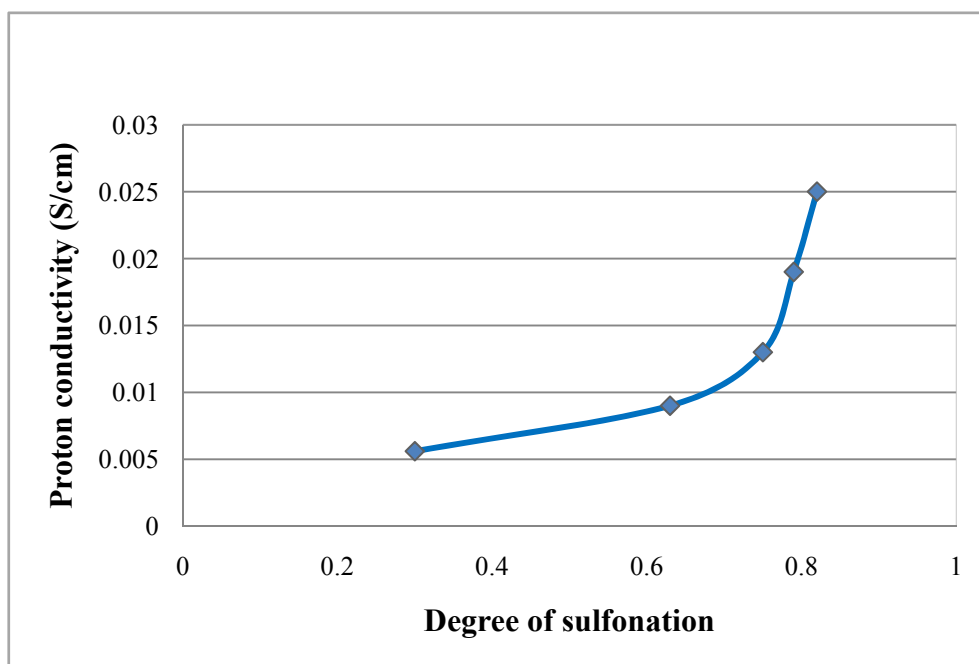


Figure 3. 16: Proton conductivity of the membranes with different DS.

The proton conductivity at DS = 0.82 is the highest measured among these SPEEK membrane in this study, but, the water uptake value is also extremely high at 80 °C. As excessively high levels of water uptake can result in membrane dimensional change leading to failures in mechanical properties, it is considered an unsuitable membrane. Table 3.5 shows that SPEEK membranes with DS close to 1.0 could be dissolved when immersed in water at room temperature. The SPEEK membrane with DS = 0.79 which possesses high proton conductivity and suitable water uptake was chosen for further study.

The proton conductivity of the composite membrane with various ZP content was measured in a temperature range from room temperature up to 100 °C. The temperature dependence of the proton conductivity at different ZP content is presented in Figure 3.17. It shows stable increase of the proton conductivity for composite membranes, which characterizes good water retention. The addition of the ZP is enhancing the polymer proton conductivity. At the same time, the SPEEK membrane lost rapidly the proton conductivity at temperatures approaching 100 °C due to dehydration. The proton conductivity of the SPEEK/ZP composite membrane with ZP content 40 wt.% is equal to 0.045 S/cm at 100 °C.

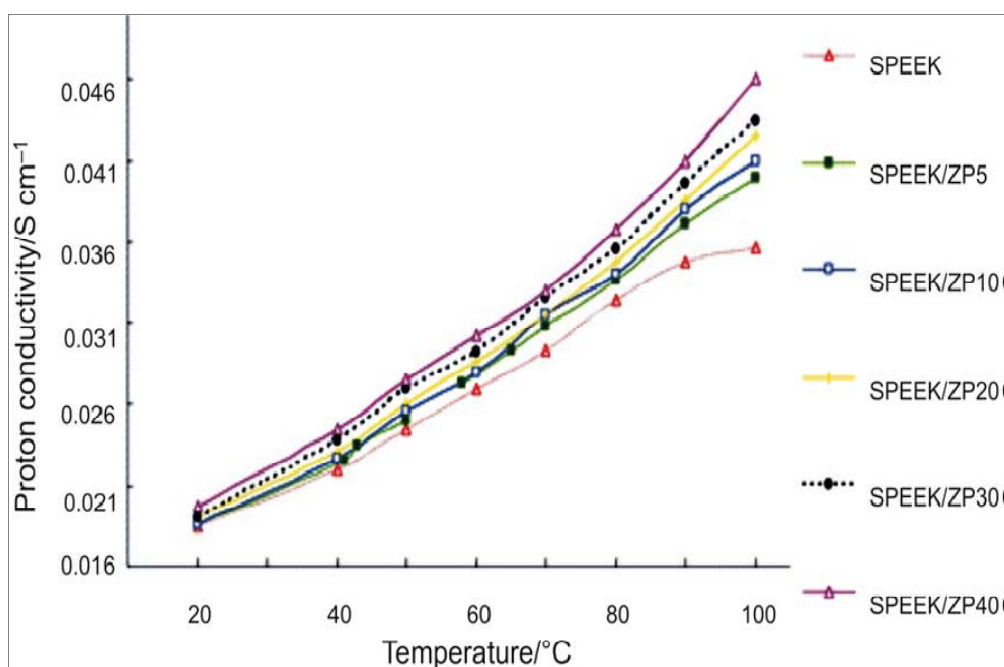


Figure 3. 17: The proton conductivity of SPEEK/ZP membranes as a function of temperature.

The increase of the proton conductivity for composite membrane with increasing the ZP content at a room temperature and 80 °C is demonstrated at Figure 3.18. As it was discussed previously, the water uptake for composite membranes decreases and the proton conductivity increases with the ZP incorporation. The proton conductivity is also stable at higher temperatures. It is the evidence that the proton conductivity is characteristic for composite material and it is not caused by the porosity of material. The incorporated ZP nano-particles enhanced the proton conductivity and decreased the material porosity on nano-scale. While ZP increases the proton conductivity, the optimized ZP content could reduce the water uptake and the methanol permeability.

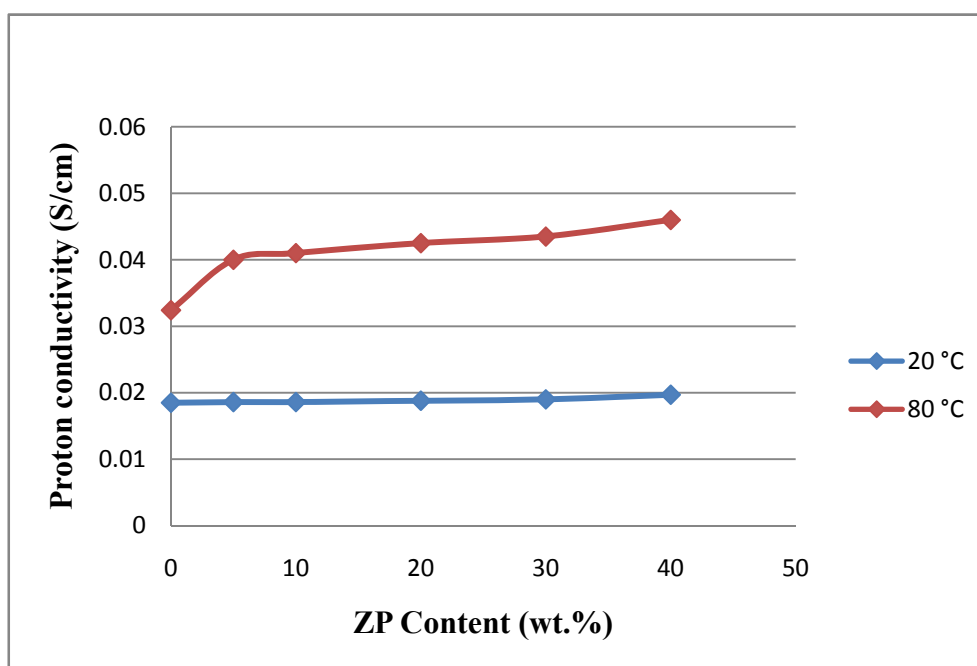


Figure 3. 18: Effect of ZP content on proton conductivity at 80 °C and room temperature.

### 3.3.9. Methanol permeability (Methanol crossover)

The methanol permeability of the composite membrane as a function of the ZP content is shown on Figure 3.19.

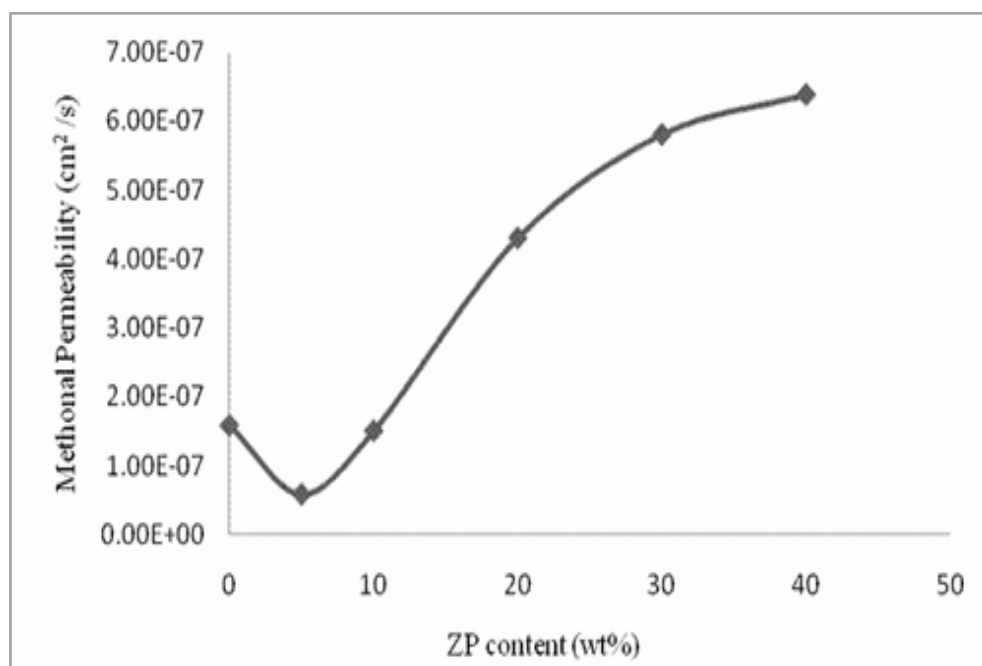


Figure 3. 19: Effect of the incorporated ZP content on methanol permeability.

The methanol permeability of the pure SPEEK as measured in a 1 M methanol solution is equal  $1.58 \times 10^{-7} \text{ cm}^2/\text{s}$ , which means that it is much lower than that of the Nafion<sup>®</sup> ( $1.39 \times 10^{-6} \text{ cm}^2/\text{s}$ ) under the same conditions. At higher methanol concentrations, the SPEEK swelling is increasing rapidly, which limits the DMFC applications. The composite membrane containing 5 wt.% of the ZP exhibited a 28 % reduction of methanol permeability ( $1.13 \times 10^{-7} \text{ cm}^2/\text{s}$ ) as compared to the pure SPEEK membrane. This value ( $1.13 \times 10^{-7} \text{ cm}^2/\text{s}$ ) is 12 times lower than that of the Nafion<sup>®</sup> 117 ( $1.39 \times 10^{-6} \text{ cm}^2/\text{s}$ ) as measured at a room temperature. However, the methanol permeability compared with that of the SPEEK membrane is increasing at ZP content higher as 5 wt.%. The decrease of the methanol permeability is believed to derive mainly from the enhanced barrier properties of the membranes due to the incorporation of the nano-sized ZP particles as the filler. The incorporated nano-sized inorganic particles block the channels to methanol passing as it was confirmed previously by water uptake results. The minimum of

the methanol permeability is observed at the ZP content equal to about 5 wt.%. At higher ZP content the mechanical stability of the membrane is decreasing and the methanol permeability is increasing. It is likely to be caused by the weaker bonding between the polymer and ZP particles and the interface is formed, which could serve also as a channel for methanol transport. For future work it is important to establish better bonding between the inorganic filler and a polymer. It will allow to keep the ZP content high, which is important factor to facilitate the decrease of the methanol permeability.

### 3.3.10. Morphology studies by SEM

The quality of the ZP dispersion in the SPEEK/ZP composite membrane was examined with SEM. Typical SEM micrographs for SPEEK and SPEEK based composite membranes are presented in Figure 3.20. The surface pictures show a dense structure without macropores (Figure 3.20, a, c). However, the cross-section of the SPEEK membrane (Figure 3.20, b) is demonstrating a developed pore structure. The cross-section of the SPEEK/5 wt.% ZP composite membrane shows much denser structure (Figure 3.20, d) and the nano-sized pore distribution. The nano-sized ZP particles are uniformly distributed within the composite membrane without agglomeration as it was confirmed by phosphorus content analysis. The presence of the 3.1 % of phosphorus for incorporated ZP particles was confirmed by using Energy Dispersive X-Ray (EDX) analysis from SEM.

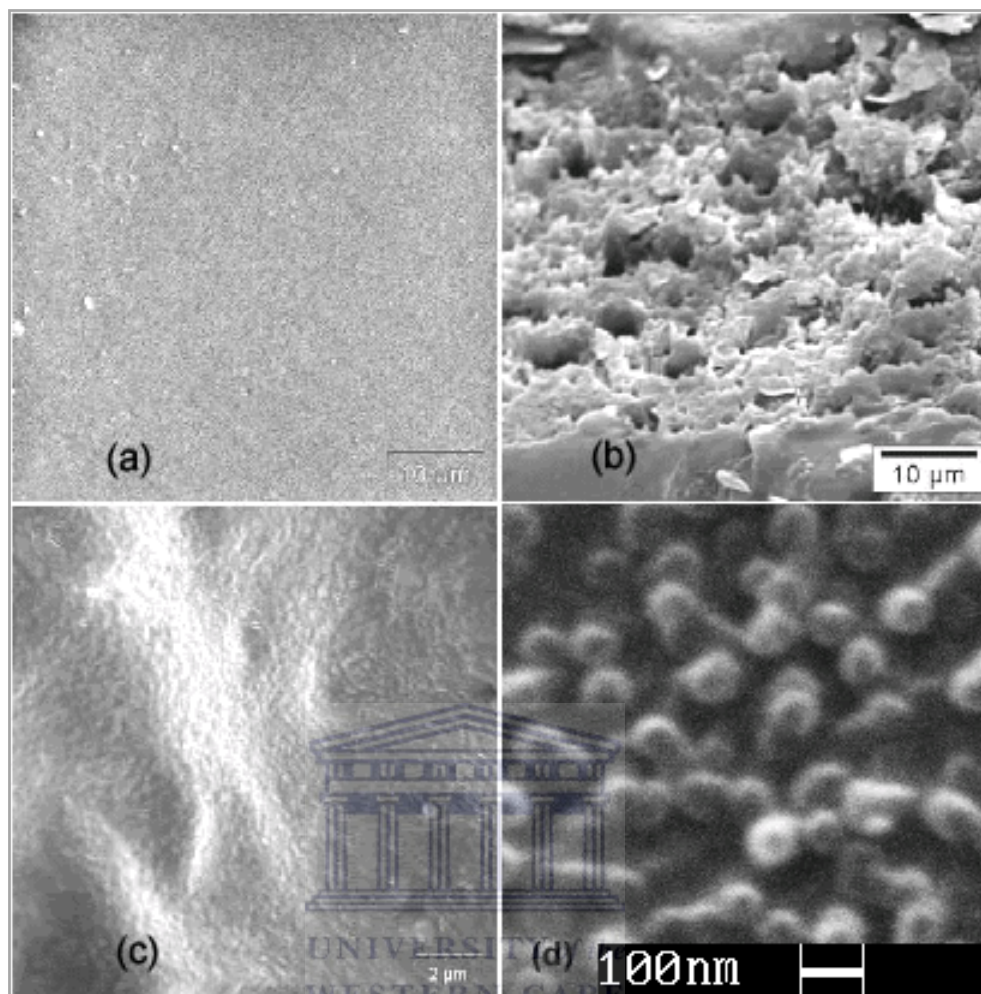


Figure 3. 20: SEM micrographs of SPEEK and SPEEK/ZP composite membrane:

- (a) Surface of the SPEEK membrane;
- (b) Cross section of the SPEEK membrane;
- (c) Surface of the composite membrane with 5 wt.% of ZP;
- (d) Cross section of the composite membrane with 5 wt.% of ZP.

### 3.4. CONCLUSIONS

DS of SPEEK increases with increasing sulfonation time. The water uptake of the SPEEK membrane increased with increasing DS and temperature, except that SPEEK membrane with DS close to 1.0, because it is soluble in water. The proton conductivities at room temperature were measured and found to increase with increasing DS and temperatures.

For the purpose of improving the properties of SPEEK membranes, especially increasing proton conductivity and reducing the extremely high water uptake, SPEEK with DS = 0.79 is established as the best material for the composite membranes.

A series of composite membranes were prepared and studied. The composite membranes were prepared by incorporating varying content of ZP into SPEEK with DS = 0.79. The proton conductivity of the SPEEK/ZP composite membranes was increased with the incorporation of increased ZP content. The high water uptake at high temperature was reduced by incorporated ZP. The methanol permeability of SPEEK/ZP with low incorporated content ZP was reduced by 28 % as compared to the SPEEK membrane. The composite membranes show a very good capability of maintaining proton conductivity at 100 °C.

Following advantages are promising for DMFC and other applications: Ease of preparation; Reasonable proton conductivity; Increased proton conductivity as compared to that of SPEEK membranes; Reduction of the high water uptake value at higher temperature; Methanol permeability was reduced by 28 % for composite membrane with 5 wt.% of ZP; Good thermal stability and mechanical properties; The membranes are substantially cheaper than the fluorinated membranes; Good stability demonstrated in maintaining proton conductivity at high temperature.

## CHAPTER 4: PREPARATION AND CHARACTERIZATION OF CROSS-LINKED PEEK MEMBRANES

### 4.1. INTRODUCTION

In the last decades, some sulfonated fluorinated and partially fluorinated ionomers were developed, however, the cost of those polymers is high due to the complex process of production.

Sulfonated polymers (as PEK, PEEK, etc.) have been studied as an alternative to Nafion<sup>®</sup> due to their many advantages, for example, good mechanical properties, high thermal stability and proton conductivity.

The proton conductivity of the sulfonated poly(etheretherketone) (SPEEK) membrane increases with increasing degree of sulfonation (DS). However, the polymers become more swollen (the SPEEK with DS close to 1 is water soluble even at room temperature) and therefore mechanically weak. This is the drawback, and it is limiting for fuel cell applications as far the sulfonated polymer membrane with high proton conductivity is concerned.

The mechanical weakness of non-cross-linked sulfonated polymers initiated several attempts to prepare more stable and mechanically stronger cross-linked proton exchange membranes. Thus cross-linked polymers and directly synthesized polymers have been developed. The cross-linked sulfonated PEEK (SPEEK) membranes were found to be much less susceptible to swelling than non-cross-linked SPEEK. However, these membranes also have got many disadvantages, like unstable in a practical environment, such as acidic environment and at increased temperatures. Besides that, the synthesis of known cross-linked SPEEK membranes is comparatively complex process, and requires using expensive materials.

In this section, the cross-linked PEEK membranes were prepared using an original and simple method. After cross-linking the water soluble SsPEEK polymer, the prepared cross-linked membranes became insoluble even in organic solvent; cross-linked membranes are stable, mechanically strong and highly proton conductive.



## 4.2. EXPERIMENTAL

### 4.2.1. Chemicals and Materials

The chemical materials used in this section are listed in Table 4.1.

Table 4. 1: List of the used chemicals and materials.

Chemicals and Materials	Specifications	Supplier
Poly(oxy-1,4-phenyleneoxy-1,4-phenylenecarbonyl-1,4-phenylene) (PEEK)	Typical $M_n$ 10,300; Typical $M_w$ 20,800	ALDRICH
Carbon cloth		ETEK
Catalyst	30 % Pt on Vulcan	ALFA
	XC-72	AESAR
	40 % Pt on Vulcan	ALFA
	XC-72	AESAR
Chlorosulfonic acid	98 %	ALDRICH
Diiodomethane	99 %	ALDRICH
Dimethylacetamide (DMAc)	99 %	ALDRICH
Dimethylformamide (DMF)	99 %	ALDRICH
Hydrogen Peroxide	30 % in water	KIMIX
1-Methyl-2-pyrrolidinone (NMP)	99 %	ALDRICH
Methanol	99 %	KIMIX
Sodium hypochlorite solution	4 % available chlorine	ALDRICH
Sodium sulfite	98 %	ALDRICH
Sulfuric acid	98 %	KIMIX

#### 4.2.2. Modification of PEEK

Initially, Sulfonated and Chlorosulfonated PEEK (SCPEEK) was prepared using the concentrated chlorosulfonic acid.

PEEK pellets were dried in a vacuum oven at 100 °C for 24 h. Thereafter, 10 g of PEEK was dissolved in 100 ml of the chlorosulfonic acid in a round bottom flask under vigorous magnetic stirring, and cooled in an ice bath. After the prescribed time, the resulting polymer was recovered by precipitating the acid polymer solution into a large excess of ice-water under mechanical agitation. The polymer precipitate was washed with deionized water to remove the excess of acids until pH = 7 after 1 week. The polymer was dried under vacuum in an oven for one week at 60 °C.

A series of SCPEEK were prepared by varying reaction times. The substitution of SO<sub>3</sub>H and SO<sub>2</sub>Cl was determined by titration.

10 g SCPEEK with IEC = 3.25 mmol/g reduced by mixing with 100 ml of 1 M Na<sub>2</sub>SO<sub>3</sub> solution in a three-neck flask under stirring at 80 °C. After complete reducing, the polymer was washed with deionized water, and dialyzed for removing residual Na<sub>2</sub>SO<sub>3</sub>. The reduced polymer SsPEEK was filtered and dried at 60 °C in a vacuum oven.

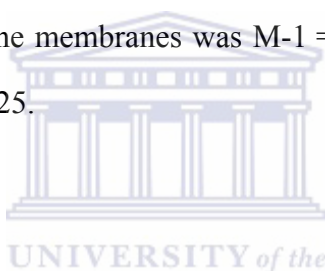
#### 4.2.3. Preparation of cross-linked PEEK membranes

Different cross-linked PEEK membranes were prepared by reacting SsPEEK with various amount of the cross-linker.

Initially, 15 wt.% polymer solution was prepared by dissolving SsPEEK in NMP.

Then, the diiodomethane was added to the SsPEEK polymer solution with sturdy stirring. The solution was cast onto the glass Petri dish. Then the solvent was removed in an oven, keeping at 130 °C under vacuum for 1 day. The membrane was peeled off from the surface of Petri dish and immersed in a 10 % NaOH solution at 90 °C for 1 day and then in 10 % H<sub>2</sub>SO<sub>4</sub> solution at 90 °C for 1 day, and finally in water for 1 day at 90 °C.

A series of cross-linked PEEK membranes were prepared with increasing addition of amount of the cross-linkers. Assuming that SsPEEK cross-linked completely with the added cross-linkers, the molar ratio of the cross-linker to SsPEEK also indicates the cross-linking degree of the membranes. The cross-linking degree of the membranes was M-1 = 0.05, M-2 = 0.10, M-3 = 0.15, M-4 = 0.20 and M-5 = 0.25.



#### 4.2.4. Characterization of the polymer and membranes

##### 4.2.4.1. Fourier Transform Infrared (FTIR)

FTIR spectra of PEEK, SPEEK, SCPEEK, SsPEEK and one of the membranes were recorded on PerkinElmer Spectrum™ 100 FTIR spectrometer equipped with the universal ATR optional accessory.

FTIR spectra were recorded in a scanning range of 400 - 4000 cm<sup>-1</sup>.

##### 4.2.4.2. Viscosity measurement

The SCPEEK are well soluble in DMAc and polymers can be characterized by viscosimetry. The viscosities of the SCPEEK were measured in DMAc with 0.2 g/l concentration of by using a Stabinger Viscometer SVM 3000 at 25 °C.

The intrinsic viscosity was taken as the arithmetical mean of reduced and inherent viscosities extrapolated to zero concentration.

#### 4.2.4.3. Ion Exchange Capacity (IEC)

The Ion Exchange Capacity (IEC) of the SCPEEK polymer and the membranes were determined by acid-base titration as the following procedure: a dry weight of 0.5 g of the polymer or membrane in the  $\text{SO}_3\text{H}^+$  form was immersed in 20 ml of saturated NaCl solution and equilibrated for 24 h. All  $\text{H}^+$  ions of the polymer were exchanged by using large excess of  $\text{Na}^+$  ions. The solution was then titrated with a 0.01 M NaOH solution and phenolphthalein was used as an acid-base indicator. The IEC was calculated by the following equations:

$$\text{IEC} = \frac{\text{Moles}_{\text{H}^+}}{\text{Mass}_{\text{sample}}} \cdot 1000 \text{ (mmol/g)} \quad (4.1)$$

#### 4.2.4.4. Determination of chloride by the Mohr method

Initially, 0.5 g of dried SCPEEK was dissolved in 20 ml of DMF in a 250 ml flask. Then 20 ml of 5 %  $\text{H}_2\text{O}_2$  solution was added, and stirred at 80 °C for 24 h.

Small quantities of  $\text{NaHCO}_3$  were added until effervescence ceased. About 2 ml of  $\text{K}_2\text{CrO}_4$  (5 %) was added and the solution was titrated with 0.1 M  $\text{AgNO}_3$  solution to the appearance of red  $\text{Ag}_2\text{Cr}_2\text{O}_4$ .

The substitution of  $\text{SO}_2\text{Cl}$  (SC) was calculated by the following equations:

$$\text{SC} = \frac{\text{Moles}_{\text{Cl}^-}}{\text{Mass}_{\text{sample}}} \cdot 1000 \text{ (mmol/g)} \quad (4.2)$$

#### 4.2.4.5. Redox titration for determination of the sulfinat

The sulfinat group content in SsPEEK was determined by redox back titration.

The redox back titration of the SsPEEK was performed as the following. 1 g SsPEEK polymer was stirred in 100 ml deionized H<sub>2</sub>O. After 2 h stirring, 5 g NaOCl (4 % active Cl) was added into the solution, the solution was heated at 40 °C for 3 h. After cooling to the room temperature, 2 g KI was added to the solution. After the oxidation, 10 ml acetic acid (HAc) was added. The solution became black, which indicated the release of free I<sub>2</sub> by NaOCl reaction with KI. Then the solution was titrated potentiometrically with 0.1 M Na<sub>2</sub>S<sub>2</sub>O<sub>3</sub> solution to determine the amount of free, unreacted NaOCl.

#### 4.2.4.6. Proton conductivity measurement

The experimental method was utilised the same as in Chapter 3.

#### 4.2.4.7. Water uptake

The experimental method was utilised the same as in Chapter 3.

#### 4.2.4.8. Methanol permeability (methanol crossover) measurements

In this Chapter, the methanol permeability of membrane was determined by using an electrochemical method<sup>[194]</sup>.

Measurements were carried out in a two-compartment plastic cell with the membrane separating the two compartments, an AUTOLAB (PGSTAT 30) electrochemical analysis system was used. The platinum mesh and platinum electrodes were used as the working and counter electrodes. The 0.5 M H<sub>2</sub>SO<sub>4</sub> was used as electrolyte. An Ag/AgCl reference electrode was used in all experiments. Cyclic Voltammograms (CV) were recorded to study the methanol permeability of the membrane. The methanol permeability was studied by introducing methanol of a known concentration in 0.5 M H<sub>2</sub>SO<sub>4</sub> on one side (side A) of the cell and

analyzing the concentration at other side (side B) for its methanol permeability determination. Chronoamperometric studies were carried out to study the methanol permeability of methanol quantitatively. The initial voltage and the potential step were -0.250 V and 0.500 mV vs. the Ag/AgCl reference electrode, respectively. The equilibrium point or the point at which the methanol concentration is the same in both compartments was found through a chronoamperometric method.

#### 4.2.4.9. Electrochemical stability by cyclic voltammetry measurement

In order to determine the electrochemical stability of the prepared membrane, the cyclic voltammetry was performed using an AUTOLAB (PGSTAT 30) electrochemical analysis system at room temperature.

The membranes were placed between a platinum counter electrode and a working platinum electrode. The reference electrode was the Ag/AgCl electrode.

The measurements were performed in both acidic and basic condition.

#### 4.2.4.10. TGA

The samples containing 10 mg of membrane material were analyzed in an argon atmosphere by using Thermal Analyzer STA 1500 (CCI-3, Rheometric Scientific) in a temperature range from 20 °C to 550 °C at a heating rate of 10 °C/min.

#### 4.2.4.11. DMFC test

##### *1. Preparation of the Membrane-Electrode Assembly (MEA) for DMFC*

Pt catalyst for the cathode and Pt-Ru for the anode supported on commercial carbon cloth was used in this study. The catalyst loading was equal to  $1.5 \text{ mg/cm}^2$  for all electrodes (anode and cathode) used in the experiments.

The catalyst ink, for both anode and cathode, was prepared by mixing the Nafion<sup>®</sup> solution in alcohol with the catalyst powders, and dispersing the powder by magnetic stirring and ultrasonic vibration in order to form the catalyst ink. The electrodes were prepared by brushing the prepared catalyst ink on carbon cloth backing layer. On each electrode, approximately  $1.5 \text{ mg/cm}^2$  of catalyst was coated. The loading was determined by weighing the dried electrode.

The Membrane Electrode Assembly (MEA) was manufactured by hot-pressing the electrode onto the membrane at  $130 \text{ }^\circ\text{C}$  and 140 bar for 2 min. The geometrical area of both electrodes was  $4 \text{ cm}^2$ . The procedure is explained on Figure 4.1 .

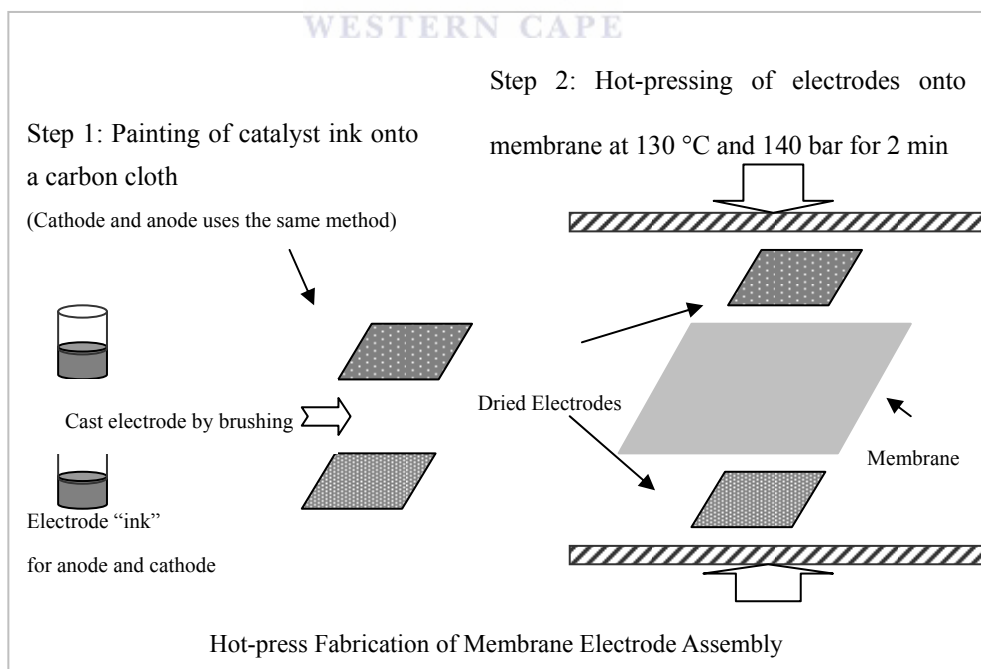


Figure 4. 1: The procedures of membrane-electrode assembly.

## 2. Assembly of Single cell and testing

The single cell was assembled by mounting the MEA into cell endplates. The endplates used were purchased from Lynntech (Figure 4.2). The flow fields for the reactants used were of serpentine configuration with three serpentine connected in parallel. The endplates are also fitted with holes to accommodate a heating cartridge and a thermocouple for the temperature controller.

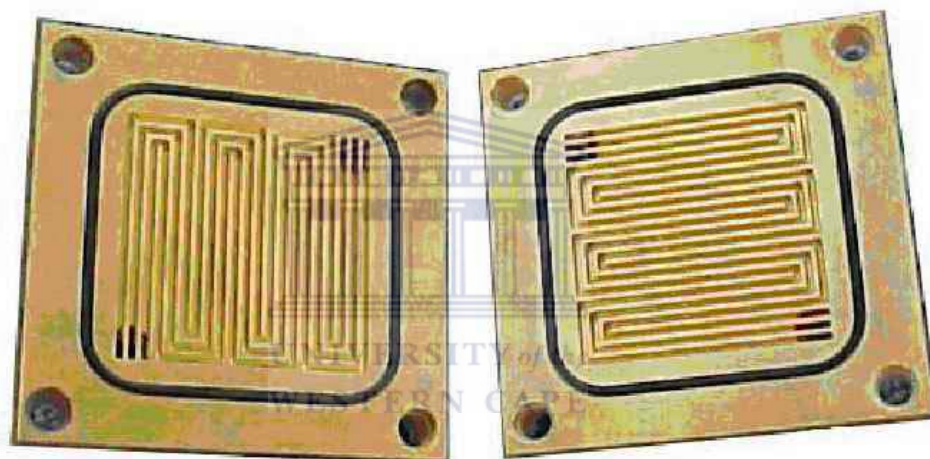


Figure 4. 2: Lynntech endplates.

The operating temperature of the cell was 70 °C. 1 M methanol solution was pumped through the DMFC anode at a flow rate of 1 ml/min, and oxygen was fed to the cathode at 0.5 l/min.

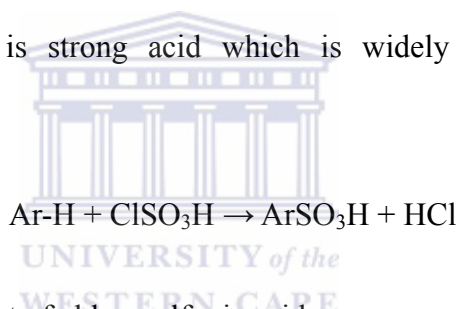
The MEA was tested on a Fuel Cell testing station. The data were collected by using an AUTOLAB (PGSTAT 30) electrochemical analysis system.

### 4.3. RESULTS AND DISCUSSION

#### 4.3.1. Modification of PEEK by chlorosulfonic acid

Sulfonation for PEEK can be performed in several ways with different sulfonating agents, such as concentrated sulfuric acid, sulfur trioxide, chlorosulfonic acid, a sulfur trioxide-triethyl phosphate complex, and trimethylsilylchlorosulfonated<sup>[119, 195, 196]</sup>. Sulfonation of PEEK in sulfuric acid is an electrophilic substitution reaction, in which the sulfonic groups are introduced into the hydroquinone segment of the polymer activated for electrophilic substitution by the ether linkage chain<sup>[189]</sup>.

Chlorosulfonic acid is a strong acid which is widely used as a powerful sulfonating agent<sup>[197]</sup>.



An equimolar amount of chlorosulfonic acid or an excess of the chlorosulfonic acid also can be used for chlorosulfonation (or chlorosulfonylation) of aromatic compounds:



In this study, chlorosulfonic acid was used in a large excess with respect to PEEK.

Under experimental conditions of this study both sulfonation and chlorosulfonation took place without degradation of material.

### 4.3.2. FTIR of investigated polymers and membranes

The comparative FTIR spectra of PEEK, SPEEK, SCPEEK, SsPEEK and one of the cross-linked membranes are shown in Figure 4.3 and Figure 4.4. The broad band at  $3450\text{ cm}^{-1}$  in SPEEK, SCPEEK, SsPEEK and a cross-linked membrane (shown in Figure 4.3) is assigned to O-H vibration from molecular water, which is adsorbed due to interacting with sulfonic acid groups.

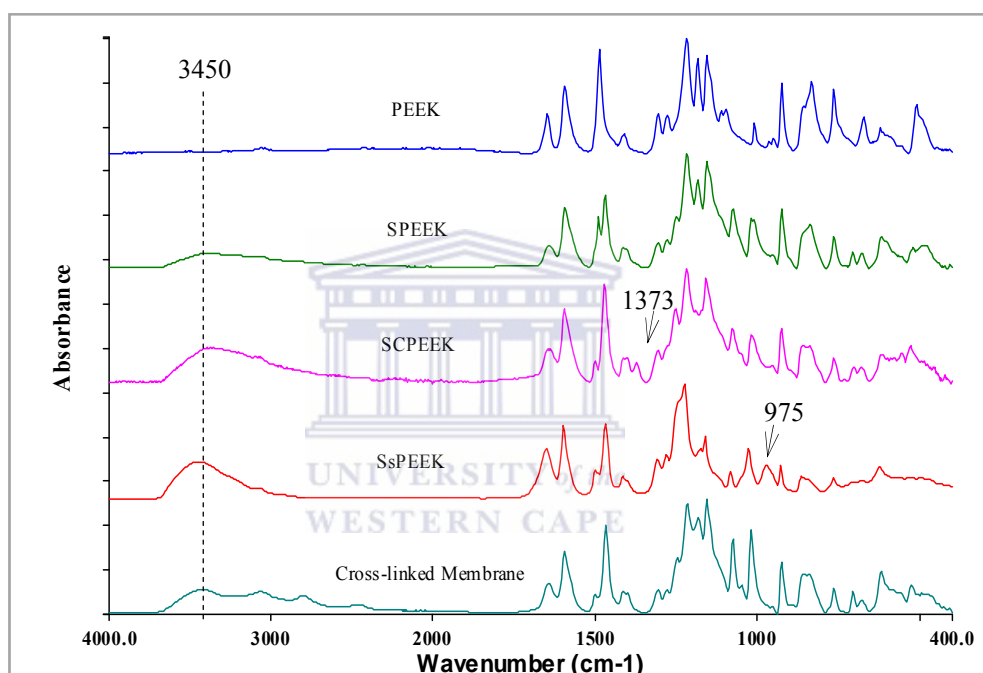


Figure 4. 3: FTIR spectra of PEEK, SPEEK, SCPEEK, SsPEEK and one of the cross-linked membranes.

Figure 4.4 is the enlarged FTIR spectra (from  $800 - 1800\text{ cm}^{-1}$ ). The aromatic C-C band at  $1488\text{ cm}^{-1}$  for PEEK was split due to new substitution. The absorption bands at  $1020$  and  $1078\text{ cm}^{-1}$  in the spectra of SPEEK and SCPEEK samples were assigned to symmetric and asymmetric stretching vibration O=S=O due to the introduction of  $\text{SO}_3\text{H}$  groups. A new absorption band, which appeared at  $1250\text{ cm}^{-1}$  in the spectra of SPEEK and SCPEEK samples, was also assigned to

the sulfonic functional group<sup>[191]</sup>. The FTIR spectra of SCPEEK is different from SPEEK and it showed characteristic band of sulfonyl group  $\text{SO}_2\text{Cl}$  at  $1373\text{ cm}^{-1}$  ( $\text{SO}_2$  asymmetric stretching vibration) in the spectra of SCPEEK<sup>[198]</sup>. The result proves that both  $\text{SO}_3\text{H}$  and  $\text{SO}_2\text{Cl}$  functional groups have been successfully introduced in PEEK polymer by using chlorosulfonic acid, but only sulfonic functional groups were introduced in PEEK by using concentrated sulfuric acid.

The S=O stretching, specifically, a symmetric stretching of the sulfinate group, is observed at  $975\text{ cm}^{-1}$  in the spectra of SsPEEK<sup>[199]</sup>. After cross-linking, the sulfinate band disappears from the spectrum of cross-linked membrane. It is explained that after the completed cross-linking reaction, the unreacted sulfinate groups have been converted to sulfonic groups by the post-treatment (hydrolysis).



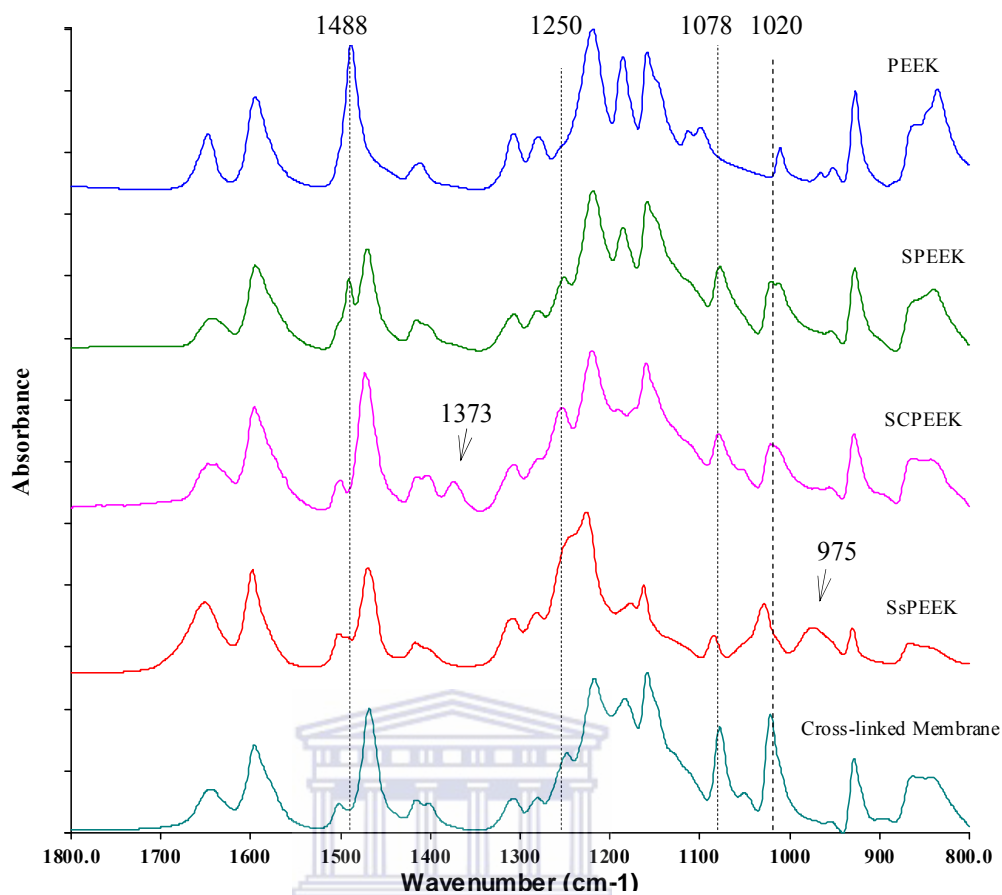


Figure 4. 4: Enlarged FTIR spectra of PEEK, SPEEK, SCPEEK, SsPEEK and one of the cross-linked membranes.

### 4.3.3. Viscosity of SCPEEK

It is difficult to measure the molecular weight of PEEK directly due to its poor solubility. Gel Permeation Chromatography (GPC) has been successfully applied to measure  $M_w$  of pure PEEK using phenol/1,2,4-trichlorobenzene 50/50 mixture at 115 °C [191].

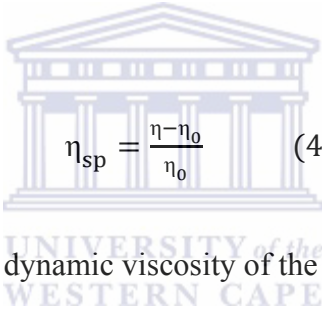
Intrinsic Viscosities provide the most significant information on the size of a polymer molecule in solution. Typically, the intrinsic viscosity provides a qualitative inference of molecular weight.

The intrinsic viscosity  $[\eta]$  is related to the molecular characteristic of a linear-chain macromolecule by the well-known Kuhn-Mark-Houwink-Sakurada relationship which is widely used in the polymer science and technology<sup>[200, 201]</sup>.

$$[\eta] = K_{\eta}M^a,$$

where  $a$  and  $K_{\eta}$  are the parameters that depend on the solvent and polymer. Once  $K$  and  $a$  are known for a combination of polymer and solvent, one may use the intrinsic viscosity to calculate the viscosity-average molar mass of a material,  $M_v$ .

It is usual to define the specific viscosity,  $\eta_{sp}$ , of a polymer solution by equation:



$$\eta_{sp} = \frac{\eta - \eta_0}{\eta_0} \quad (4.3),$$

where  $\eta$  and  $\eta_0$ , are the dynamic viscosity of the solution and solvent.

The intrinsic viscosity was taken as the arithmetical mean of reduced and inherent viscosities extrapolated to zero concentration.

For real polymer solutions, the dependence of the specific viscosity on mass concentration is often more complex than this simple theory predicts. The polymer molecule is not necessarily a sphere nor is it much larger as compared to the solvent molecule. In this case, it is discussable to use the simplification of spheric geometry. To parameterize the concentration dependence of specific viscosity, one defines the intrinsic viscosity,  $[\eta]$ , as:

$$[\eta] = \lim_{c \rightarrow 0} \frac{\eta_{sp}}{c} \quad (4.4),$$

where  $c$  is the concentration of the polymer solution. Like other parameters obtained by extrapolating to infinite dilution, the intrinsic viscosity describes the interaction of a single average polymer molecule with an infinite volume of solvent. It is assumed that  $[\eta]$  is proportional to the molecular weight.

The measured viscosity values for SCPEEK are shown in Figure 4.5. The viscosity values are not changing with increasing reaction time. So, the molecular weight was not reduced with increasing reaction time. It proves that during the PEEK modification by concentrated chlorosulfonic acid there was no degradation of polymer.

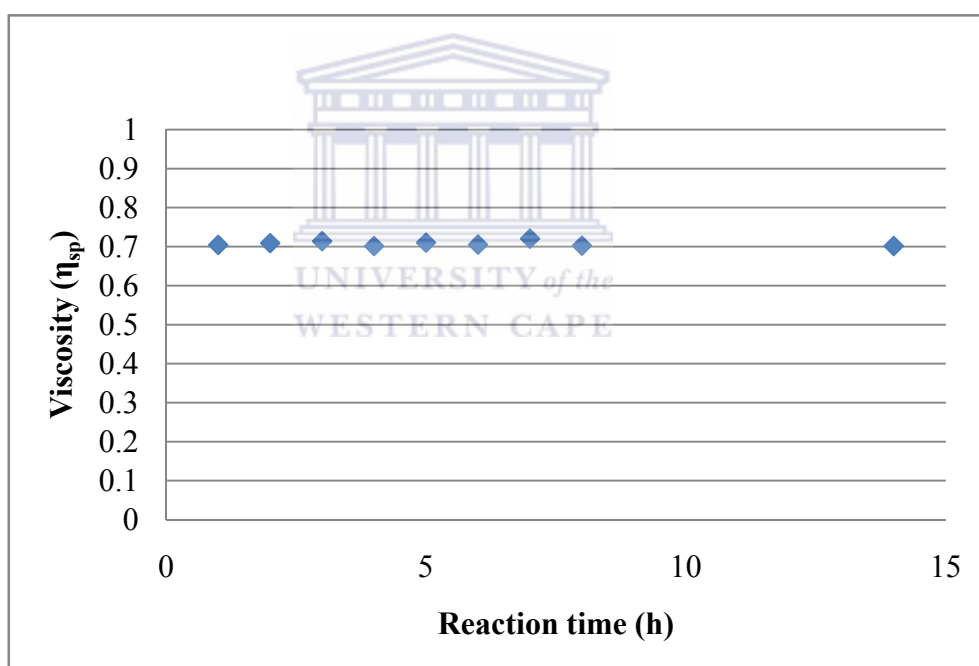


Figure 4. 5: Viscosities of SCPEEK.

#### 4.3.4. IEC of SCPEEK

The ion exchange capacity (IEC) of SCPEEK characterizes the number of

sulfonic groups which has been substituted on PEEK. Figure 4.6 shows IEC of SCPEEK as a function of reaction time. It increases rapidly with increasing reaction time first 4 h, but the increase is becoming more moderate after 4 h.

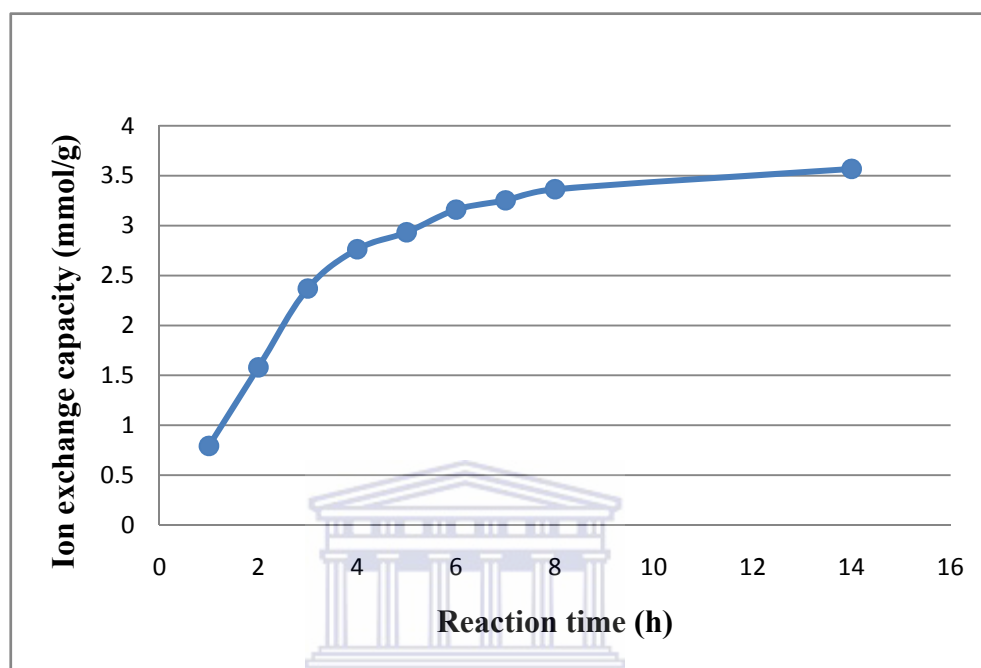


Figure 4. 6: Ion exchange capacity of SCPEEK.

Jin *et al.* investigated that sulfonation of PEEK and it was concluded that by using concentrated sulfuric acid the DS is limited to 1.0. The  $^{13}\text{C}$  NMR spectrum of sulfonated PEEK confirms that substitution is predominantly at site 1, not 2 or 3 (see Figure 4.7), that is in the phenyl ring flanked by two ethers <sup>[185]</sup>.

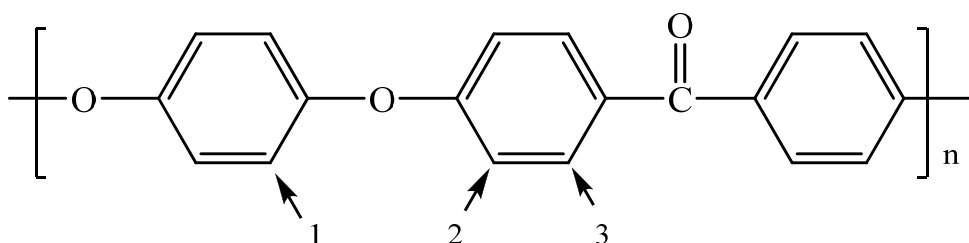


Figure 4. 7: Structure of PEEK positions marked with arrows are possible sites of substitution.

Thus, IEC of SPEEK by using concentrated sulfuric acid is also limited to 2.7 mmol/g. However, the results show that IEC of SCPEEK exceeded 2.7 mmol/g after 6 h. This is a strong evidence that sulfonation of PEEK by using concentrated chlorosulfonic acid apparently proceeds further substitution at sites 2 and 3. It is indicating that a highly proton conductive sulfonated PEEK can be prepared by using chlorosulfonic acid.

#### 4.3.5. Chlorine analysis

The FTIR results show that the SO<sub>2</sub>Cl groups are introduced in modified PEEK by using HSO<sub>3</sub>Cl. The number of substituted SO<sub>2</sub>Cl groups was determined by chloride analysis.

Subsequently, degree of chlorosulfonation (DC) was calculated by using following equation:

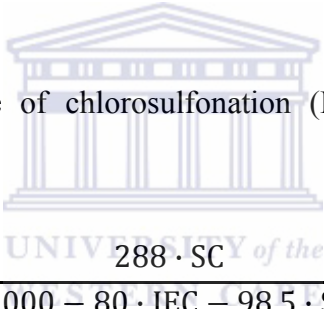

$$DC = \frac{288 \cdot SC}{(1000 - 80 \cdot IEC - 98.5 \cdot SC)} \quad (4.5)$$

Figure 4.8 shows that SC and DC quickly increases first 8 h with increasing reaction time. The results show that the chlorosulfonating reaction was rapid with increasing reaction time, but slow down after 8 h.

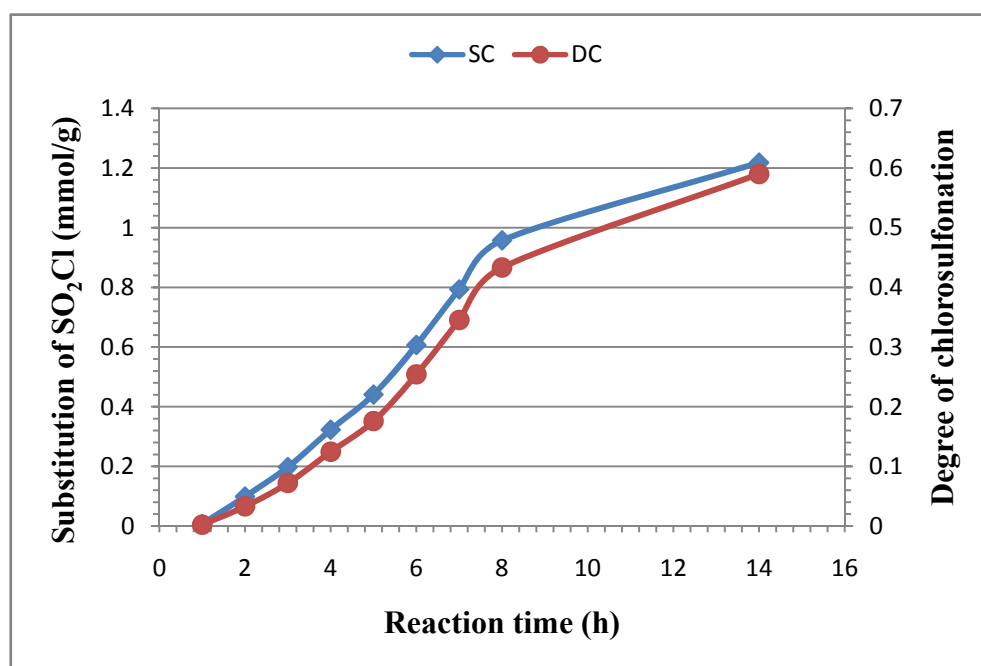


Figure 4. 8: Substitution of SO<sub>2</sub>Cl and degree of chlorosulfonation.

Energy Dispersive X-Ray (EDX) results (see Figure 4.9) also show that the content of chlorine in SCPEEK increases with increasing reaction time.

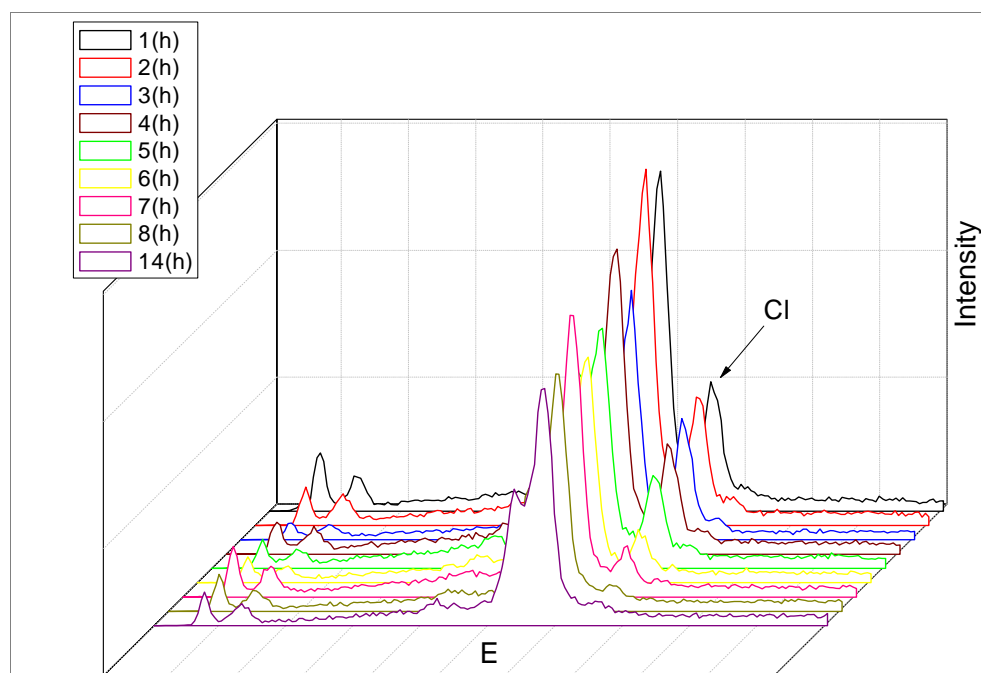


Figure 4. 9: Energy Dispersive X-ray spectroscopy of SCPEEK.

#### 4.3.6. Degree of substitution

The degree of sulfonation (DS) was calculated by the following equation:

$$DS = \frac{288 \cdot IEC}{(1000 - 80 \cdot IEC - 98.5 \cdot SC)} \quad (4.6)$$

The total substitution is the sum of  $SO_3H$  and  $SO_2Cl$ :

$$TS = IEC + SC \quad (4.7)$$

DT also can be calculated as:

$$DT = DS + DC \quad (4.8)$$

DS, DC and DT are shown in figure 4.10. They all increase with increasing reaction time.

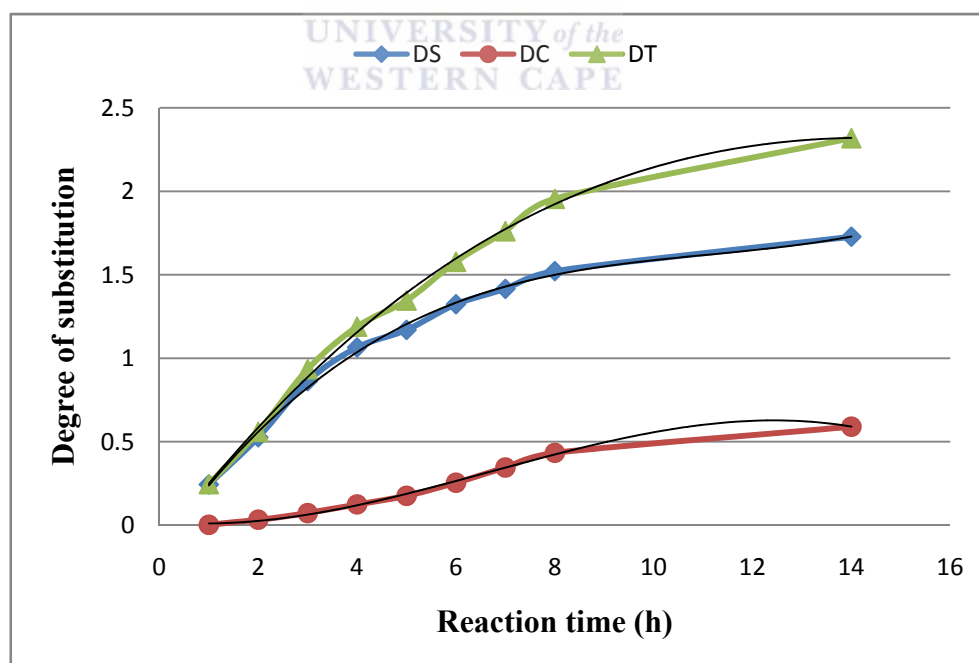


Figure 4. 10: Degree of substitutions of SCPEEK.

#### 4.3.7. Redox titration for determination of the sulfinite

One of the SCPEEKs (6 h) was converted to SsPEEK. The content of sulfinite group in SsPEEK can be calculated by the equation:

$$C_s = \frac{\text{Moles}_{\text{SO}_2^-}}{\text{Mass}_{\text{sample}}} \cdot 1000 \text{ (mmol/g)} \quad (4.9)$$

From determination of the content of sulfinite group in SsPEEK the conversion rate of  $\text{SO}_2\text{Cl}$  to  $\text{SO}_2\text{Na}$  was determined as equal to 78 %.

#### 4.3.8. IEC of the cross-linked membranes

The IEC of the cross-linked membrane characterizes the number of  $\text{SO}_3\text{H}$  in the membrane, and also indicates the ease of ion flow within the membrane. The IEC of the starting SCPEEK was 3.25 mmol/g. In principle, IEC of the cross-linked membrane might be higher than that of the noncross-linked SCPEEK. The sulfinite groups, which will not participate in cross-linking reaction, will be converted to sulfonate groups by hydrolysis during protonation. However, IEC of the membranes was slightly lower than that of expected value. The possible reasons for IEC reduction are the presence of residual solvent, metal ion, etc.

Figure 4.11 shows that the IEC of the membranes reduces with increasing cross-linking degree. It is due to reacting of sulfinite groups with the cross-linker, thus reducing the unreacted sulfinite groups for converting to  $\text{SO}_3\text{H}$ .

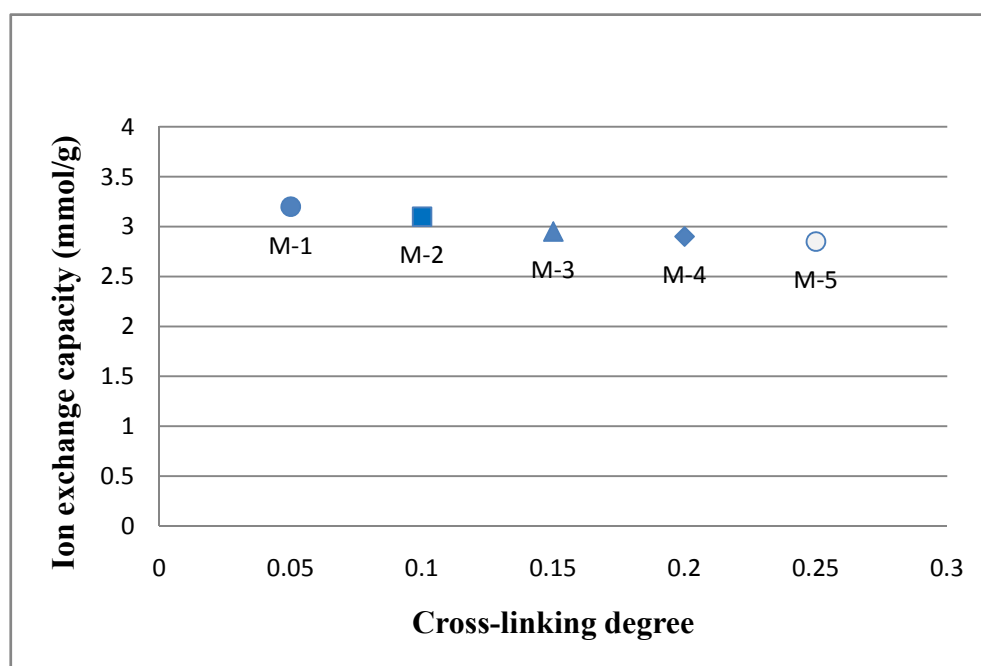


Figure 4. 11: IEC of the cross-linked membranes.

The images of the prepared membranes after drying in oven are shown in Figure 4.12. The membrane gradually became darker with increasing cross-linking degree, because amount of the released  $I_2$  was increased after cross-linking reaction.

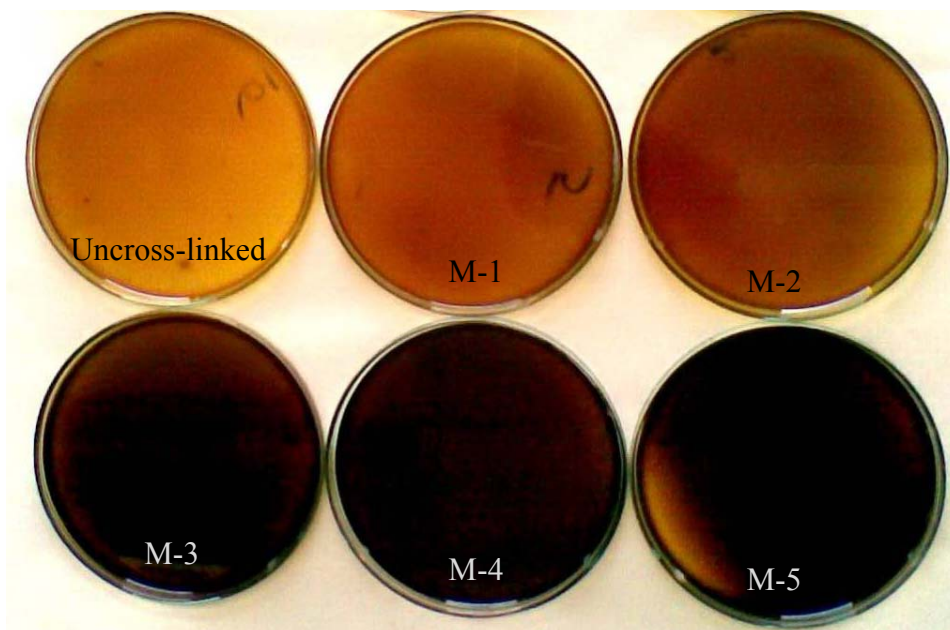


Figure 4. 12: Image of the prepared membranes.

#### 4.3.9. Water uptake of the cross-linked membranes

The water uptake is determined by the presence of hydrophilic groups ( $\text{SO}_3\text{H}$ ) in the membrane structure. Water can be found in two states – bounded and free (absorbed). There was no clear separation between these two states observed using TG analysis.

From this study it was concluded, that the membrane without cross-linking and with high content of the sulfonic group is not applicable in fuel cells due to its infinity of water uptake, which means solubility in water.

The water uptake of the cross-linked membrane is shown in Figure 4.13. It shows the water uptake of the cross-linked membranes as a function of temperature. The water uptake of all investigated membranes increases with increasing temperature in a range from room temperature to 80 °C. The water uptake of the cross-linked membrane with low cross-linking degree exhibited

strong temperature dependence. At temperatures above 45 °C, the rapid increase of the water uptake is observed. The trend of the water uptake for membranes confirmed the influence of the cross-linking on the membrane properties. The water uptake of the M-5 with a high cross-linking degree is obviously reduced, and only slightly increases with increasing temperature.

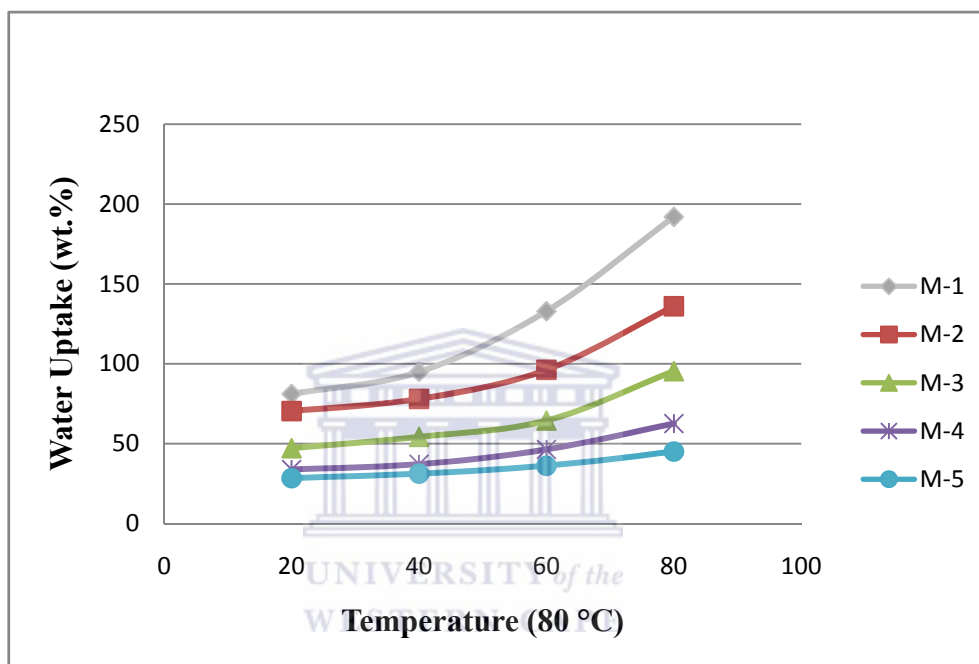


Figure 4. 13: Water uptake of the cross-linked membranes.

As it was described in Chapter 3, the water uptake of SPEEK membrane decreases with decreasing IEC. For the cross-linked membranes, their IEC are just slightly decreased with increasing cross-linking degree. However, the water uptake of the cross-linked membranes obviously decreases with increasing cross-linking degree (shown in Figure 4.14). The membrane with a low cross-linking degree will show high water uptake and low mechanical strength. At the same time, the membrane with high cross-linking degree will show low water uptake.

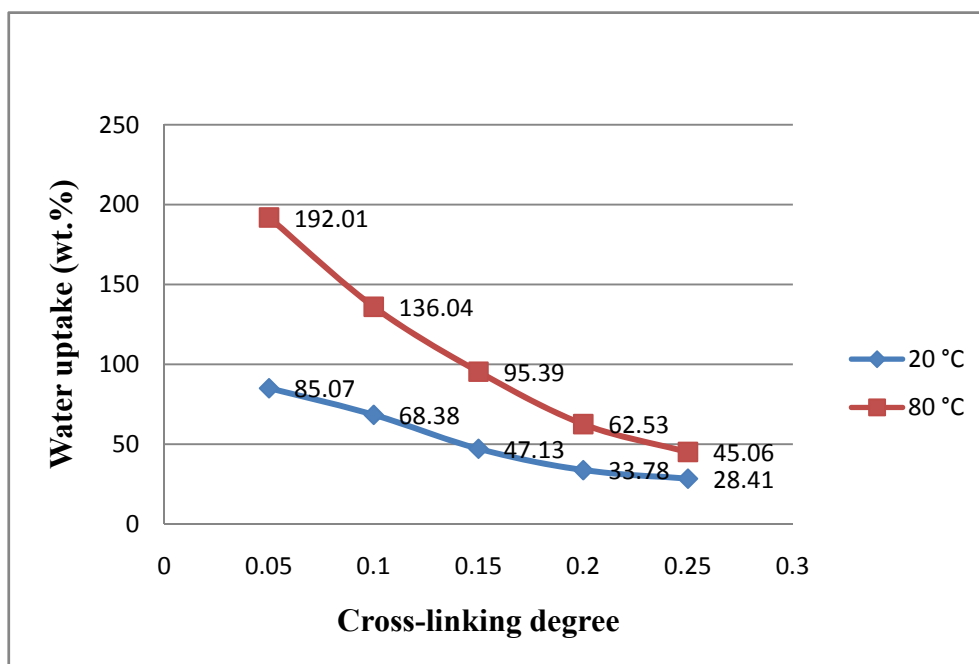


Figure 4. 14: The dependence of water uptake on cross-linking degree.

The main reason is that the increasing of the cross-linking degree is strengthening the polymer chain in membrane. The cross-linkages between polymer chains form a three-dimensional network and prevent the polymer swelling to infinity, in other words, dissolving. This is due to the elastic retraction forces of the network, and is accompanied by a decrease in entropy of the chains, as they become denser as compared to starting polymer (shown in Figure 4.15).

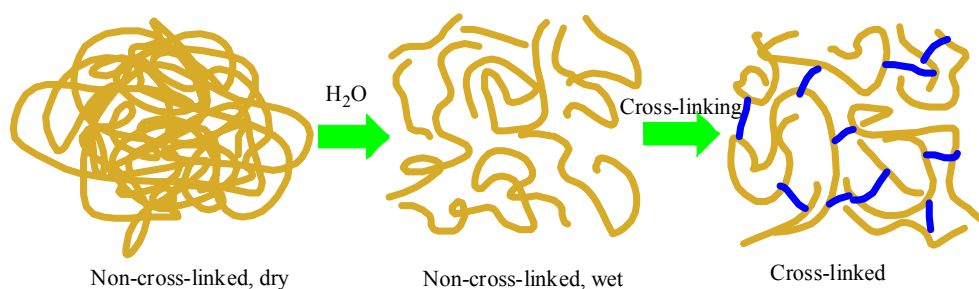


Figure 4. 15: Schematic diagram of the cross-linking membrane.

#### 4.3.10. Proton conductivity of the cross-linked membranes

The proton conductivity is one of the most important properties of the proton exchange membrane from point view of application. The proton conductivities of the cross-linked membranes were measured at temperatures ranging from 20 °C to 80 °C and the results show that the proton conductivity of the membranes as a function of temperature in Figure 4.16.

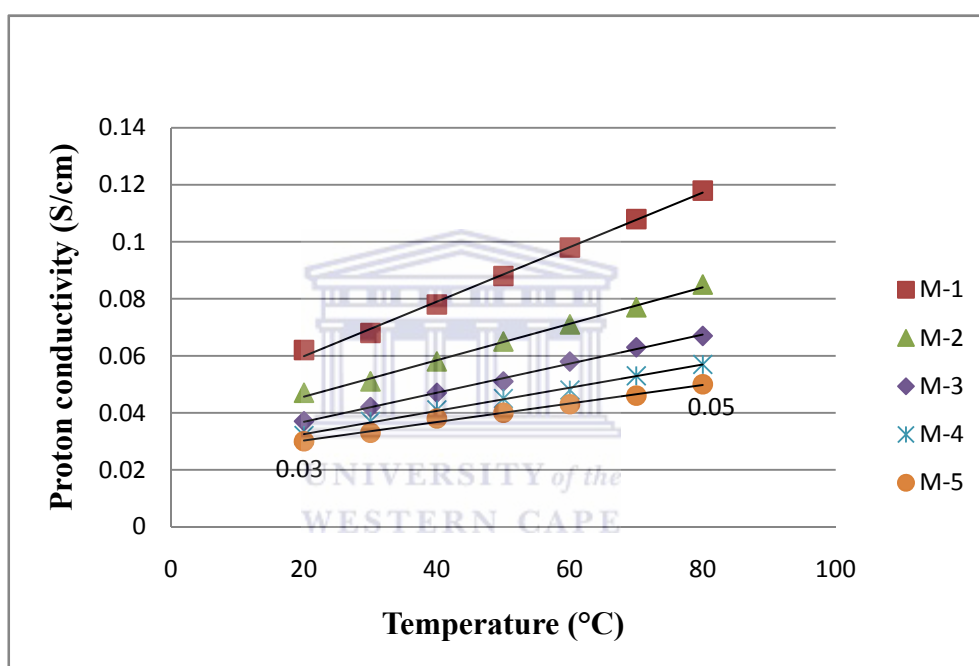


Figure 4. 16: proton conductivity of the membranes as a function of temperature.

Figure 4.17 shows the dependence of proton conductivity on cross-linking degree. It was found that the cross-linking significantly affects the proton conductivity. After cross-linking, the structure of membranes becomes more dense, which leads to the reduction of the mobility of  $H^+$  and amount of retaining structural water around sulfonic acid groups<sup>[202]</sup>. Therefore the proton conductivity is compromised. The results show that the cross-linked membrane M-1 exhibits the highest proton conductivity in all the cross-linked membrane, and the proton

conductivity of the cross-linked membranes reduces with increasing cross-linking degree both at room temperature and 80 °C.

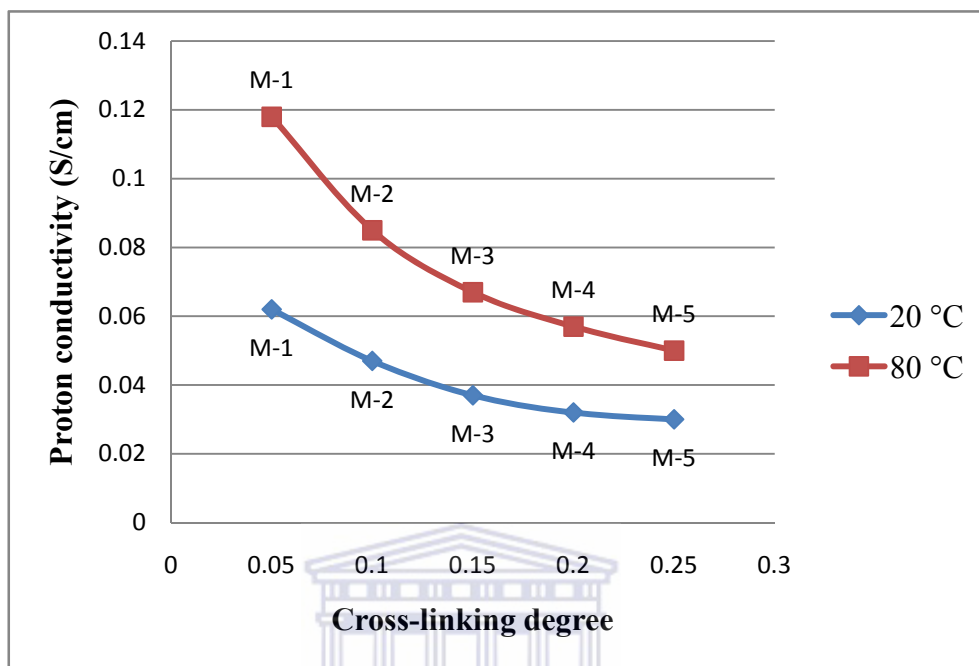


Figure 4. 17: Effect proton conductivity on cross-linking degree.

The structure of proton exchange membranes has been extensively studied by many researchers, and it is well known that the protons transfer between ionic clusters consisting of polar groups such as  $\text{SO}_3\text{H}$ . The number of ionic clusters increases<sup>[203]</sup> with increase of the number of  $\text{SO}_3\text{H}$  groups and water content in the membrane. Cross-linking significantly improves the mechanical strength of the membranes and reduces the water uptake of the membranes. However, it is also reducing the proton conductivity.

Figure 4.18 shows Arrhenius plot of proton conductivity as a function of temperature for the cross-linked membranes and Nafion<sup>®</sup> 117 membrane. The relation between proton conductivity and temperature in general follows the Arrhenius equation. From the Arrhenius equation, the activation energy of

membrane conductivity can be calculated. The activation energy of Nafion<sup>®</sup> 117 membrane is 7.04 kJ/mol, which is in agreement with the literature value. The activation energy for Nafion<sup>®</sup> 115 membrane is equal to 9.45 kJ/mol [204]. As can be seen, the proton conductivity of the cross-linked membranes increases continuously with increasing temperature.

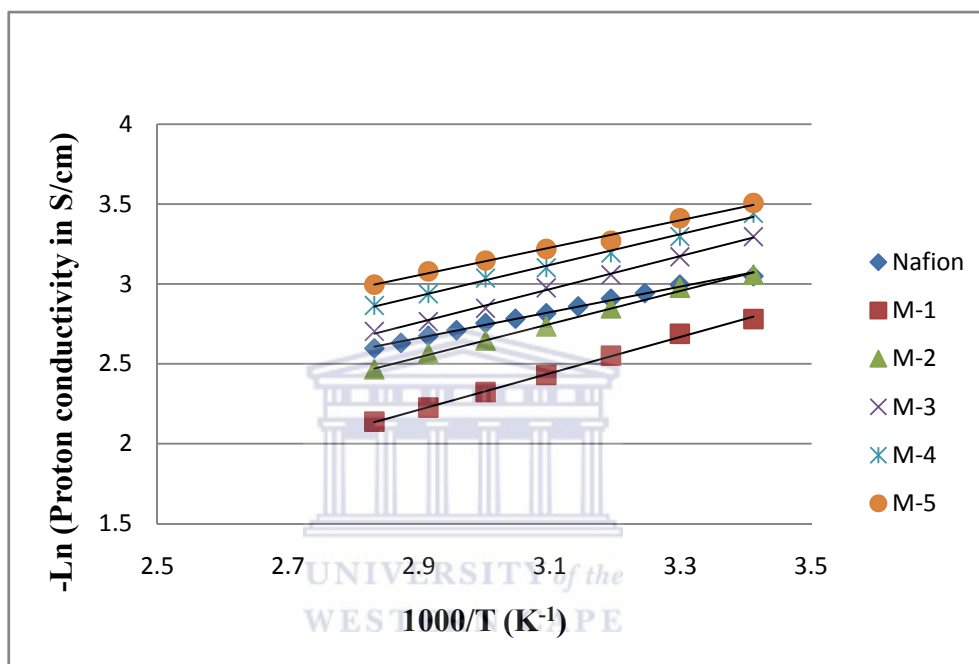


Figure 4. 18: Arrhenius plot of proton conductivity as a function of temperature for the cross-linked membranes and Nafion<sup>®</sup> 117 membrane.

It could be observed (see Figure 4.17), that the proton conductivity of cross-linked membranes trend to decrease with increasing cross-linking degree. It might be explained that proton conductivity is a function of ion exchange capacity and water uptake, both of which are affected by the level of cross-linking. The adding of cross-linker is facilitating, the cross-linking, which lead to structural reorientation and decrease of the polymer chain mobility. Therefore, the cross-linked membranes have compact network structure and lower proton exchangeable sites than uncross-linked one, which result in less dense and smaller

hydrophilic paths for water absorption and water mobility and hinder the mobility of  $H^+$  in the water phase, that is why the proton conductivity is compromised. Moreover, the cross-linked membranes exhibit more rigid backbone than the uncross-linked one, which also resists water uptake, water percolation, methanol permeability, and results in the decrease of the proton conductivity due to the reduction of suitable structural vacancies to retain water around sulfonic acid groups<sup>[202, 205, 206]</sup>.

#### 4.3.11. Methanol permeability (methanol crossover)

In order to achieve high overall efficiency of DMFC, two major obstacles, namely, low activity of the methanol electro-oxidation catalysts and crossover of methanol through the polymer electrolyte membrane have to be overcome<sup>[194]</sup>. The methanol permeability from anode to cathode lowers the fuel utilization, affects the oxygen cathode activity and causes the excess thermal load in the cell. The fluorosulfonic acid membranes, such as Nafion<sup>®</sup> are widely used as proton exchange membranes due to their excellent chemical and thermal stability and excellent proton conductivity. However, it has been found that over 40 % of the methanol can be wasted in DMFCs across such membranes due to high methanol permeability<sup>[207]</sup>. The methanol permeability at temperatures higher as 80 °C is increasing to such extent that the membrane is not suitable for DMFC applications anymore.

The methanol permeability of the cross-linked membranes was determined by using an electrochemical method<sup>[194]</sup>.

Initially, CV behaviour of methanol solutions in  $H_2SO_4$  with different concentrations has been studied. Figure 4.19 shows the cyclic voltammetry curves obtained on platinum mesh electrode for various concentrations of methanol on

the methanol added side. The methanol oxidation current increases with an increase in methanol concentration. It can be observed from these results that the onset of methanol oxidation on these electrodes is almost independent of the concentration of methanol.

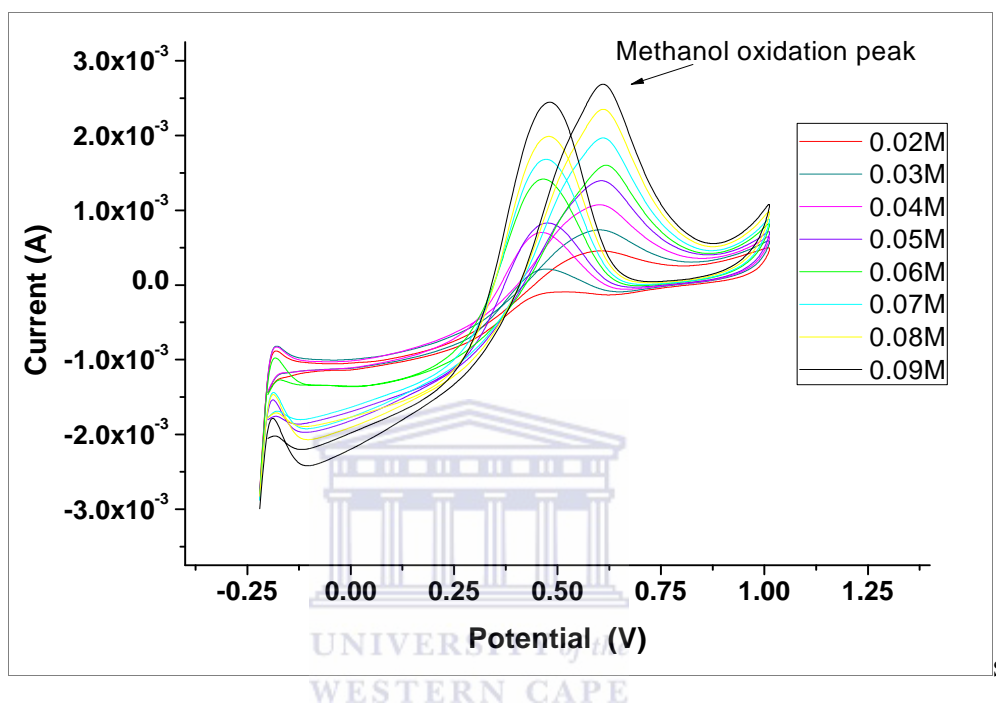


Figure 4. 19: Cyclic voltammety curves for the methanol at various concentrations.

Figure 4.20 shows that the relation between a peak current of methanol oxidation and a methanol concentration is linear. Therefore, CV method could be applied to measure quantitatively the concentration of the methanol in  $\text{H}_2\text{SO}_4$  solution. The methanol permeability of Nafion<sup>®</sup> 117 membrane was determined as  $3.81 \times 10^{-6} \text{ cm}^2/\text{s}$  after 5 h long exposure. It is slightly smaller than that of value measured by GC.

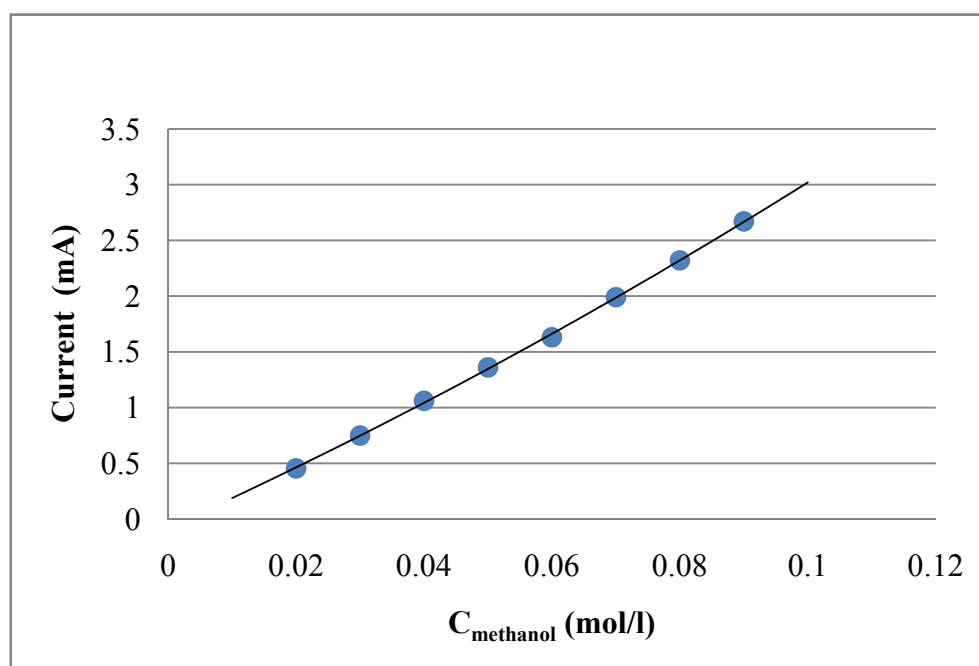


Figure 4. 20: The relation between peak current and methanol concentration.

Subsequently, the methanol permeability of the cross-linked membrane was determined, and it is shown in Figure 4.21:

The results show that the methanol permeability also reduces with increasing cross-linking degree. Like water uptake, the methanol cross over is also affected by the cross-linking degree (or cross-linking extent). The results show that the methanol permeability of M-5 was  $2.21 \times 10^{-7} \text{ cm}^2/\text{s}$ , much lower than that of Nafion<sup>®</sup> 117 membrane.

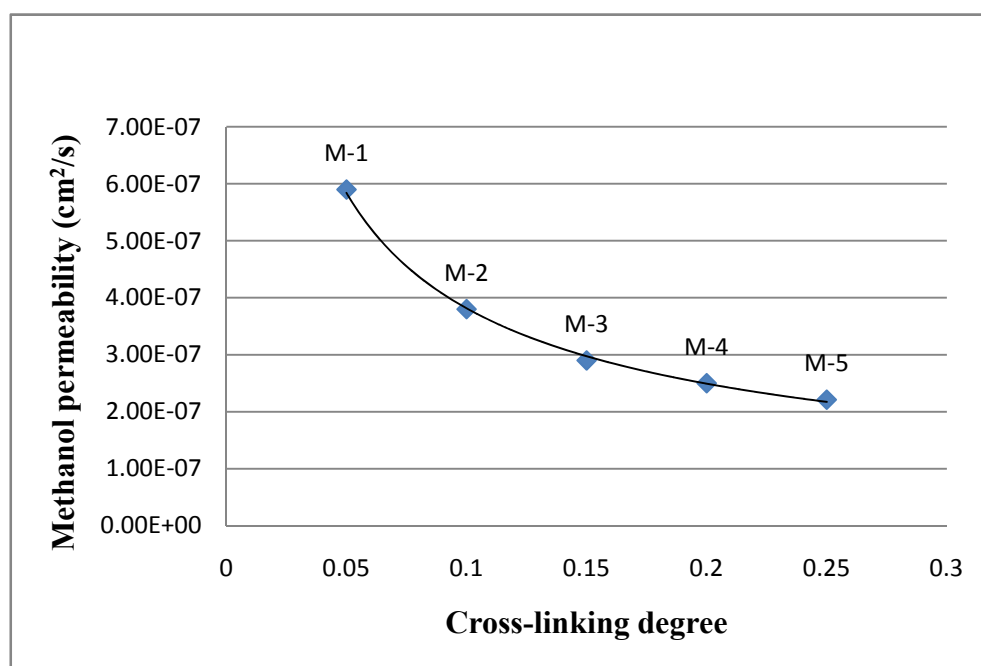


Figure 4. 21: The influence of cross-linking degree on methanol permeability of the cross-linked PEEK membranes.

#### 4.3.12. SEM of the cross-linked membrane

The SEM cross-section images of the cross-linked membranes are displayed in Figure 4.22. The images show that the all dried cross-linked membranes are dense, and no microporous structure is presented. This is important to decrease the methanol permeability via the micropores which would serve as a pathway for methanol.

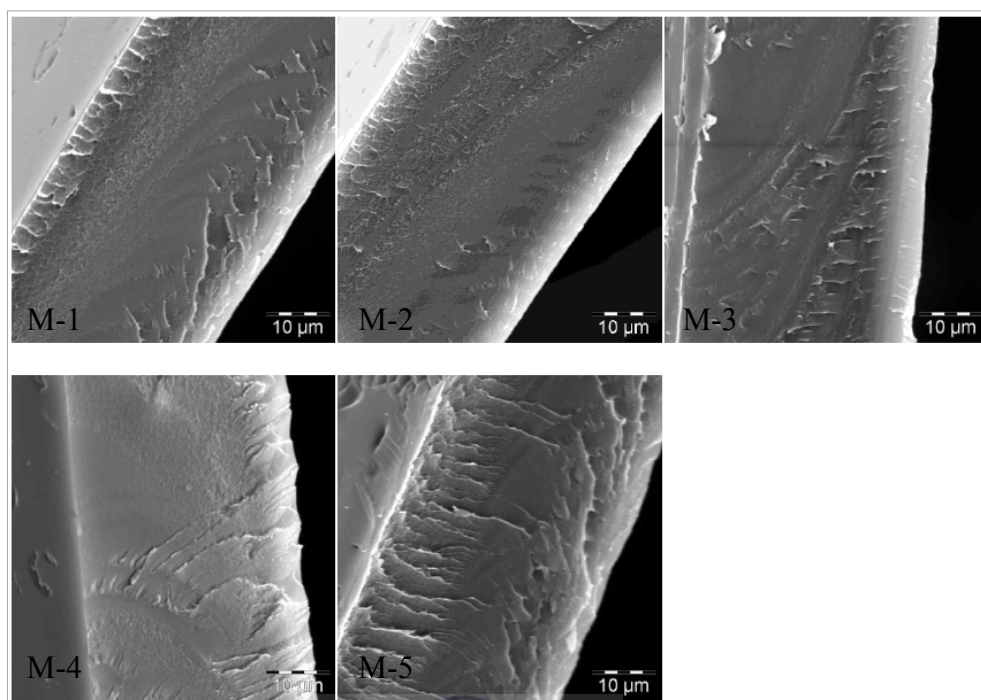


Figure 4. 22: The SEM cross section images of the cross-linked membranes.

#### 4.3.13 Thermal stability of the cross-linked membrane

The thermal stability of the cross-linked membranes was analyzed by TGA. The similar TGA curves of M-1 and M-5 are shown in Figure 4.23. The cross-linked membrane is thermally stable up to about 250 °C. In the curve of the cross-linked membranes, three subsequent steps of weight loss are observed. The absorbed water in the membranes causes the first weight loss. The second weight loss is related to the decomposition of the sulfonic acid groups from main chain of PEEK. The third weight loss is attributed to the polymer decomposition at temperatures higher than 400 °C. The decomposition kinetics of M-5 is slower than that of M-1. One of the reasons might be that the content of the sulfonic acid group in M-5 is lower than that of M-1. Furthermore, the cross-linking also improves the thermal stability of the membrane.

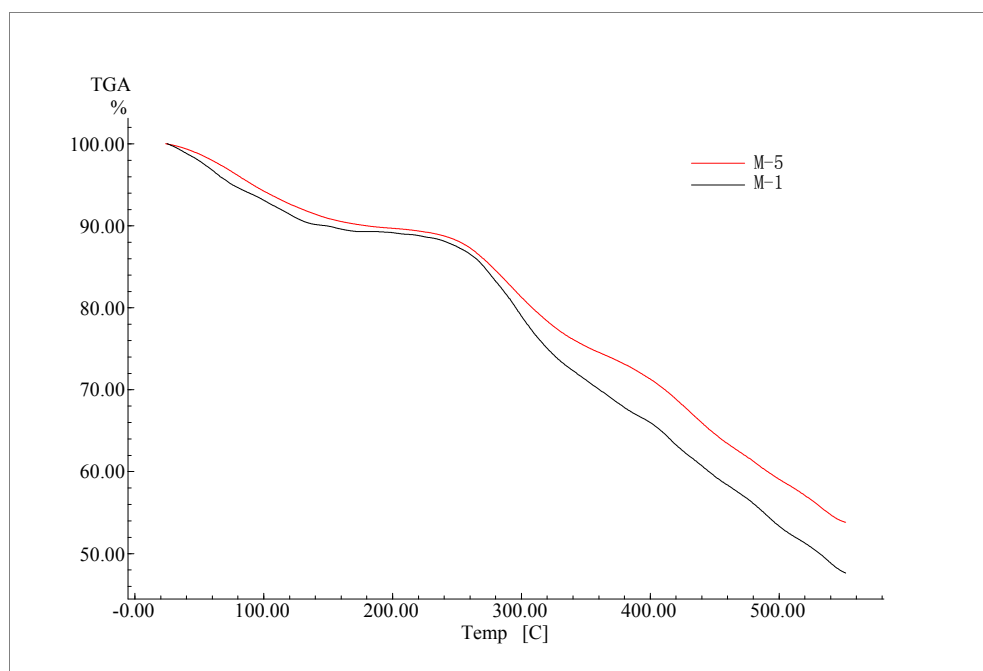


Figure 4. 23: The TGA curves of cross-linked membranes M-1 and M-5.

#### 4.3.14. Electrochemical stability

The electrochemical stability of the proton conducting membrane is very important for practical use in fuel cell <sup>[208]</sup>.

The redox behavior of the electrolytic membrane was investigated by cyclic voltammetry on the Pt/electrolyte interface. The electrochemical potential stability window is limited in its cathodic and anodic extremes by the reduction and the oxidation of the membrane or residual water or chloride ions, with a possible reaction of the polymer chain, where the reduction or oxidation of the polymer or  $H^+$  ion can take place. A broad stability window during the reduction and oxidation cycles is important for the practical use of these materials in contact with the electrolyte <sup>[209]</sup>.

Fig 4.24 presents the second (red) and 100th circle (black) of the cyclic voltammogram of the Pt electrode using the prepared membrane in 1 M KOH.

The cyclic voltammogram is only slightly changed after 100 cycles as shown in Figure 4.24. It demonstrates that the prepared membrane is very stable in the tested potential range.

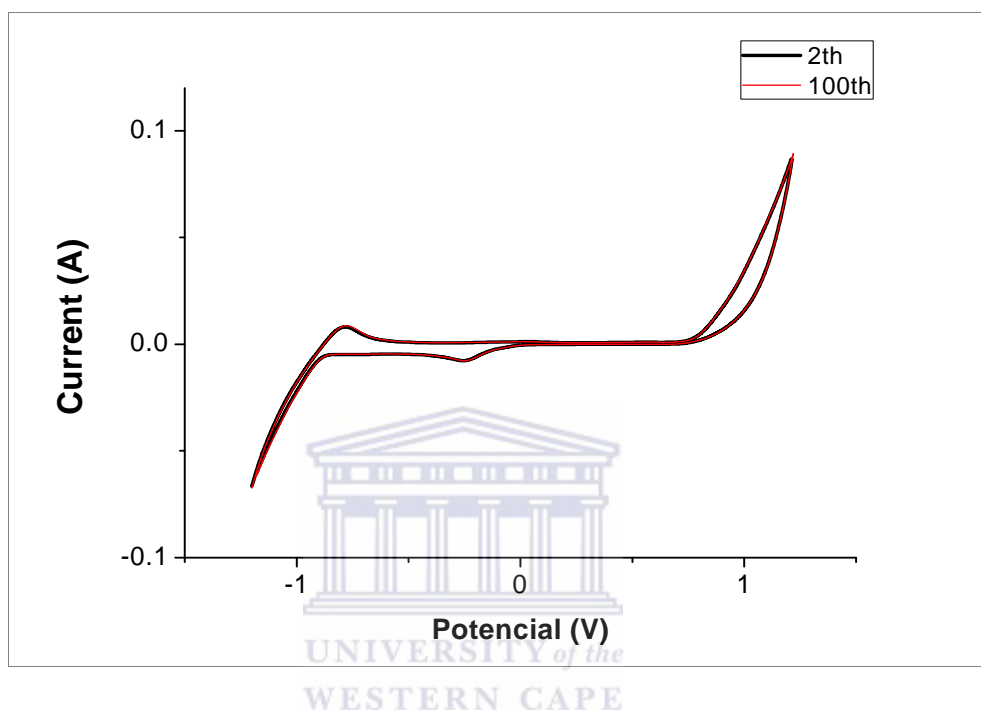


Figure 4. 24: Cyclic voltammetry of prepared membrane in 1 M KOH solution.

Performed in symmetrical Pt| electrolyte| Pt cell at a room temperature and a scan rate: 50 mv/s.

Black curve: the second circle, Red curve: the 100th circle (both circles are almost superposed).

Fig 4.25 presents the second (black) and 100th circle (green) of the cyclic voltammogram of the Pt electrode using the prepared membrane in 0.5 M sulfuric acid. A couple of redox peaks located at 0.5 and 0.7 V is due to the oxidation and reduction of Pt. The cyclic voltammogram show only slightly changes after 100 cycles as shown in Figure 4.25. It demonstrates that the prepared membrane is

stable in the measured potential range.

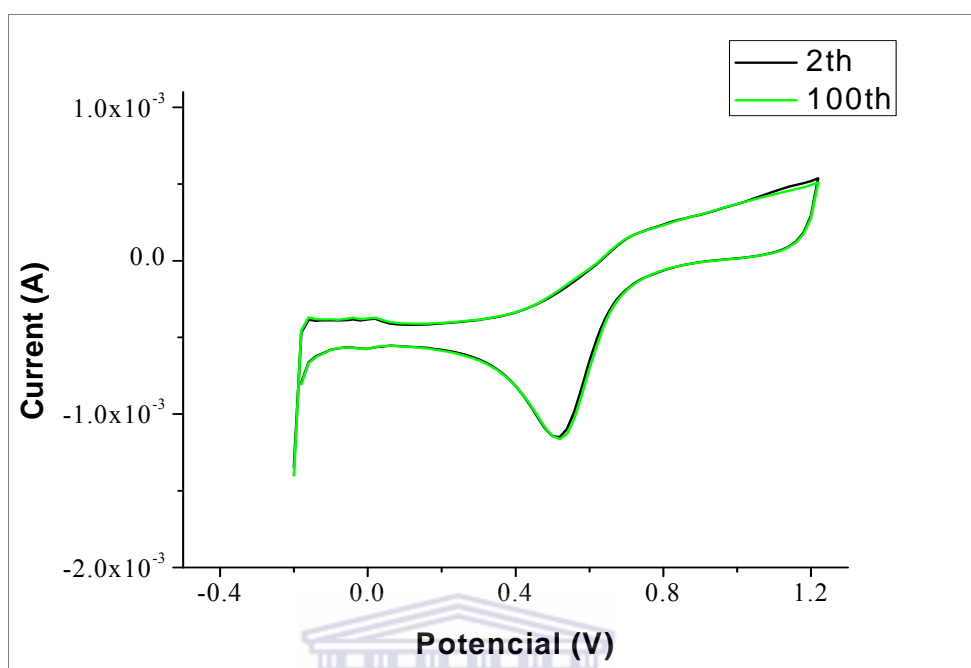


Figure 4. 25: Cyclic voltammetry of prepared membrane in 0.5 M H<sub>2</sub>SO<sub>4</sub>.

Performed in symmetrical Pt| electrolyte| Pt cell at a room temperature and a scan rate: 50 mv/s.

Black curve: the second circle, Green curve: the 100th circle (both circles are almost superposed).

The cross-linked membranes are also stable in hot solutions of strong acids and bases (see Table 4.2). There was no weight loss detected after 1 week long boiling in both NaOH and H<sub>2</sub>SO<sub>4</sub> solution.

Table 4. 2: Chemical stability of cross-linked membranes.

Cross-linked PEEK membranes	SPEEK membranes (high DS)
Stable in boiling water	Unstable
Stable in boiling NaOH solution (10 %)	Unstable
Stable in boiling HCl (10 %)	Stable
Stable in boiling H <sub>2</sub> SO <sub>4</sub> (10 %)	Stable
Stable in DMAC, NMP (unsolvable)	Unstable (soluble)

#### 4.3.15 Performance of membranes in DMFC

A discharge curve of a single DMFC using a cross-linked membrane (M-5 thickness = 50  $\mu\text{m}$ ) is shown in Figure 4.26. The curve was established after 100 h of operation in the DMFC testing station. The operating temperature of the cell was 70 °C. 1 M methanol solution was pumped through the DMFC anode at a flow rate of 1 ml/min, and oxygen was fed to the cathode at 0.5 l/min. The open circuit potential is 0.69 V. A power density 40.8 mW/cm<sup>2</sup> was reached with a current density of 204 mA/cm<sup>2</sup> at 0.2 V. From these results, the application of a prepared cross-linked membrane single DMFC, shows better performance compared with Nafion<sup>®</sup>. The reasons might be that the methanol permeability of the cross-linked membrane is lower than that of Nafion<sup>®</sup>, and membrane thickness reduction. It is suggested that the cross-linked membrane is a promising alternative proton exchange membrane for DMFC application.

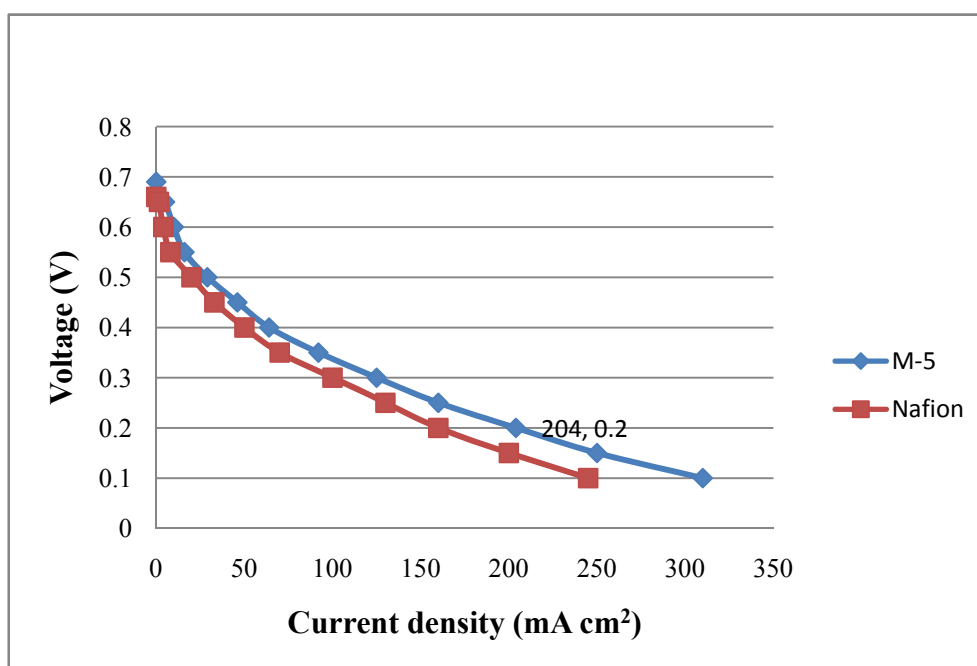


Figure 4. 26: The cell performance of a cross-linked membrane single cell vs. Nafion<sup>®</sup> 117 single cell.



#### 4.4. CONCLUSIONS

A novel cross-linked membrane with high proton conductivity and stability was successfully developed. The cross-linked membranes were prepared by cross-linking SsPEEK. SsPEEK was synthesized by reducing SCPEEK. SCPEEK was prepared via a chlorosulfonation by the strong acid, chlorosulfonic acid.

The results show that it is a good method to prepare a high SO<sub>3</sub>H content polymer. Simultaneously, another functional group can be substituted on the main chain of the polymer for further cross-linking.

The cross-linked membranes are highly proton conductive, mechanically and chemically stable, they show reduced water uptake, reduced methanol permeability and they show characteristic improvement with increasing cross-linking degree.

The stability, low methanol permeability, suitable water uptake and high proton conductivity of the cross-linked membranes makes them suitable candidates for DMFC applications.

A cross-linked membrane was applied in a DMFC and a considerable performance improvement was found as compared to commercial Nafion<sup>®</sup> 117 membranes.

## CHAPTER 5: OVERALL SUMMARY AND RECOMMENDATIONS

### 5.1. OVERALL SUMMARY

Poly(etheretherketone) (PEEK) was established as suitable starting material for membrane preparation due to its low cost and high mechanical stability.

Chapter 3 presents a new SPEEK/ZP composite proton exchange membrane for DMFC application.

Initially, PEEK was sulfonated by concentrated sulphuric acid. A series of SPEEK membranes were prepared and studied. For SPEEK membrane with DS ranging from 0.3 to 0.82 the proton conductivity values from  $5.6 \times 10^{-3}$  to  $2.5 \times 10^{-2}$  S/cm is observed at a room temperature. The proton conductivity of SPEEK membranes and the water uptake is increasing with increasing DS. The methanol permeability of SPEEK membrane is also rising with increasing DS. It was also found that the extremely high water uptake of SPEEK membrane with high DS is reducing the strength of the membrane, and the membrane become brittle after drying and water removal.

Subsequently, for the purpose of improving the properties of the SPEEK membranes, especially increasing proton conductivity and reducing the high water uptake, SPEEK with DS = 0.79 was established as the material to prepare a series of SPEEK/ZP composite membranes.

The SPEEK/ZP composite membranes were prepared by incorporating ZP into the SPEEK polymer matrix. The ZP was synthesized by phosphorization of nano-sized  $ZrO_2$ . The incorporated ZP is increasing the proton conductivity of the membrane. The proton conductivity for SPEEK/ZP composite membrane containing 40 wt.% of ZP, is equal to  $1.97 \times 10^{-2}$  S  $cm^{-1}$  at a room temperature. The membrane at the same time is thermally and chemically stable. The level of proton conductivity is comparable to that of the recast Nafion<sup>®</sup> membrane. A study of the water uptake of the SPEEK/ZP composite membrane has shown

reduced water uptake as compared to that of a pure SPEEK membrane at 80 °C. The methanol permeability of the membrane with a low ZP nano-particle content is reduced by 28 % as compared to that of the pure SPEEK membrane and it is 12 times lower than that of Nafion<sup>®</sup> membrane.

In Chapter 4 the main achievement of this study is presented. A novel cross-linked PEEK membrane was developed using original and simple procedure. The low cost and environmentally friendly material was produced, which is suitable for DMFC applications.

Initially, PEEK was sulfonated and chlorosulfonated by using concentrated chlorosulfonic acid. It was shown that the SCPEEK with the DS higher as 1 was synthesized via concentrated sulphuric acid. It was proved that the highly proton conductive polymer can be prepared via this method. SsPEEK was prepared by reducing SCPEEK. In this process the sulfonyl chloride was transformed to the sulfinate group.

The cross-linked membranes were prepared also by covalent cross-linking of the water soluble SsPEEK. In the process of cross-linking, the water uptake was extremely reduced. The increase of the cross-linking degree led to further reduction of the water uptake. For highly cross-linked membrane the observed water uptake is low and practically independent from temperature in a temperature range suitable for DMFC applications. At the same time slight decrease of the proton conductivity was observed. However, the proton conductivity of membranes is still high. In a single cell DMFC test, cross-linked PEEK membrane demonstrated better performance as compared to the commercial Nafion<sup>®</sup> membrane. Due to the low cost, high proton conductivity, suitable water uptake and low methanol permeability, the novel cross-linked PEEK membranes are considered suitable for use in DMFCs (also for H<sub>2</sub>-PEMFC) and might be alternative to Nafion<sup>®</sup> membrane.

## 5.2. RECOMMENDATIONS

In order to succeed in DMFC application the development of the proton

exchange membranes should be focused on achieving high power output and long term stability. Optimization of the MEA preparation procedure will be required for successful commercialization of these membranes in high performance DMFCs. In order to prevent the delamination, it is suggestible to use a PEEK based material instead of Nafion<sup>®</sup> solution for preparing the catalyst ink. The development of improved electrodes and optimized electrode-membrane assembly is in progress.

Further optimization of the composite membrane using appropriate procedures might be needed in order to enhance the stability and proton conductivity of the membrane.

It could be suggestible in a future research (some of the investigations are ongoing) to apply the developed cross-linking procedure to different polymers, to experiment with new cross-linking agents (which might also include polymers) and combine with ionic cross-linking (Figure 5.1).

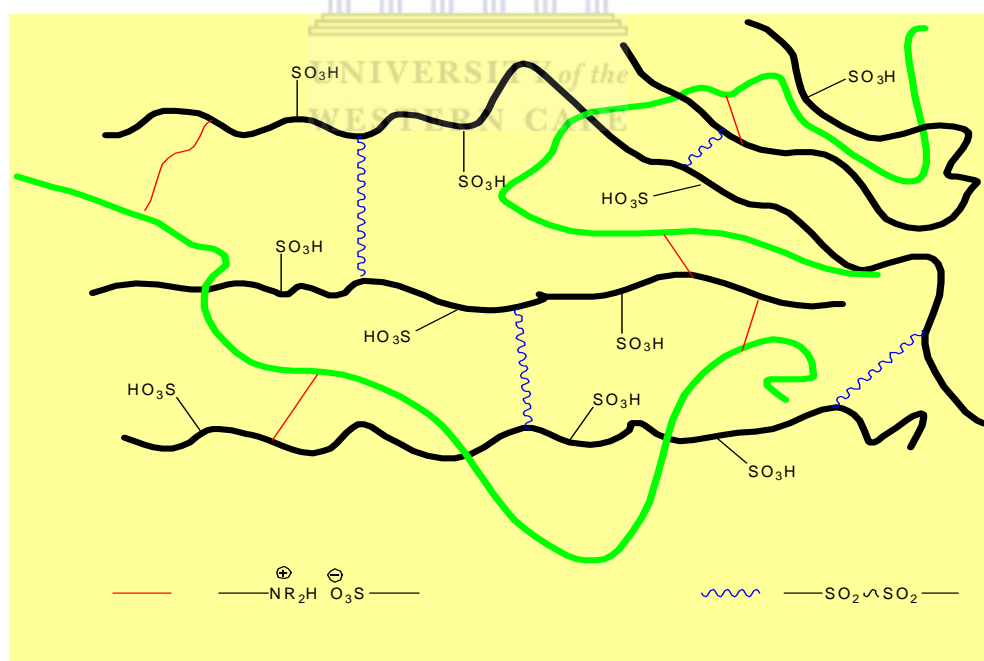


Figure 5. 1: Schematic diagram of a cross-linked membrane.

The attention will be paid to further studies of the lifetime of both composite and cross-linked membranes in DMFC and H<sub>2</sub>-PEMFC.

**REFERENCES**

1. Fanchi, J.R. and K.W. Tjan, *Energy in the 21st century*. 2005: Ebrary.
2. Williams, R.H., *Fuel cells convert a fuel's energy directly into electricity, without combustion and without moving parts*. Technology Review, 1994: p. 22-30.
3. Brandon, N. and D. Hart, *An Introduction to Fuel Cell Technology and Economics*. Imperial College Centre for Energy Policy and Technology: Occasional Paper No, 1999. **1**.
4. Appleby, A.J., *Recent developments and application of the polymer fuel cell*. Phil. Trans. Royal Soc. London A, 1996. **354**: p. 1681.
5. Cruickshank, J. and K. Scott, *The degree and effect of methanol crossover in the direct methanol fuel cell*. Journal of Power Sources, 1998. **70**(1): p. 40-47.
6. Singh, D., D.M. Lu, and N. Djilali, *A two-dimensional analysis of mass transport in proton exchange membrane fuel cells*. International Journal of Engineering Science, 1999. **37**(4): p. 431-452.
7. Hoogers, G., *Fuel Cell Technology Handbook*. 2003: CRC Press.
8. Wakefield, E.H., *History of the Electric Automobile: Battery-only Powered Cars*. 1994: Society of Automotive Engineers.
9. Thomas, S., et al., *Fuel Cells-Green Power*. 1999: Los Alamos National Laboratory.
10. Appleby, A.J. and F.R. Foulkes, *Fuel Cell Handbook*. 1989: Van Nostrand Reinhold.
11. Handbook, F.C., *US Department of Energy*. National Energy Technology Laboratory (NETL), ottobre, 2000.
12. Steele, B.C.H., *Material science and engineering: The enabling technology for the commercialisation of fuel cell systems*. Journal of Materials Science, 2001. **36**(5): p. 1053-1068.
13. Smotkin, E.S. and R.R. Diaz-Morales, *New Electrocatalysts By*

- Combinatorial Methods*. Annual Review of Materials Research, 2003. **33**(1): p. 557-579.
14. McVeigh, J., et al., *Winner, loser, or innocent victim? Has renewable energy performed as expected?* Solar Energy, 2000. **68**(3): p. 237-255.
  15. Chalk, S.G., P.G. Patil, and S.R. Venkateswaran, *The new generation of vehicles: market opportunities for fuel cells*. Journal of Power Sources, 1996. **61**(1-2): p. 7-13.
  16. Kalhammer, F.R. and T.R. Schneider, *Energy Storage*. Annual Review of Energy, 1976. **1**(1): p. 311-343.
  17. Lovins, A.B. and L.H. Lovins, *Energy Forever*. American Prospect, 2002. **13**(3): p. 30-34.
  18. Santi, E., et al., *A fuel cell based domestic uninterruptible power supply*. Applied Power Electronics Conference and Exposition, 2002. APEC 2002. Seventeenth Annual IEEE, 2002. **1**.
  19. Li, Y., Q. Fu, and M. Flytzani-Stephanopoulos, *Low-temperature water-gas shift reaction over Cu-and Ni-loaded cerium oxide catalysts*. Applied Catalysis B, Environmental, 2000. **27**(3): p. 179-191.
  20. Fatsikostas, A.N., D.I. Kondarides, and X.E. Verykios, *Production of hydrogen for fuel cells by reformation of biomass-derived ethanol*. Catalysis Today, 2002. **75**(1-4): p. 145-155.
  21. Dincer, I., *Technical, environmental and exergetic aspects of hydrogen energy systems*. International Journal of Hydrogen Energy, 2002. **27**(3): p. 265-285.
  22. Stambouli, A.B. and E. Traversa, *Solid oxide fuel cells (SOFCs): a review of an environmentally clean and efficient source of energy*. Renewable and Sustainable Energy Reviews, 2002. **6**(5): p. 433-455.
  23. Song, C., *Fuel processing for low-temperature and high-temperature fuel cells Challenges, and opportunities for sustainable development in the 21st century*. Catalysis Today, 2002. **77**(1-2): p. 17-49.
  24. Lee, H.S., K.S. Jeong, and B.S. Oh, *An experimental study of controlling strategies and drive forces for hydrogen fuel cell hybrid vehicles*.

- International Journal of Hydrogen Energy, 2003. **28**(2): p. 215-222.
25. Badwal, S.P.S. and K. Foger, *Solid oxide electrolyte fuel cell review*. Ceramics International, 1996. **22**(3): p. 257-265.
26. Carrette, L., K.A. Friedrich, and U. Stimming, *Fuel Cells: Principles, Types, Fuels, and Applications*. ChemPhysChem, 2000. **1**(4): p. 162-193.
27. Steele, B.C.H. and A. Heinzel, *Materials for fuel-cell technologies*. Nature, 2001. **414**(6861): p. 345-52.
28. Larminie, J. and A. Dicks, *Fuel Cell Systems Explained*. Second Edition ed. 2003: John Wiley and Sons. 15.
29. Gregor, H., *Fuel cell technology handbook*. 2003, CRC Press, New York.
30. L. Carrette, K.A.F.U.S., *Fuel Cells - Fundamentals and Applications*. FUEL CELLS, 2001. **1**(1): p. 5-39.
31. Cacciola, G., V. Antonucci, and S. Freni, *Technology up date and new strategies on fuel cells*. Journal of Power Sources, 2001. **100**(1-2): p. 67-79.
32. Meier-Haack, J., et al., *Membranes from sulfonated block copolymers for use in fuel cells*. Separation and Purification Technology, 2005. **41**(3): p. 207-220.
33. Perry, M.L. and T.F. Fuller, *A Historical Perspective of Fuel Cell Technology in the 20th Century*. Journal of The Electrochemical Society, 2002. **149**: p. S59.
34. Kalhammer, F.R., *Polymer electrolytes and the electric vehicle*. Solid State Ionics, 2000. **135**(1-4): p. 315-323.
35. Kordesch, K.V. and G.R. Simader, *Environmental Impact of Fuel Cell Technology*. Chemical Reviews, 1995. **95**(1): p. 191-207.
36. Acres, G.J.K., et al., *Electrocatalysts for fuel cells*. Catalysis Today, 1997. **38**(4): p. 393-400.
37. Haile, S.M., *Fuel cell materials and components*. Acta Materialia, 2003. **51**(19): p. 5981-6000.

## References

---

38. Gasteiger, H.A., et al., *Activity benchmarks and requirements for Pt, Pt-alloy, and non-Pt oxygen reduction catalysts for PEMFCs*. Applied Catalysis B, Environmental, 2005. **56**(1-2): p. 9-35.
39. Papageorgopoulos, D.C., M. Keijzer, and F.A. de Bruijn, *The inclusion of Mo, Nb and Ta in Pt and PtRu carbon supported electrocatalysts in the quest for improved CO tolerant PEMFC anodes*. Electrochimica Acta, 2002. **48**(2): p. 197-204.
40. Mehta, V. and J.S. Cooper, *Review and analysis of PEM fuel cell design and manufacturing*. Journal of Power Sources, 2003. **114**(1): p. 32-53.
41. Trimm, D.L. and Z.I. Onsan, *Onboard fuel conversion for hydrogen-fuel-cell-driven vehicles*. Catalysis Reviews - Science and Engineering, 2001. **43**(1 & 2): p. 31-84.
42. Han, J. and E.S. Park, *Direct methanol fuel-cell combined with a small back-up battery*. Journal of Power Sources, 2002. **112**(2): p. 477-483.
43. McNicol, B.D., D.A.J. Rand, and K.R. Williams, *Fuel cells for road transportation purposes -- yes or no?* Journal of Power Sources, 2001. **100**(1-2): p. 47-59.
44. Miesse, C.M., et al., *Direct formic acid fuel cell portable power system for the operation of a laptop computer*. Journal of Power Sources, 2006. **162**(1): p. 532-540.
45. Maynard, H.L. and J.P. Meyers, *Miniature fuel cells for portable power: Design considerations and challenges*. Journal of Vacuum Science & Technology B: Microelectronics and Nanometer Structures, 2002. **20**: p. 1287.
46. Osaka, T. and M. Datta, *Energy Storage Systems in Electronics*. 2000: CRC Press.
47. Billings, R. and S. Saathoff, *Fuel cells as backup power for digital loop carrier systems*. Telecommunications Energy Conference, 2004. INTELEC 2004. 26th Annual International, 2004: p. 88-91.
48. Lee, J.H., T.R. Lalk, and A.J. Appleby, *Modeling electrochemical performance in large scale proton exchange membrane fuel cell stacks*. Journal of Power Sources, 1998. **70**(2): p. 258-268.

- 
49. Wang, L., et al., *A parametric study of PEM fuel cell performances*. International Journal of Hydrogen Energy, 2003. **28**(11): p. 1263-1272.
50. Vielstich, W., *Electrochemical energy conversion: methanol fuel cell as example*. Journal of the Brazilian Chemical Society, 2003. **14**: p. 503-509.
51. Mikkola, M., *Experimental Studies on Polymer Electrolyte Membrane Fuel Cell Stacks*. 2001, HELSINKI UNIVERSITY OF TECHNOLOGY. p. 17.
52. Kikuchi, E., et al., *Steam reforming of methane in membrane reactors: comparison of electroless-plating and CVD membranes and catalyst packing modes*. Catalysis Today, 2000. **56**(1-3): p. 75-81.
53. Baxter, S.F., V.S. Battaglia, and R.E. White, *Methanol Fuel Cell Model: Anode*. Journal of The Electrochemical Society, 1999. **146**: p. 437.
54. Tazi, B. and O. Savadogo, *Parameters of PEM fuel-cells based on new membranes fabricated from Nafion(R), silicotungstic acid and thiophene*. Electrochimica Acta, 2000. **45**(25-26): p. 4329-4339.
55. Grot, W.G., *Perfluorinated ion exchange polymers and their use in research and industry*. Macromol. Symp, 1994. **82**: p. 161-172.
56. Arimura, T., et al., *The effect of additives on the ionic conductivity performances of perfluoroalkyl sulfonated ionomer membranes*. Solid State Ionics, 1999. **118**(1-2): p. 1-10.
57. Costamagna, P. and S. Srinivasan, *Quantum jumps in the PEMFC science and technology from the 1960s to the year 2000 Part II. Engineering, technology development and application aspects*. Journal of Power Sources, 2001. **102**(1-2): p. 253-269.
58. Bruijn, F., *The current status of fuel cell technology for mobile and stationary applications*. Green Chemistry, 2005. **7**(3): p. 132-150.
59. Li, Q., et al., *Approaches and Recent Development of Polymer Electrolyte Membranes for Fuel Cells Operating above 100 °C*. Chemistry of Materials, 2003. **15**(26): p. 4896-4915.
60. Haubold, H.G., et al., *Nano structure of NAFION: a SAXS study*. Electrochimica Acta, 2001. **46**(10-11): p. 1559-1563.

- 
61. Rozière, J. and D.J. Jones, *Non-fluorinated polymer materials for proton exchange membrane fuel cells*. Annual Review of Materials Research, 2003. **33**: p. 503-555.
62. Moore Iii, R.B. and C.R. Martin, *Morphology and chemical properties of the Dow perfluorosulfonate ionomers*. Macromolecules, 1989. **22**(9): p. 3594-3599.
63. Zaluski, C. and G. Xu, *Blends of Nafion and Dow Perfluorosulfonated Ionomer Membranes*. Macromolecules, 1994. **27**(23): p. 6750-6754.
64. James, P.J., et al., *In situ rehydration of perfluorosulphonate ion-exchange membrane studied by AFM*. Polymer, 2000. **41**(11): p. 4223-4231.
65. Ghielmi, A., et al., *Proton exchange membranes based on the short-side-chain perfluorinated ionomer*. Journal of Power Sources, 2005. **145**(2): p. 108-115.
66. Savadogo, O., *Emerging membranes for electrochemical systems: (I) solid polymer electrolyte membranes for fuel cell systems*. Journal of New Materials for Electrochemical Systems, 1998. **1**(1): p. 47-66.
67. Claus D. Eisenbach, J.H.K.F., *Blends of rigid-rod and flexible macromolecules*. Macromolecular Rapid Communications, 1994. **15**(2): p. 117-124.
68. Kuver, A. and K. Potje-Kamloth, *Comparative study of methanol crossover across electropolymerized and commercial proton exchange membrane electrolytes for the acid direct methanol fuel cell*. Electrochimica Acta, 1998. **43**(16-17): p. 2527-2535.
69. Yoshida, N., et al., *Characterization of Flemion® membranes for PEFC*. Electrochimica Acta, 1998. **43**(24): p. 3749-3754.
70. Scott, K., W.M. Taama, and P. Argyropoulos, *Performance of the direct methanol fuel cell with radiation-grafted polymer membranes*. Journal of Membrane Science, 2000. **171**(1): p. 119-130.
71. Bae, B. and D. Kim, *Sulfonated polystyrene grafted polypropylene composite electrolyte membranes for direct methanol fuel cells*. Journal of Membrane Science, 2003. **220**(1-2): p. 75-87.

72. Costamagna, P. and S. Srinivasan, *Quantum jumps in the PEMFC science and technology from the 1960s to the year 2000: Part I. Fundamental scientific aspects*. Journal of Power Sources, 2001. **102**(1-2): p. 242-252.
73. Du, X., et al., *Performances of proton exchange membrane fuel cells with alternate membranes*. Physical Chemistry Chemical Physics, 2001. **3**(15): p. 3175-3179.
74. Surampudi, S., et al., *Advances in direct oxidation methanol fuel cells*. Journal of Power Sources, 1994. **47**(3): p. 377-385.
75. Heinzl, A. and V.M. Barragan, *A review of the state-of-the-art of the methanol crossover in direct methanol fuel cells*. Journal of Power Sources, 1999. **84**(1): p. 70-74.
76. Gupta, B., et al., *Materials research aspects of organic solid proton conductors*. Solid state ionics, 1993. **61**(1-3): p. 213-218.
77. Scherer, G.G., *Polymer membranes for fuel cells*. Ber. Bunsenges. Phys. Chem, 1990. **94**: p. 1008-1014.
78. Lehtinen, T., et al., *Electrochemical characterization of PVDF-based proton conducting membranes for fuel cells*. Electrochimica Acta, 1998. **43**(12-13): p. 1881-1890.
79. Steck, A.E., In: O. Savadogo, PR Roberge and TN Veziroglu, Editors. Proceedings of the First International Symposium on New Materials for Fuel-Cell Systems, Montréal, Canada, 1995: p. 74.
80. Wei, J., C. Stone, and A.E. Steck, *Trifluorostyrene and substituted trifluorostyrene copolymeric compositions and ion-exchange membranes formed therefrom*. 1995, Google Patents.
81. Daniel I. Livingston, P.M.K.R.S.C., *Poly- $\alpha,\beta,\beta$ -trifluorostyrene*. Journal of Polymer Science, 1956. **20**(96): p. 485-490.
82. Sankir, M., et al., *Proton exchange membrane for DMFC and H<sub>2</sub>/air fuel cells: Synthesis and characterization of partially fluorinated disulfonated poly(arylene ether benzonitrile) copolymers*. Journal of Membrane Science, 2007. **299**(1-2): p. 8-18.
83. Penner, R.M. and C.R. Martin, *Ion Transporting Composite Membranes*.

- Journal of The Electrochemical Society, 1985. **132**: p. 514.
84. Croce, F., L. Settimi, and B. Scrosati, *Superacid ZrO<sub>2</sub>-added, composite polymer electrolytes with improved transport properties*. Electrochemistry Communications, 2006. **8**(2): p. 364-368.
85. Ren, S., et al., *Sulfated zirconia-Nafion composite membranes for higher temperature direct methanol fuel cells*. Journal of Power Sources, 2006. **157**(2): p. 724-726.
86. Chen, L.-C., et al., *Nafion/PTFE and zirconium phosphate modified Nafion/PTFE composite membranes for direct methanol fuel cells*. Journal of Membrane Science, 2008. **307**(1): p. 10-20.
87. Helen, M., B. Viswanathan, and S.S. Murthy, *Synthesis and characterization of composite membranes based on [alpha]-zirconium phosphate and silicotungstic acid*. Journal of Membrane Science, 2007. **292**(1-2): p. 98-105.
88. Bauer, F. and M. Willert-Porada, *Microstructural characterization of Zr-phosphate-Nafion(R) membranes for direct methanol fuel cell (DMFC) applications*. Journal of Membrane Science, 2004. **233**(1-2): p. 141-149.
89. Xu, W., et al., *Low methanol permeable composite Nafion/silica/PWA membranes for low temperature direct methanol fuel cells*. Electrochimica Acta, 2005. **50**(16-17): p. 3280-3285.
90. Shao, Z.-G., et al., *Hybrid Nafion-inorganic oxides membrane doped with heteropolyacids for high temperature operation of proton exchange membrane fuel cell*. Solid state ionics, 2006. **177**(7-8): p. 779-785.
91. Kim, Y.S., et al., *Fabrication and characterization of heteropolyacid (H<sub>3</sub>PW<sub>12</sub>O<sub>40</sub>)/directly polymerized sulfonated poly(arylene ether sulfone) copolymer composite membranes for higher temperature fuel cell applications*. Journal of Membrane Science, 2003. **212**(1-2): p. 263-282.
92. Saarinen, V., et al., *On the swelling properties of proton conducting membranes for direct methanol fuel cells*. Solid state ionics, 2007. **178**(7-10): p. 533-537.
93. Taylor, E.P., et al., *Counterion dependent crystallization kinetics in blends of a perfluorosulfonate ionomer with poly(vinylidene fluoride)*. Polymer,

2006. **47**(21): p. 7425-7435.
94. Cho, K.-Y., et al., *Preparation and characteristics of Nafion membrane coated with a PVdF copolymer/recast Nafion blend for direct methanol fuel cell*. Journal of Power Sources, 2006. **159**(1): p. 524-528.
95. Cho, K.-Y., et al., *A coated Nafion membrane with a PVdF copolymer/Nafion blend for direct methanol fuel cells (DMFCs)*. Solid state ionic, 2005. **176**(39-40): p. 3027-3030.
96. Kim, H.J., et al., *Nafion-Nafion/polyvinylidene fluoride-Nafion laminated polymer membrane for direct methanol fuel cells*. Journal of Power Sources, 2004. **135**(1-2): p. 66-71.
97. Cho, K.-Y., et al., *Characteristics of PVdF copolymer/Nafion blend membrane for direct methanol fuel cell (DMFC)*. Electrochimica Acta, 2004. **50**(2-3): p. 583-588.
98. Zhai, Y., et al., *A novel H<sub>3</sub>PO<sub>4</sub>/Nafion-PBI composite membrane for enhanced durability of high temperature PEM fuel cells*. Journal of Power Sources, 2007. **169**(2): p. 259-264.
99. Wycisk, R., et al., *Direct methanol fuel cell membranes from Nafion-polybenzimidazole blends*. Journal of Power Sources, 2006. **163**(1): p. 9-17.
100. Huang, L.-N., et al., *Nafion/PTFE/silicate composite membranes for direct methanol fuel cells*. Journal of Power Sources, 2006. **161**(2): p. 1096-1105.
101. Lin, H.-L., et al., *Nafion/PTFE composite membranes for direct methanol fuel cell applications*. Journal of Power Sources, 2005. **150**: p. 11-19.
102. Liu, F., et al., *Nafion/PTFE composite membranes for fuel cell applications*. Journal of Membrane Science, 2003. **212**(1-2): p. 213-223.
103. Liu, J., et al., *Nafion-polyfurfuryl alcohol nanocomposite membranes for direct methanol fuel cells*. Journal of Membrane Science, 2005. **246**(1): p. 95-101.
104. Kang, J.-S., et al., *Preparation of Nafion® nanocomposite membrane modified by phosphoric acid-functionalized 3-APTES*. Colloids and Surfaces A: Physicochemical and Engineering Aspects, 2008. **313-314**: p.

- 207-210.
105. Chalkova, E., et al. *Composite materials for PEM fuel cells operating at high temperature and low relative humidity*. in *Meeting Abstracts*. 2005. Los Angeles, CA.
106. Tricoli, V., N. Carretta, and M. Bartolozzi, *Comparative investigation of proton and methanol transport in fluorinated ionomeric membranes*. *Journal of The Electrochemical Society*, 2000. **147**(4): p. 1286-1290.
107. Wang, H. and G.A. Capuano, *Behavior of Raipore radiation-grafted polymer membranes in H<sub>2</sub>/O<sub>2</sub> fuel cells*. *Journal of The Electrochemical Society*, 1998. **145**(3): p. 780-784.
108. Jiang, R., H.R. Kunz, and J.M. Fenton, *Composite silica/Nafion(R) membranes prepared by tetraethylorthosilicate sol-gel reaction and solution casting for direct methanol fuel cells*. *Journal of Membrane Science*, 2006. **272**(1-2): p. 116-124.
109. Johnson, B.C., et al., *Synthesis and characterization of sulfonated poly(arylene ether sulfones)*. *Journal of polymer science. Polymer chemistry edition*, 1984. **22**(3): p. 721-737.
110. Nolte, R., et al., *Partially sulfonated poly(arylene ether sulfone) - A versatile proton conducting membrane material for modern energy conversion technologies*. *Journal of Membrane Science*, 1993. **83**(2): p. 211-220.
111. Nabe, A., E. Staude, and G. Belfort, *Surface modification of polysulfone ultrafiltration membranes and fouling by BSA solutions*. *Journal of Membrane Science*, 1997. **133**(1): p. 57-72.
112. Arnold, C. and R.A. Assink, *Development of sulfonated polysulfone membranes for redox flow batteries*. *Journal of Membrane Science*, 1988. **38**(1): p. 71-83.
113. Pozniak, G., M. Bryjak, and W. Trochimczuk, *Sulfonated polysulfone membranes with antifouling activity*. *Die Angewandte Makromolekulare Chemie*, 1995. **233**: p. 23-31.
114. Kerres, J., W. Cui, and S. Reichle, *New sulfonated engineering polymers via the metalation route. I. Sulfonated poly(ethersulfone) PSU Udel? via*

- metalation-sulfination-oxidation*. Journal of Polymer Science Part A Polymer Chemistry, 1996. **34**(12): p. 2421-2438.
115. Kerres, J., et al., *Development and characterization of crosslinked ionomer membranes based upon sulfinated and sulfonated PSU crosslinked PSU blend membranes by disproportionation of sulfinic acid groups*. Journal of Membrane Science, 1998. **139**(2): p. 211-225.
116. Zhang, W., C.M. Tang, and J. Kerres, *Development and characterization of sulfonated-unmodified and sulfonated-aminated PSU Udel(R) blend membranes*. Separation and Purification Technology, 2001. **22-23**: p. 209-221.
117. Walker, M., et al., *Proton-conducting polymers with reduced methanol permeation*. Journal of Applied Polymer Science, 1999. **74**(1): p. 67-73.
118. Kerres, J., et al., *Application of Different Types of Polyaryl-Blend-Membranes in DMFC*. Journal of New Materials for Electrochemical Systems, 2002. **5**(2): p. 97-107.
119. Bauer, B., et al., *Electrochemical characterisation of sulfonated polyetherketone membranes*. Journal of New Materials for Electrochemical Systems, 2000. **3**(2): p. 93-98.
120. Zaidi, S.M.J., et al., *Proton conducting composite membranes from polyether ether ketone and heteropolyacids for fuel cell applications*. Journal of Membrane Science, 2000. **173**(1): p. 17-34.
121. Kreuer, K.D., *On the development of proton conducting polymer membranes for hydrogen and methanol fuel cells*. Journal of Membrane Science, 2001. **185**(1): p. 29-39.
122. Kreuer, K.D., *On the development of proton conducting materials for technological applications*. Solid state ionics, 1997. **97**(1-4): p. 1-15.
123. Bailly, C., et al., *The sodium salts of sulphonated poly(aryl-ether-ether-ketone) (PEEK): Preparation and characterization*. Polymer, 1987. **28**(6): p. 1009-1016.
124. Li, L., J. Zhang, and Y. Wang, *Sulfonated poly(ether ether ketone) membranes for direct methanol fuel cell*. Journal of Membrane Science, 2003. **226**(1-2): p. 159-167.

125. Hübner, G. and E. Roduner, *EPR investigation of HO• radical initiated degradation reactions of sulfonated aromatics as model compounds for fuel cell proton conducting membranes*. Journal of Materials Chemistry, 1999. **9**(2): p. 409-418.
126. Sundet, S.A., *Reverse osmosis membrane, casting solution, and processes for making same*. 1986.
127. Konagaya, S. and M. Tokai, *Synthesis of ternary copolyamides from aromatic diamine (m-phenylenediamine, diaminodiphenylsulfone), aromatic diamine with carboxyl or sulfonic group (3,5-diaminobenzoic acid, 2,4-diaminobenzenesulfonic acid), and iso- or terephthaloyl chloride*. Journal of Applied Polymer Science, 2000. **76**(6): p. 913-920.
128. Yamada, O., et al., *Polymer electrolyte fuel cells based on main-chain-type sulfonated polyimides*. Electrochimica Acta, 2005. **50**(13): p. 2655-2659.
129. Genies, C., et al., *Soluble sulfonated naphthalenic polyimides as materials for proton exchange membranes*. Polymer, 2001. **42**(2): p. 359-373.
130. Zhang, Y., et al., *Molecular design considerations in the synthesis of high conductivity PEMs for fuel cells*. American Chemical Society, Polymer Preprints, Division of Polymer Chemistry, 1999. **40**(2): p. 480-481.
131. Cornet, N., et al., *Sulfonated polyimide membranes: A new type of ion-conducting membrane for electrochemical applications*. Journal of New Materials for Electrochemical Systems, 2000. **3**(1): p. 33-42.
132. Besse, S., et al., *Sulfonated Polyimides for Fuel Cell Electrode Membrane Assemblies (EMA)*. Journal of New Materials for Electrochemical Systems, 2002. **5**(2): p. 109-112.
133. Guo, X., et al., *Novel sulfonated polyimides as polyelectrolytes for fuel cell application. 2. Synthesis and proton conductivity of polyimides from 9,9-bis(4-aminophenyl)fluorene-2,7-disulfonic acid*. Macromolecules, 2002. **35**(17): p. 6707-6713.
134. Blachot, J.F., et al., *Anisotropy of structure and transport properties in sulfonated polyimide membranes*. Journal of Membrane Science, 2003. **214**(1): p. 31-42.
135. Yin, Y., et al., *Synthesis, proton conductivity and methanol permeability of*

- a novel sulfonated polyimide from 3-(2',4'-diaminophenoxy)propane sulfonic acid.* Polymer, 2003. **44**(16): p. 4509-4518.
136. Asano, N., K. Miyatake, and M. Watanabe, *Hydrolytically stable polyimide ionomer for fuel cell applications.* Chemistry of Materials, 2004. **16**(15): p. 2841-2843.
137. Gunduz, N. and J.E. McGrath, *Synthesis and characterization of sulfonated polyimides.* American Chemical Society, Polymer Preprints, Division of Polymer Chemistry, 2000. **41**(1): p. 182-183.
138. Woo, Y., et al., *Synthesis and characterization of sulfonated polyimide membranes for direct methanol fuel cell.* Journal of Membrane Science, 2003. **220**(1-2): p. 31-45.
139. Guo, Q., et al., *Sulfonated and crosslinked polyphosphazene-based proton-exchange membranes.* Journal of Membrane Science, 1999. **154**(2): p. 175-181.
140. Carter, R., et al., *Blended polyphosphazene/polyacrylonitrile membranes for direct methanol fuel cells.* Electrochemical and Solid-State Letters, 2002. **5**(9).
141. Kerres, J., et al., *Cross-linked polyaryl blend membranes for polymer electrolyte fuel cells.* Fuel Cells, 2004. **4**(1-2): p. 105-112.
142. Kerres, J., *Covalent-ionically cross-linked poly(etheretherketone)-basic polysulfone blend ionomer membranes.* Fuel Cells, 2006. **6**(3-4): p. 251-260.
143. Zhang, W., et al., *Novel covalently cross-linked poly(etheretherketone) ionomer membranes.* Journal of Power Sources, 2006. **155**(1): p. 3-12.
144. Kerres, J.A., *Blended and Cross-Linked Ionomer Membranes for Application in Membrane Fuel Cells.* Fuel Cells, 2005. **5**(2): p. 230-247.
145. Mikhailenko, S.D., et al., *Properties of PEMs based on cross-linked sulfonated poly(ether ether ketone).* Journal of Membrane Science, 2006. **285**(1-2): p. 306-316.
146. Jones, D.J., et al., *High-temperature DMFC stack operating with non-fluorinated membranes.* Fuel Cells Bulletin, 2005. **2005**(10): p. 12-15.

- 
147. Mikhailenko, S.D., S.M.J. Zaidi, and S. Kaliaguine, *Sulfonated polyether ether ketone based composite polymer electrolyte membranes*. Catalysis Today, 2001. **67**(1-3): p. 225-236.
148. Othman, M.H.D., A.F. Ismail, and A. Mustafa, *Proton conducting composite membrane from sulfonated poly(ether ether ketone) and boron orthophosphate for direct methanol fuel cell application*. Journal of Membrane Science, 2007. **299**(1-2): p. 156-165.
149. Nagarale, R.K., G.S. Gohil, and V.K. Shahi, *Sulfonated poly(ether ether ketone)/polyaniline composite proton-exchange membrane*. Journal of Membrane Science, 2006. **280**(1-2): p. 389-396.
150. Mecheri, B., et al., *Sulfonated polyether ether ketone and hydrated tin oxide proton conducting composites for direct methanol fuel cell applications*. Journal of Power Sources, 2008. **178**(2): p. 554-560.
151. Powers, E.J. and G. Serad, *History and Development of Polybenzimidazoles*. High Performance Polymers: Their Origin and Development, 1986: p. 355-373.
152. Samms, S.R., S. Wasmus, and R.F. Savinell, *Thermal stability of proton conducting acid doped polybenzimidazole in simulated fuel cell environments*. Journal of The Electrochemical Society, 1996. **143**(4): p. 1225-1232.
153. Vogel, H. and C.S. Marvel, *Polybenzimidazoles, new thermally stable polymers*. Journal of Polymer Science, Part A: Polymer Chemistry, 1996. **34**(7): p. 1125-1153.
154. Bouchet, R. and E. Siebert, *Proton conduction in acid doped polybenzimidazole*. Solid state ionics, 1999. **118**(3-4): p. 287-299.
155. Glipa, X., et al., *Investigation of the conduction properties of phosphoric and sulfuric acid doped polybenzimidazole*. Journal of Materials Chemistry, 1999. **9**(12): p. 3045-3049.
156. Wainright, J.S., et al., *Acid-doped polybenzimidazoles: A new polymer electrolyte*. Journal of The Electrochemical Society, 1995. **142**(7).
157. Glipa, X., et al., *Synthesis and characterisation of sulfonated polybenzimidazole: A highly conducting proton exchange polymer*. Solid

- state ionics, 1997. **97**(1-4): p. 323-331.
158. Xing, B. and O. Savadogo, *The effect of acid doping on the conductivity of polybenzimidazole (PBI)*. Journal of New Materials for Electrochemical Systems, 1999. **2**(2): p. 95-101.
159. Gieselman, M.B. and J.R. Reynolds, *Water-soluble polybenzimidazole-based polyelectrolytes*. Macromolecules, 1992. **25**(18): p. 4832-4834.
160. Xing, B. and O. Savadogo, *Hydrogen/oxygen polymer electrolyte membrane fuel cells (PEMFCs) based on alkaline-doped polybenzimidazole (PBI)*. Electrochemistry Communications, 2000. **2**(10): p. 697-702.
161. Hoel, D. and E. Grunwald, *High protonic conduction of polybenzimidazole films [3]*. Journal of Physical Chemistry, 1977. **81**(22): p. 2135-2136.
162. Aharoni, S.M. and M.H. Litt, *Synthesis and some properties of poly-(2, 5-trimethylene benzimidazole) and poly-(2, 5-trimethylene benzimidazole hydrochloride)*. Journal of Polymer Science Polymer Chemistry Edition, 1974. **12**(3): p. 639-650.
163. Wang, J.T., et al., *A direct methanol fuel cell using acid-doped polybenzimidazole as polymer electrolyte*. Journal of Applied Electrochemistry, 1996. **26**(7): p. 751-756.
164. Wainright, J.S., J.-t. Wang, and R.F. Savinell. *Direct methanol fuel cells using acid doped polybenzimidazole as a polymer electrolyte*. in *Proceedings of the Intersociety Energy Conversion Engineering Conference*. 1996.
165. Wang, J. and L. Chen, *Selectivity coefficients of class-selective enzyme electrodes*. Biosensors and Bioelectronics, 1996. **11**(8): p. 751-756.
166. Preston, P.N., *Benzimidazoles and congeneric tricyclic compounds. part 1*. 1981: New York: Wiley.
167. Linkous, C.A., et al., *Development of new proton exchange membrane electrolytes for water electrolysis at higher temperatures*. International Journal of Hydrogen Energy, 1998. **23**(7): p. 525-529.

168. Lin, H.-L., et al., *Preparation of a low proton resistance PBI/PTFE composite membrane*. Journal of Power Sources, 2007. **164**(2): p. 481-487.
169. Lee, J.K. and J. Kerres, *Synthesis and characterization of sulfonated poly(arylene thioether)s and their blends with polybenzimidazole for proton exchange membranes*. Journal of Membrane Science, 2007. **294**(1-2): p. 75-83.
170. Chuang, S.-W., S.L.-C. Hsu, and C.-L. Hsu, *Synthesis and properties of fluorine-containing polybenzimidazole/montmorillonite nanocomposite membranes for direct methanol fuel cell applications*. Journal of Power Sources, 2007. **168**(1): p. 172-177.
171. Carollo, A., et al., *Developments of new proton conducting membranes based on different polybenzimidazole structures for fuel cells applications*. Journal of Power Sources, 2006. **160**(1): p. 175-180.
172. Zaidi, S.M.J., *Preparation and characterization of composite membranes using blends of SPEEK/PBI with boron phosphate*. Electrochimica Acta, 2005. **50**(24): p. 4771-4777.
173. Daletou, M.K., N. Gourdoupi, and J.K. Kallitsis, *Proton conducting membranes based on blends of PBI with aromatic polyethers containing pyridine units*. Journal of Membrane Science, 2005. **252**(1-2): p. 115-122.
174. Allcock, H.R., M.A. Hofmann, and R.M. Wood, *Phosphonation of Aryloxyphosphazenes*. Macromolecules, 2001. **34**(20): p. 6915-6921.
175. Allcock, H.R., et al., *Phenyl phosphonic acid functionalized poly[aryloxyphosphazenes] as proton-conducting membranes for direct methanol fuel cells*. Journal of Membrane Science, 2002. **201**(1-2): p. 47-54.
176. Zhou, X., et al., *High temperature transport properties of polyphosphazene membranes for direct methanol fuel cells*. Electrochimica Acta, 2003. **48**(14-16): p. 2173-2180.
177. Kreuer, K.D., *Proton Conductivity: Materials and Applications*. Chem. Mater, 1996. **8**: p. 610.
178. Savadogo, O., *Emerging membranes for electrochemical systems: Part II. High temperature composite membranes for polymer electrolyte fuel cell*

- (PEFC) applications. *Journal of Power Sources*, 2004. **127**(1-2): p. 135-161.
179. Kobayashi, T., et al., *Proton-conducting polymers derived from poly (ether-etherketone) and poly (4-phenoxybenzoyl-1, 4-phenylene)*. *Solid state ionics*, 1998. **106**(3-4): p. 219-225.
180. Mikhailenko, S.D., et al., *Proton conducting membranes based on cross-linked sulfonated poly (ether ether ketone)(SPEEK)*. *Journal of Membrane Science*, 2004. **233**(1-2): p. 93-99.
181. Vaivars, G., et al., *Inorganic membranes based on zirconium phosphate for fuel cells*. *Journal of Solid State Electrochemistry*, 2004. **8**(11): p. 882-885.
182. Vaivars, G., et al., *Inorganic direct methanol fuel cell*. *Journal of Energy in Southern Africa*, 2003: p. 47-50.
183. Vaivars, G., et al., *Phosphorized zirconium oxide nanoparticles*. *Applied Organometallic Chemistry*, 2005. **19**(10): p. 1096-1100.
184. Pivovar, B.S., Y. Wang, and E.L. Cussler, *Pervaporation membranes in direct methanol fuel cells*. *Journal of Membrane Science*, 1999. **154**(2): p. 155-162.
185. Jin, X., et al., *A sulphonated poly (aryl ether ketone)*. *British Polymer Journal*, 1985. **17**(1): p. 4-10.
186. Samms, S.R., S. Wasmus, and R.F. Savinell, *Thermal Stability of Proton Conducting Acid Doped Polybenzimidazole in Simulated Fuel Cell Environments*. *Journal of The Electrochemical Society*, 2005. **143**: p. 1225.
187. Shibuya, N. and R.S. Porter, *A kinetic study of PEEK sulfonation in concentrated sulfuric acid by ultraviolet-visible spectroscopy*. *Polymer*, 1994. **35**(15): p. 3237-3242.
188. Takeshi Ogawa, C.S.M., *Polyaromatic ether-ketones and ether-keto-sulfones having various hydrophilic groups*. *Journal of Polymer Science: Polymer Chemistry Edition*, 1985. **23**(4): p. 1231-1241.
189. Xing, P., et al., *Synthesis and characterization of sulfonated poly(ether ether ketone) for proton exchange membranes*. *Journal of Membrane Science*, 2004. **229**(1-2): p. 95-106.

- 
190. Kaliaguine, S., et al., *Properties of SPEEK based PEMs for fuel cell application*. Catalysis Today, 2003. **82**(1-4): p. 213-222.
191. Devaux, J., et al., *On the molecular-weight determination of a poly(aryl-ether-ether-ketone) (peek)*. Polymer, 1985. **26**(13): p. 1994-2000.
192. Colomban, P. and A. Novak, *Nature of the protonic species and the gel-crystal transition in hydrated zirconium phosphate*. Journal of Molecular Structure, 1989. **198**: p. 277-295.
193. Bondars, B., et al., *Powder diffraction investigations of plasma sprayed zirconia*. Journal of Materials Science, 1995. **30**(6): p. 1621-1625.
194. Ramya, K. and K.S. Dhathathreyan, *Direct methanol fuel cells: determination of fuel crossover in a polymer electrolyte membrane*. Journal of Electroanalytical Chemistry, 2003. **542**: p. 109-115.
195. Bonnet, B., et al., *Hybrid organic-inorganic membranes for a medium temperature fuel cell*. Journal of New Materials for Electrochemical Systems, 2000. **3**(2): p. 87-92.
196. Genova-Dimitrova, P., et al., *Ionomeric membranes for proton exchange membrane fuel cell (PEMFC): Sulfonated polysulfone associated with phosphoantimonic acid*. Journal of Membrane Science, 2001. **185**(1): p. 59-71.
197. Cremllyn, R.J.W., *Chlorosulfonic Acid: A Versatile Reagent*. 1 ed. 2002: Royal Society of Chemistry. 4.
198. De Carvalho Barcellos, M., et al., *Development of new sulphonyl resin from modification of commercial resin*. Polymer Bulletin, 2005. **55**(1-2): p. 61-70.
199. U. Zoller, *The Chemistry of Sulphonic Acids, Esters and their Derivatives*, ed. Saul Patai. 1991: Wiley.
200. Rabek, J.F., *Experimental methods in polymer chemistry: physical principles and applications*. 1980: Wiley.
201. Brandrup, J., E.H. Immergut, and E.A. Grulke, *Polymer handbook*. 2003: Wiley & Sons.

## References

---

202. Hofmann, M.A., et al., *Synthesis of polyphosphazenes with sulfonimide side groups*. *Macromolecules*, 2002. **35**(17): p. 6490-6493.
203. Nasef, M.M. and H. Saidi, *Preparation of crosslinked cation exchange membranes by radiation grafting of styrene/divinylbenzene mixtures onto PFA films*. *Journal of Membrane Science*, 2003. **216**(1-2): p. 27-38.
204. Yeo, R.S., *Ion clustering and proton transport in Nafion membranes and its applications as solid polymer electrolyte*. *Journal of The Electrochemical Society*, 1983. **130**(3): p. 533-538.
205. Qiao, J., T. Hamaya, and T. Okada, *New highly proton-conducting membrane poly(vinylpyrrolidone)(PVP) modified poly(vinyl alcohol)/2-acrylamido-2-methyl-1-propanesulfonic acid (PVA-PAMPS) for low temperature direct methanol fuel cells (DMFCs)*. *Polymer*, 2005. **46**(24): p. 10809-10816.
206. Rhim, J.-W., et al., *Crosslinked poly(vinyl alcohol) membranes containing sulfonic acid group: proton and methanol transport through membranes*. *Journal of Membrane Science*, 2004. **238**(1-2): p. 143-151.
207. Beattie, P.D., et al., *Ionic conductivity of proton exchange membranes*. *Journal of Electroanalytical Chemistry*, 2001. **503**(1-2): p. 45-56.
208. Vassal, N., E. Salmon, and J.F. Fauvarque, *Electrochemical properties of an alkaline solid polymer electrolyte based on P(ECH-co-EO)*. *Electrochimica Acta*, 2000. **45**(8-9): p. 1527-1532.
209. Lewandowski, A., K. Skorupska, and J. Malinska, *Novel poly(vinyl alcohol)-KOH-H<sub>2</sub>O alkaline polymer electrolyte*. *Solid state ionics*, 2000. **133**(3-4): p. 265-271.